AFCRL-65-65

MC 63-78-R1

RESEARCH OF AERODYNAMIC METHODS OF PRODUCING ANTENNA WINDOWS IN A PLASMA SHEATH

RICHARD H. ADAMS
JOSEPH J. ROSSI

CONTRACT NO. AF19(628)-3852
PROJECT NO. 4642 TASK NO. 464202

SCIENTIFIC REPORT NO. 1

OCTOBER 1964

PREPARED FOR
AIR FORCE CAMBRIDGE RESEARCH LABORATORIES
OFFICE OF AEROSPACE RESEARCH
UNITED STATES AIR FORCE
BEDFORD, MASSACHUSETTS

MITHRAS, INC.
AEROTHERMODYNAMICS – ELECTROMAGNETICS – QUANTUM PHYSICS
701 CONCORD AVENUE, CAMBRIDGE, MASS. 02138

MITHRAS, INC.
701 Concord Avenue
Cambridge, Massachusetts
02138

AFCRL-65-65

MC 63-78-R1

RESEARCH OF AERODYNAMIC METHODS OF PRODUCING ANTENNA WINDOWS IN A PLASMA SHEATH

by

Richard H. Adams
Joseph J. Rossi

Contract No. AF19(628)-3852

Project No. 4642

N. .04202

Scientific Report No. 1

October 1964

Prepared
for

Air Force Cambridge Research Laboratories
Office of Aerospace Research
United States Air Force
Bedford, Massachusetts

ABSTRACT

Two aerodynamic methods of creating transmission "windows" in typical plasma sheaths surrounding re-entry vehicles have been investigated: (1) the use of jets of coolant from flush nozzles which penetrate across the plasma slab and then mix with the ionized gases as they are carried downstream, (2) the use of a physical flow diverter to bypass some of the ionized flow laterally around the antenna. Equations are developed for the lateral jet penetration in a supersonic stream and for one-dimensional mixing for both perfect gases and real gases in thermodynamic equilibrium. The assumption of real-air equilibrium thermodynamics yields coolant requirements considerably below the perfect gas values for the jet injection method. It is concluded that the jet injection method will reduce a 200 mc. signal attenuation to 3 db. with modest jet flow rates of helium on a typical re-entry trajectory. Conversely, the use of a physical flow diverter is not an effective method of creating a transmission window where the ionization layer is not adjacent to the vehicle surface or where the attenuation needs to be reduced more than 10 db.

FOREWORD

This report was prepared by MITHRAS, Inc., of Cambridge, Massachusetts, for the Microwave Physics Laboratory, Air Force Cambridge Research Laboratories, Hanscom Field, Bedford, Massachusetts, under Contract AF 19(628)-3852. The work was initiated by Mr. Walter Rothman and monitored by him and Mr. John F. Lennon.

The investigations whose results are reported here were conducted during the period 14 October 1963 to 14 October 1964. They were directed by Mr. Jacques A. F. Hill and carried out by Mr. Joseph J. Rossi and Mr. Richard H. Adams. This report was written by Mr. Joseph J. Rossi and Mr. Richard H. Adams. The research program is being continued under the same contract number.

TABLE OF CONTENTS

TABLE OF CONTENTS (Concluded)

LIST OF FIGURES

LIST OF FIGURES (Continued)

LIST OF FIGURES (Concluded)

LIST OF SYMBOLS

M_j	Mach number
θ_c	cone angle
ω_p	plasma frequency, RAD/SEC
ω_c	electron collision frequency, RAD/SEC
Ne	electron density
$\bar{c}$	average velocity of electron
N_j	concentration of j^{th} species
Q_j	electron cross-section of j^{th} species
T	temperature
P	pressure
ρ	density
V	velocity
$f(\gamma)$	tabulated function of the isentropic exponent at the stagnation region
C_D	drag coefficient, $D / \left(\frac{1}{2} \rho_\infty U_\infty^2 \cdot A \right)$
C_L	lift coefficient, $L / \left(\frac{1}{2} \rho_\infty U_\infty^2 A \right)$
W	weight, or width of jet
A	area
$(W/C_L A)$	re-entry glide parameter
h	enthalpy
H	stagnation enthalpy
ΔF_N	incremental force normal to jet
ΔF_S	incremental force tangent to jet
$\dot{m}$	mass flow of jet
V_j	average velocity of jet along its centerline at station S
S	approximate path length from orifice along centerline of jet

σ	parameter describing turning of jet, arc tan (y/x)
x	distance along body
y	distance normal to body
c	coefficient describing the percent by weight of coolant present in a mixed flow
R	gas constant
C_p	specific heat, $(\frac{\partial h}{\partial T})_p$
$C_{Q_{1,2}}$	coolant injection coefficient $\dot{m}/\rho_1 U_1 A_{1,2}$
δ	plasma thickness
N	axial force normal to vehicle surface
α	angle of attack
C_{N_α}	stability derivative, describes the rate of change of body normal force with changing angle of attack
b, a	major and minor axes of ellipse

SUBSCRIPTS

1, 2	value of variable at particular point in the flow
∞	free stream condition
s	separated region condition
e	external region, refers to condition in shock layer
te	stagnation condition external to separated region
a	refers to air property
c	coolant or cone property
i, j	injected gas condition, or jet condition
x	value of varjable at stations along body
o	sea level conditions or jet exit condition
RA	ram condition existing just in front of expanding jet

SUPERSCRIPTS

*	denotes variables normalized with respect to external region properties
o	denotes free stream conditions

1. INTRODUCTION

The plasma sheath surrounding a hypersonic re-entry vehicle attenuates the radio signals transmitted to and from the vehicle, often to the point of complete blackout. Much work has been done on the physics of the interaction of the plasma and the electromagnetic wave near the vehicle, and experimental flight data supporting theories and prediction is now becoming available.

On experimental manned re-entry vehicles the blackout problem has been solved by on board recorders which store data during the blackout and then playback the data once the blackout region has been passed. The manned Mercury vehicles have merely "lived with" the blackout problem. However, with the advent of the Apollo program and other manned vehicle programs, particularly manned maneuvering vehicles, the importance of uninterrupted radio contact with the vehicle during re-entry has increased. This necessitates developing methods of creating "windows" through the plasma sheath.

Under contract AF 19(628)-3852 with the Microwave Physics Laboratory of AFCRL, MITHRAS, Inc., has conducted a study of aerodynamic methods of creating radio windows through the plasma sheath surrounding a re-entry vehicle. In the course of this study, two techniques have been develcped. One uses jets of coolant from flush nozzles which penetrate across the layer of ionized flow and then mix with it as they are carried downstream. The other uses a physical flow diverter to bypass some of the ionized flow laterally around the antenna. The region of separated flow behind the flow diverter, through which the antenna looks, is kept cool by low-velocity coolant injection.

2. SUMMARY AND CONCLUSIONS

The plasma sheath properties on typical re-entry vehicle shapes have been investigated by treating the sheath as a homogeneous slab bounded by free space. Typical shapes for which the attenuation of a 200 Mc. signal was determined during re-entry are the cone, the flat plate, and a blunt nosed body.

Two aerodynamic methods of creating transmission "windows" in the plasma sheath have been investigated; (1) the use of jets of coolant from flush nozzles which penetrate across the plasma slab and then mix with it as they are carried downstream, (2) the use of a physical flow diverter to bypass some of the ionized flow laterally around the antenna. Equations were developed for the lateral jet penetration in a supersonic stream and for one-dimensional mixing for both perfect gases and real gases in thermodynamic equilibrium. Charts of coolant required to achieve transmission of a 200 Mc. signal on typical vehicles were derived.

Finally, the effect of the use of a side jet on the vehicle aerodynamics was briefly investigated.

The results of the above summarized investigations have led to the following conclusions with regard to the problem of achieving a transmission "window" in a plasma sheath.

(1) With the approximation of thermodynamic equilibrium, transmission losses at 200 Mc are negligible for temperatures below 3000°K at all pressures of interest.

(2) If it is assumed that an average transmitting frequency for re-entry vehicles is in the 200 megacycles range and the plasma thickness is 0.2 ft., then transmission is possible,

(a) for a cone only if $M_\infty \sin \theta_c \leq 6$

(b) for a flat plate only if the angle of attack and wing loadings are low

(c) for a blunt body only far back on the body.

(3) Jet penetration across the entire shock layer at typical antenna installations may be achieved with practical nozzle geometries and coolant supply pressures.

(4) The jet method can reduce the plasma temperature to levels at which transmission is possible with modest jet mass flows.

(5) The assumption of real-air equilibrium thermodynamics yields coolant requirements considerably below the perfect-gas values for the jet injection method.

(6) The effects of the side jet on the re-entry vehicle aerodynamics are slight, typically causing a trim angle-of-attack less than one degree.

(7) The use of a physical flow diverter is not an effective method of creating a transmission window where the ionization layer is not adjacent to the vehicle surface or where the attenuation needs to be reduced more than 10 db.

3. PLASMA SHEATH PROPERTIES ON TYPICAL VEHICLES

3.1 Transmission Through a Plasma Sheath

The electromagnetic wave incident on a boundary such as the discontinuity in going from an antenna surface to an ionized flow field reflects some energy at the surface and transmits some energy. This problem may be simplified by considering only normally incident waves. If the plasma slab is considered bounded on both sides by free space and considered homogenous rather than containing the high temperature and density gradients generally surrounding a hypervelocity vehicle, further mathematical simplifications are possible.

When an electromagnetic wave is imposed upon a medium containing free electrons such as a plasma, each electron may be considered to act as a miniature antenna and to absorb energy from the wave. Since the electron is accelerated by the electric field, the energy of the wave may be thought of as being converted into energy of the electrons. This conversion of energy results in a decrease of signal strength through reflection and absorption effects. A tractable expression for the attenuation in transmitting through a plasma sheath can be derived by solving Maxwell's equations and the equations of motion for the electrons in this field. Plane-wave solutions to Maxwell's equations for homogenous media, for the case of a bounded plasma shown in Figure 3.1, were presented in Reference 1. This theory was used to calculate transmission losses through a plasma sheath since analyses involving more mathematical rigor are extremely laborious and many times present insolvable expressions. In view of other related uncertainties (i.e. non-equilibrium effects, viscous interactions, and electron-heavy particle collision cross-section) such rigor is not clearly warranted. For example Figure 3.2, taken from Reference 2, shows approximately a 35 db difference in transmitting through a bounded plasma slab when a non-equilibrium rather than an equilibrium gas flow field is assumed.

This change due to the selected gas model is significantly greater than what one would expect if more complex plasma models were chosen.

The solutions for a bounded plasma slab in terms of signal attenuation as a function of plasma frequency, ω_p, collision frequency, ω_c, and signal frequency, ω, for thickness, δ, of 0.1 ft. and 0.2 ft. are presented in Figure 3.3. This figure illustrates the relative importance of the various parameters over the range of interest for re-entry vehicles. The 3 db attenuation line was chosen as a reasonable blackout limit.

3.2 Plasma Sheath Properties Related to Flow

The solutions shown in Figure 3.3 for a plane wave in passing through a plasma slab, if an equilibrium gas is assumed, show that the attenuation of a signal is a function only of the following four variables;

ω signal frequency

ω_p plasma frequency

ω_c electron collision frequency

δ plasma thickness

In turn, in the case of an equilibrium gas, both the plasma frequency and the collision frequency are solely a function of the state properties of the gas. Once these properties are known the attenuation resulting in transmitting through a plasma sheath with a given signal frequency and plasma thickness can be solved for.

The relations describing the plasma and collision frequencies are as follows:

$$\omega_p = 56.4 \sqrt{N_e} \quad \text{RAD/SEC} \tag{3.1}$$

N_e = electron/meter ^{3}

$$\omega_c = \bar{c} \; \Sigma \; N_j \; Q_j \tag{3.2}$$

$\bar{c}$ = average velocity of electron

N_j = concentration of j^{th} species

Q_j = electron cross-section of j^{th} species

The estimate for the electron cross-section has been taken from Reference 3 and results in the following formula for the collision frequency:

$$\omega_c = 5.0 \cdot 10^{12} \; \frac{P}{T} \tag{3.3}$$

T = °K

P = ATM

The electron density for real air can be determined from Feldman [4]. Lin's curves [4], however, can be approximated to within a factor of 2 by the following empirical formula from Reference 3.

$$N_e = 1.87 \cdot 10^{20} \left(\frac{P}{P_o}\right)^{0.6} \left(\frac{T - 1400}{3500}\right)^{8.7} \tag{3.4}$$

$$1800 < T\,°K < 7000$$

$$10^{-6} < \left(P/P_o\right) < 10$$

For the same range of conditions the density ratio can be approximated by,

$$\log_{10}\left(\frac{P}{P_o}\right) = \log_{10}\left(\frac{P}{P_o}\right) - \frac{T^\circ K}{6000} - 0.6 \qquad (3.5)$$

By using equations 3.1 through 3.5 plus the relations describing the attenuation of a signal passing through a bounded plasma slab with the assumption of a constant signal frequency and plasma thickness, the attenuation may be found as a function of pressure and temperature.

For illustrative purpose a signal frequency of 200 megacycles and plasma thickness of 0.1 ft. and 0.2 ft. were chosen for the results presented in Figure 3.4 through 3.7, and throughout this study. These figures describe the temperature criteria necessary for cooling sufficiently to prevent blackout. It is seen that, if the local flow over an antenna is cooled to approximately 3000° K, and equilibrium is achieved, transmission is clearly possible. The use of electrophilic gases in combination with an injected coolant would allow a further decrease in attenuation which is not shown in these figures.

3.3 Example of Basic Configurations

In order to establish the magnitude of the problems of transmitting through a plasma sheath, several basic configuration shapes were chosen for comparison. No specific vehicle has been chosen for analysis since it is felt that a flexibility of choice of the vehicle should be maintained so that the results of the study may have the broadest application possible. With this in mind, a few basic vehicle shapes which could in composition make up a more complex vehicle shape were studied. The shapes studied were a cone, a flat plate at angle-of-attack and a blunt body.

The total attenuation of a 200 Mc. signal transmitted through a 0.1 ft. and 0.2 ft. plasma slab on these various bodies was taken as a realistic example of interest in the study. As will become evident in section 4.3, the local velocity in the region of the plasma is a most significant parameter in

the injection of a coolant to reduce attenuation.

3.3.1 Cones

For the data dealing with cones, no specific trajectories are required as the plasma frequency on cones may conveniently be related to the hypersonic similarity parameter, $M_\infty \sin \theta_c$, as suggested by Romig (Reference 5).

The various flow properties on the surface of a cone as related to $M_\infty \sin \theta_c$ are presented in Figures 3.8 through 3.11. The density and temperature plots (Figures 3.8 and 3.9) along with the relations of section 3.2 allow the calculation of plasma frequency and collision frequency as presented in Figure 3.12. The shock layer thickness may be determined from the shock wave angle as defined in Figure 3.10. The cone surface velocity presented in Figure 3.11, as pointed out previously, is an important parameter when the injection of a coolant is considered.

The relationship of total attenuation of a 200 Mc signal through a 0.1 ft and 0.2 ft bounded plasma for a cone at an altitude of 210,000 ft as a function of the hypersonic similarity parameter is presented in Figure 3.13. This figure was derived from the plasma and collision frequency data of Figure 3.12, and used in conjunction with the bounded plasma attenuation data of Figure 3.3. Note the close relationship between the shape of the total attenuation curve of Figure 3.13 and the shape of the plasma frequency curve of Figure 3.12. Bearing this similarity in mind, and observing that transmission is possible at 210,000 ft for cones if $M_\infty \sin \theta_c \leq 10$, then it may be concluded that transmission of a 200 Mc signal is possible down to 55,000 ft altitude for cones of plasma thickness on the order of 0.2 ft and $M_\infty \sin \theta_c \leq 6$.

3.3.2 Flat Plate

Data computed for a flat plate was derived by assuming that a body, one of whose surfaces was a flat plate, followed an equilibrium glide trajectory at an angle of attack for maximum C_L. This configuration was chosen as the two-dimensional flat plate pressures are applicable to the under

surface of a flat-bottomed body, delta wing, etc. For computational purposes the shock wave angle was assumed constant at 53° 44'. The calculated trajectories for different values of $W/C_L A$ are shown in Figure 3.14 and the surface velocities on the plate are presented in Figure 3.15.

The plasma frequencies for varying $W/C_L A$ are presented in Figure 3.16. Figure 3.17 shows the trend of plasma and collision frequencies with $W/C_L A$ for the specific altitude of 210,000 ft. The attenuation as a function of $W/C_L A$ for 210,000 ft altitude, a transmission frequency of 200 Mc and plasma thickness of 0.1 ft and 0.2 ft is presented in Figure 3.18. Note the similarity between this figure and Figure 3.13 which presented the attenuation on a cone for the same conditions. The strong function of attenuation with $W/C_L A$ is evident in Figure 3.18. A low $W/C_L A$, or a low wing loading lowers the attenuation rapidly on a flat plate as would be expected since this has the effect of dissipating the kinetic energy of the body in a region of low density and therefore small electron concentration.

3.3.3 Blunt Body

Pressures on a blunted, hemisphere cylinder are given by the following equation from Reference 6:

$$\frac{P_x}{P_\infty} = \frac{f(\gamma) M_\infty^2 C_D^{1/2}}{X/D} + 0.44$$

This equation has been derived for equilibrium air at speeds consistent with blast wave theory. The formula has been compared with experimental equilibrium gas flows and found to be in good agreement (Reference 6).

P_x is surface pressure along body

$f(\gamma)$ is a tabulated function of the isentropic exponent at the stagnation region

C_D = 0.097 drag coefficient for hemisphere cylinder

X/D is a body station non-dimensionalized with respect to hemisphere nose diameter

Equilibrium gas properties at the stagnation point are derived from equilibrium normal shock tables and then an isentropic expansion (i.e., body streamline) is traced on a Mollier chart to the calculated body pressure. Equilibrium properties are then read off.

Since the additional variables of a non-uniform flow field with distance from the nose is added in the case of a blunt body a specific flight condition has been chosen as an example. The conditions chosen are V = 25.000 ft/sec and h = 250,000 ft. The surface velocity variation with body location, X/D, is presented in Figure 3.19. The plasma frequency calculated with the aid of Reference 6 is presented in Figure 3.20 along with the plasma frequency and collision frequency data of Reference 7. The attenuation as a function of X/D is presented in Figure 3.21. Note that for the example chosen an antenna would have to be located about 100 body diameters aft of the nose for suitable transmission at 200 Mc.

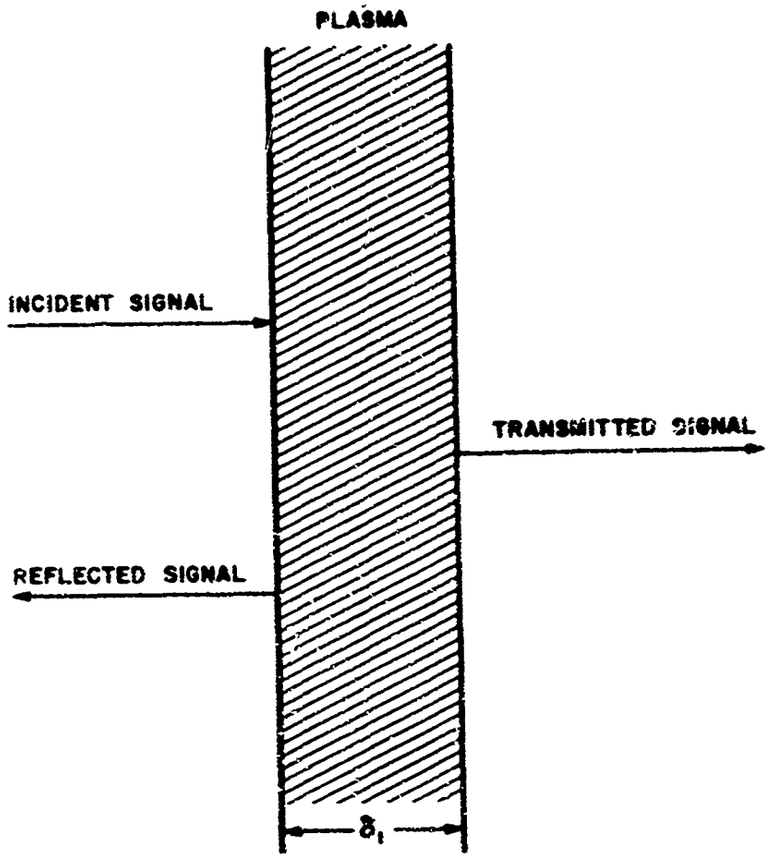

Figure 3.1. Bounded plasma

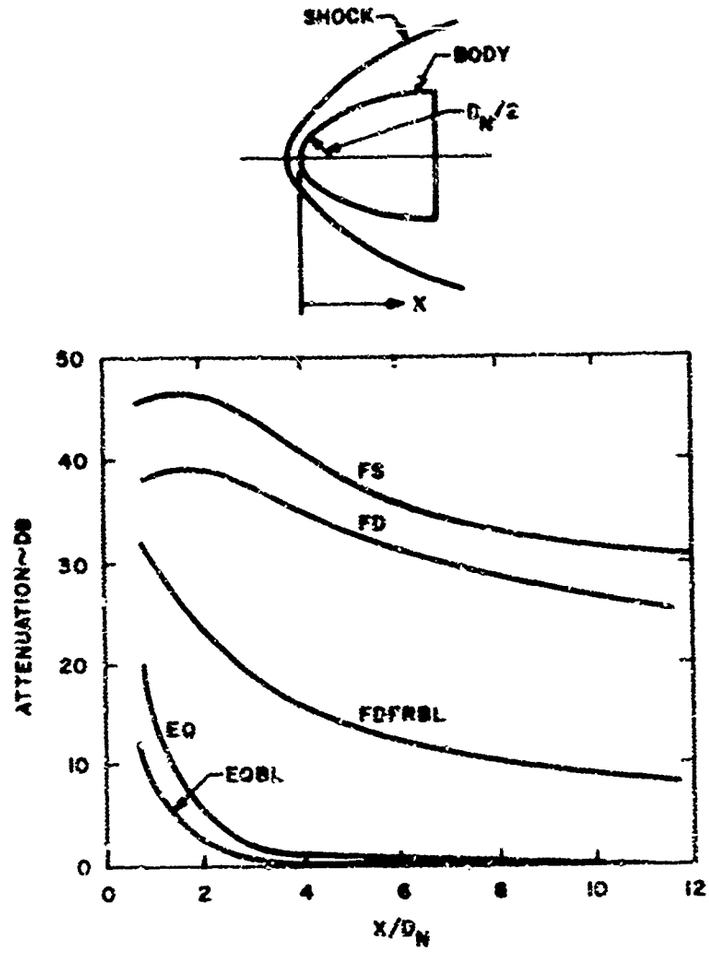

FS — Flow field in which chemical and ionic reaction rates vanish downstream of shock wave, but shock is at equilibrium.

FD — Flow field in which chemical reaction rates vanish downstream of freeze point on each streamline.

FDFRBL — Same as FD but with boundary layer corrections to temperature, density, and velocity and also with allowance for finite rate recombination of electrons along streamlines.

EG — Flow field in which chemical and ionic reactions are everywhere in equilibrium.

EQBL — Same as EQ but with boundary-layer corrections to temperature and density.

Figure 3.2. Attenuation on a blunt body versus distance for various assumed flow fields.

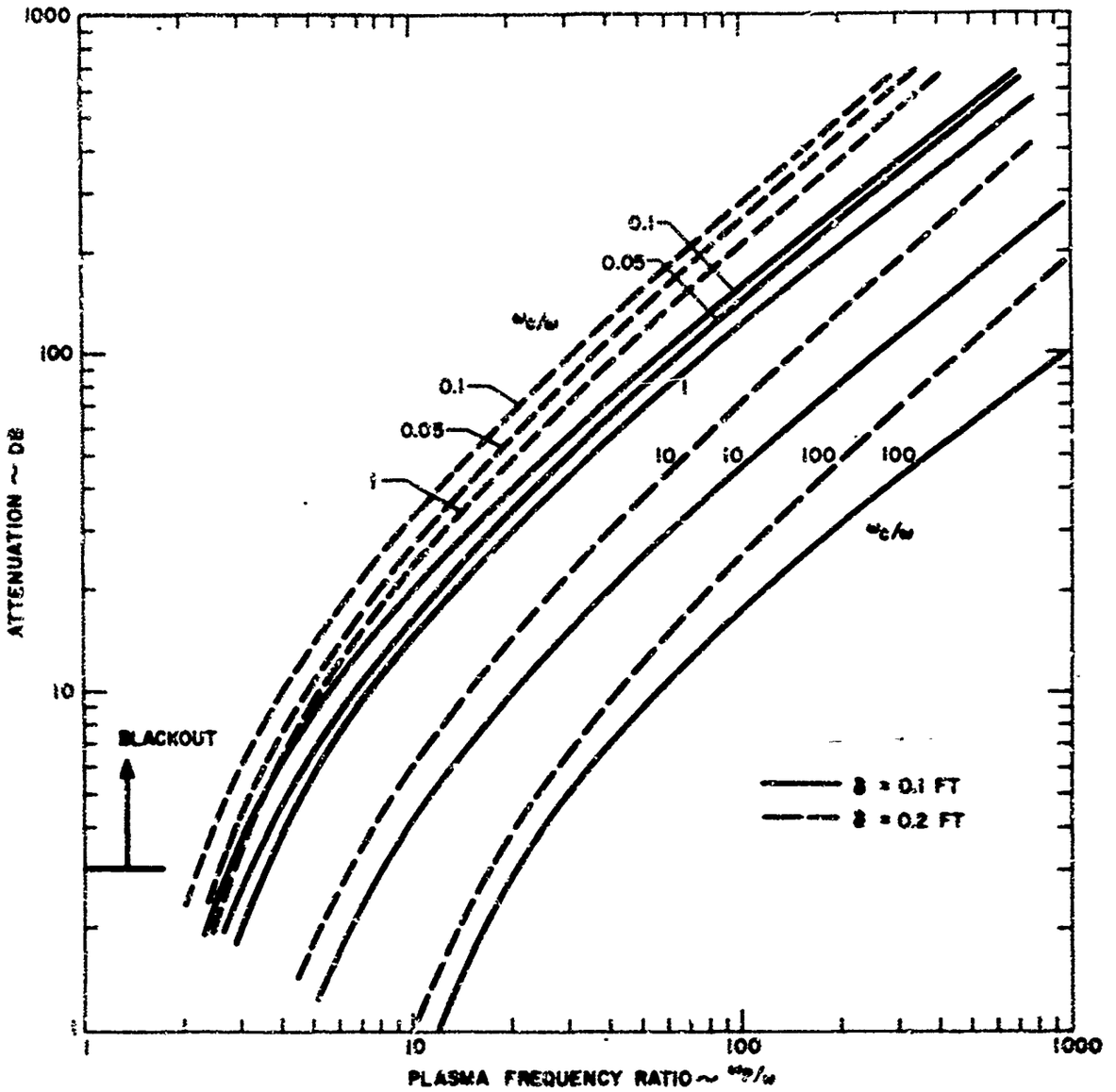

Figure 3.3. Variation of attenuation with plasma frequency ratio and collision frequency ratio for a bounded plasma.

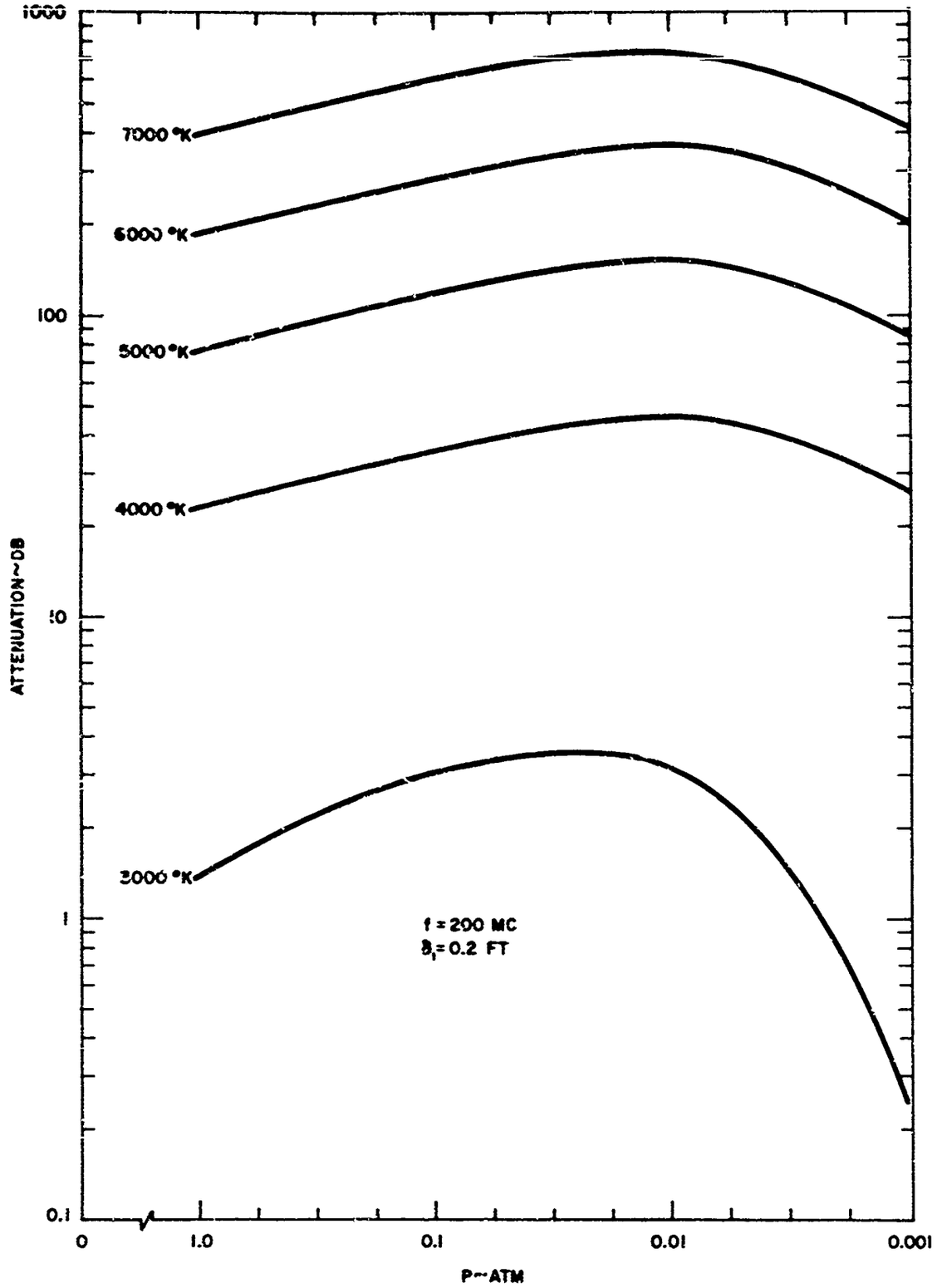

Figure 3.4. Attenuation as a function of pressure and temperature for a plasma thickness of .2'.

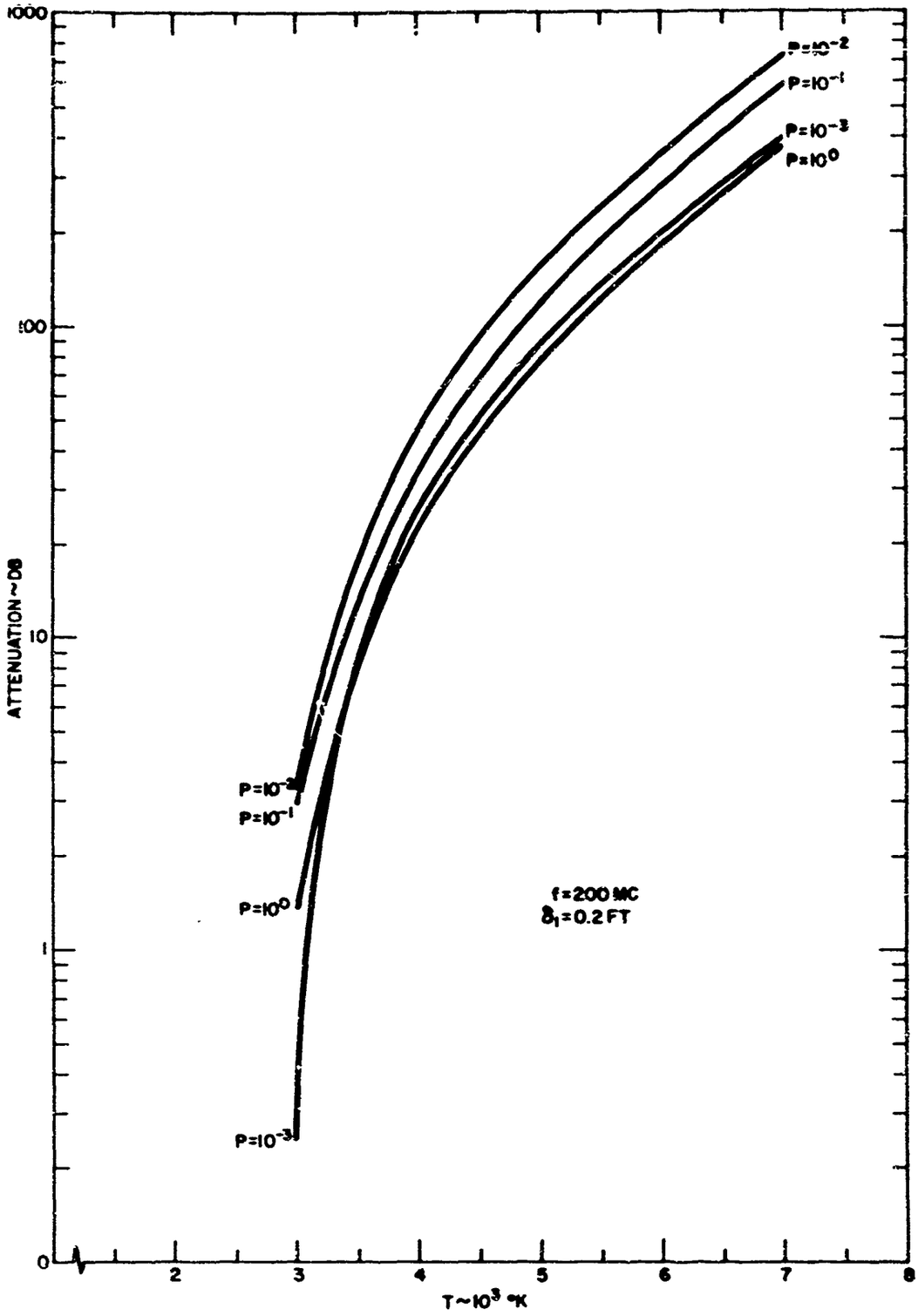

Figure 3.5. Attenuation as a function of pressure and temperature for a plasma thickness of .2'.

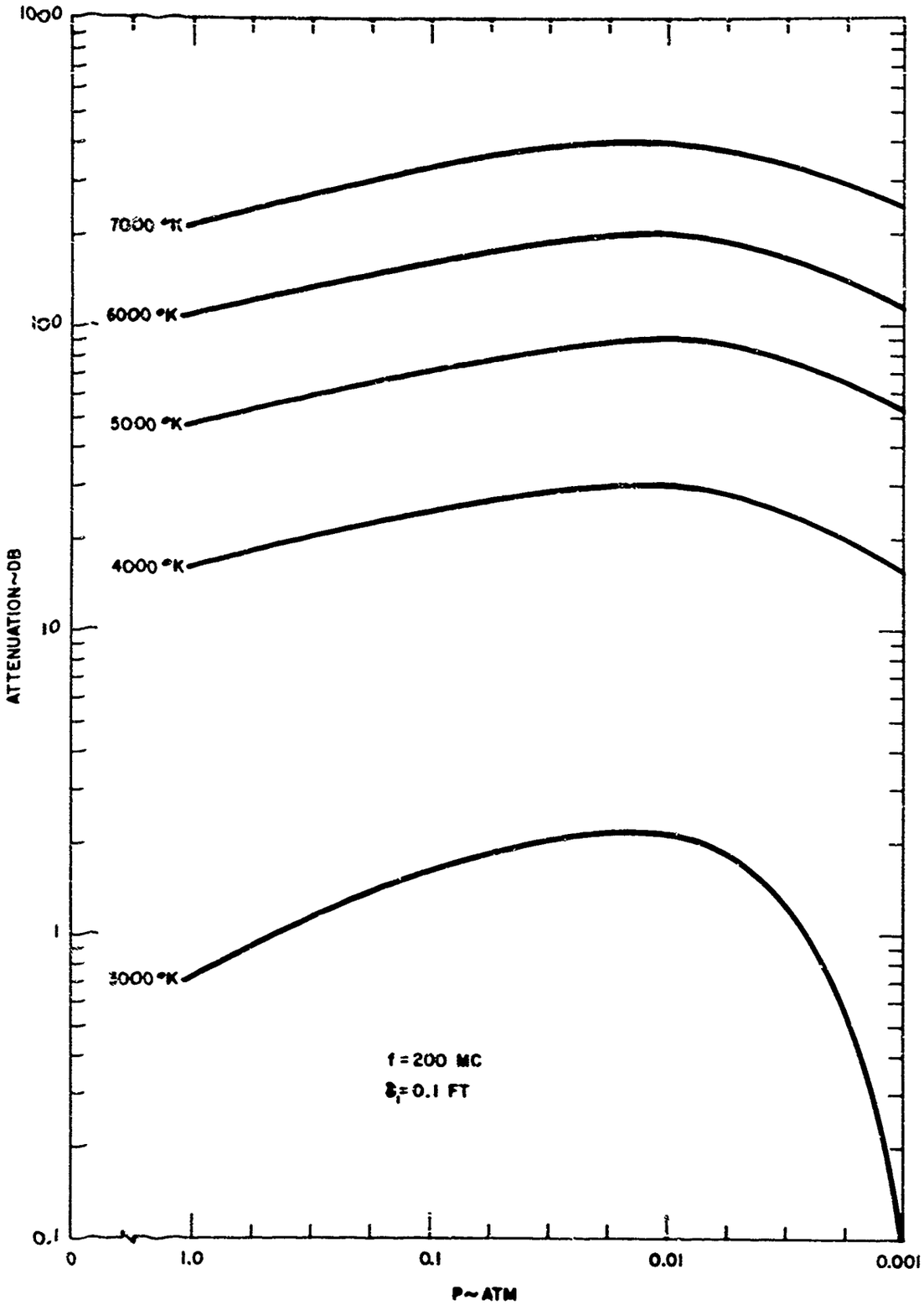

Figure 3.6. Attenuation as a function of pressure and temperature for a plasma thickness of .1'.

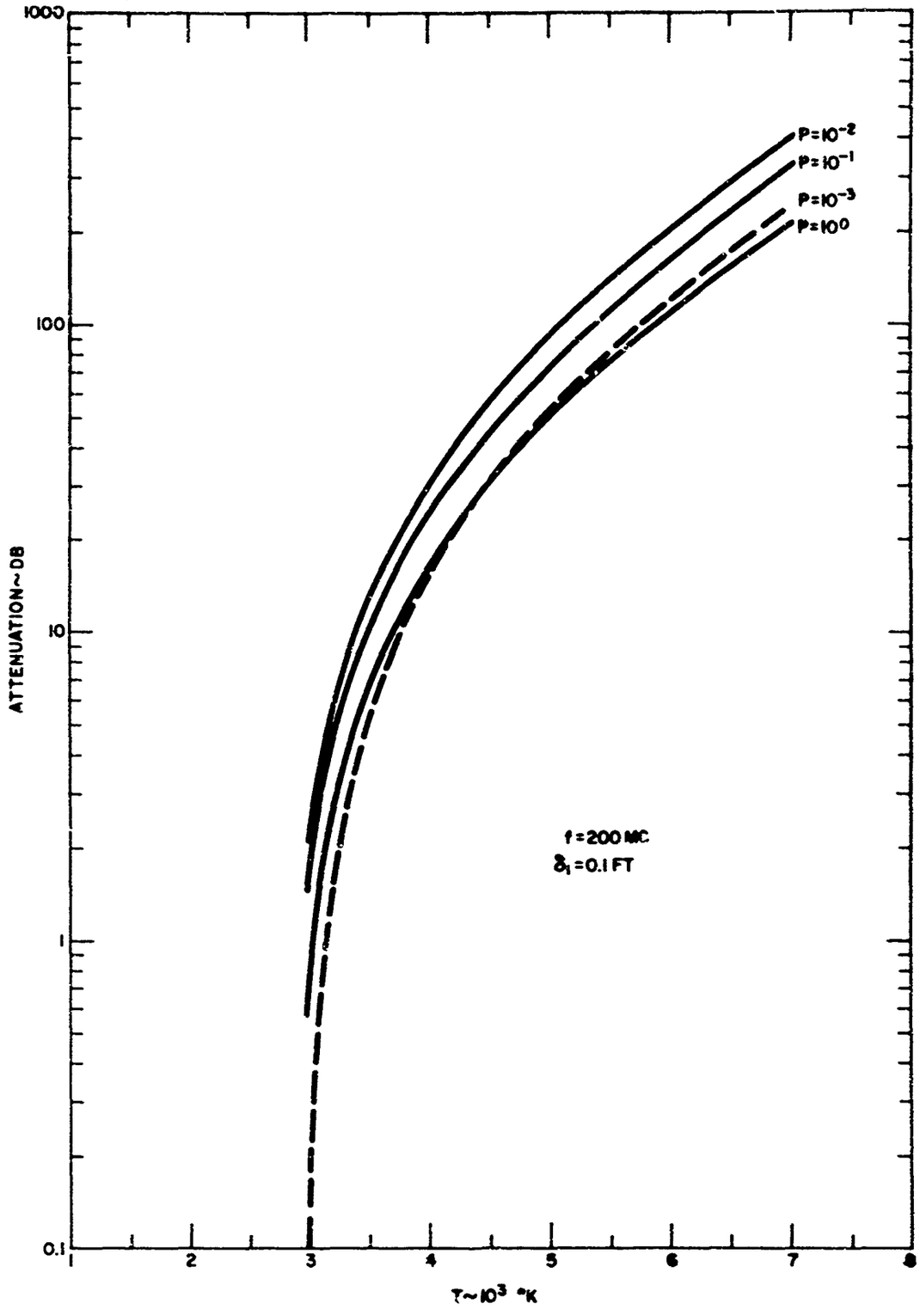

Figure 3.7. Attenuation as a function of pressure and temperature for a plasma thickness of .1'.

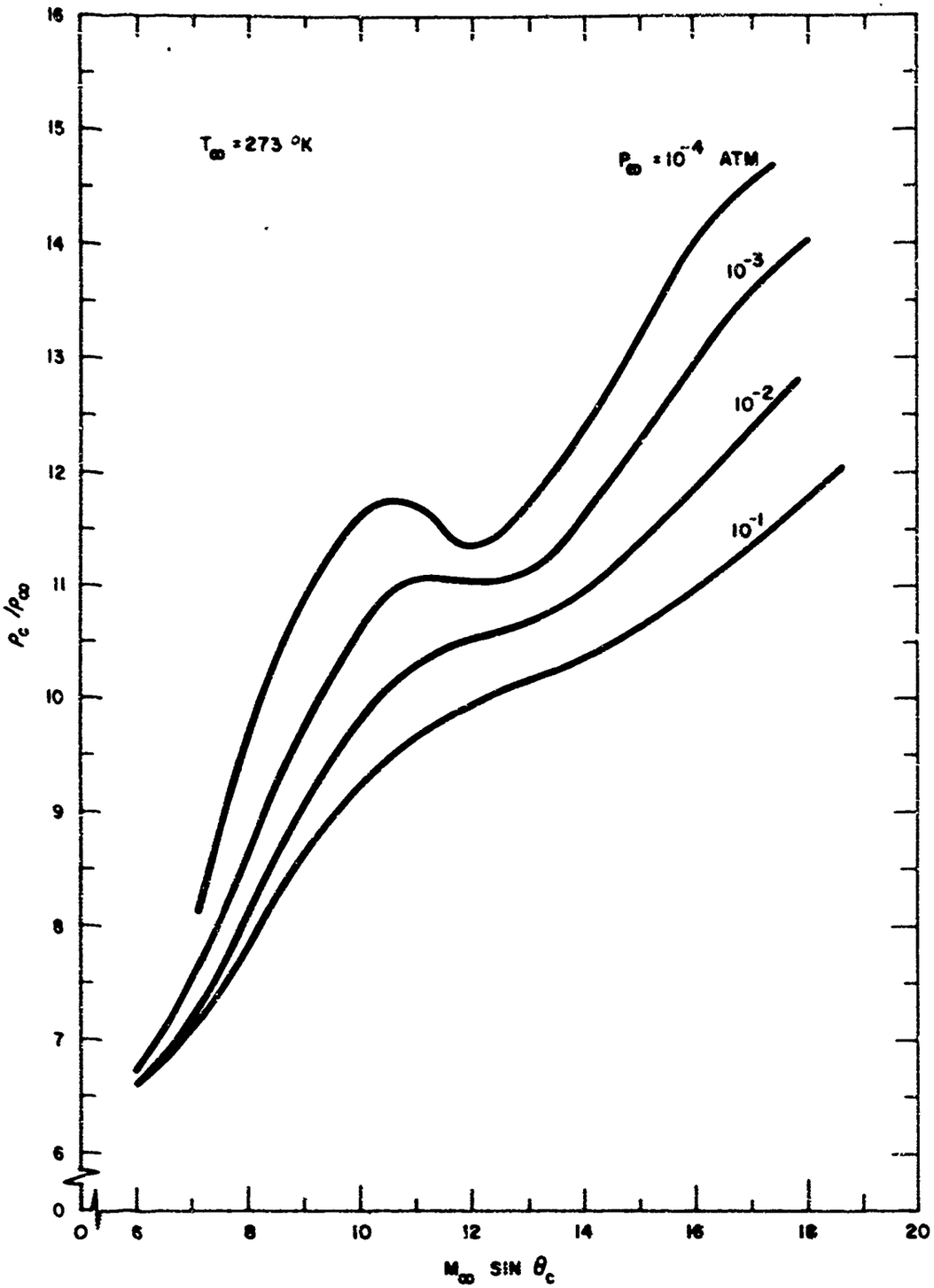

Figure 3.8. Ratio of cone surface density to free stream density versus hypersonic similarity parameter.

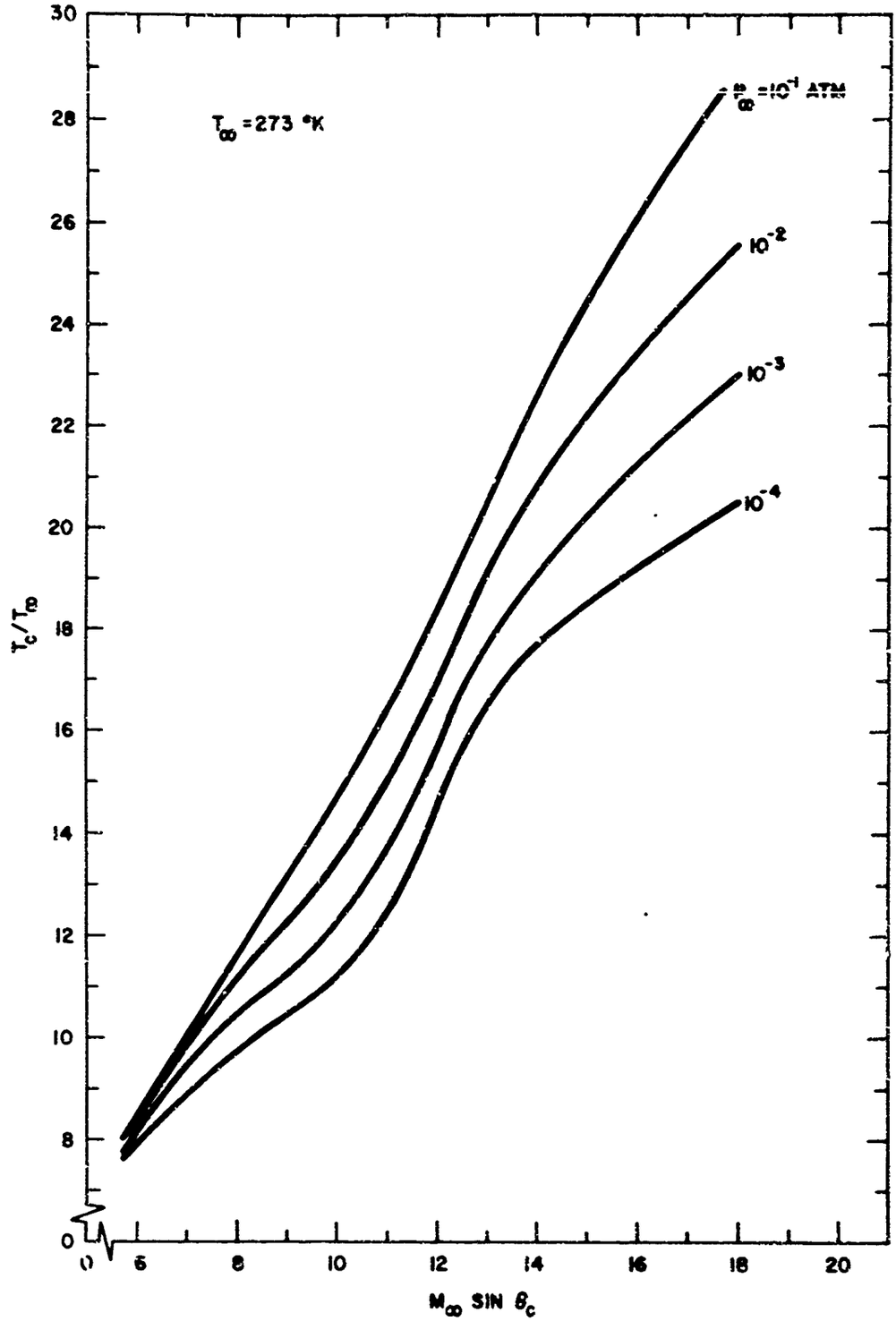

Figure 3.9. Ratio of cone surface temperature to free stream temperature versus hypersonic similarity parameter.

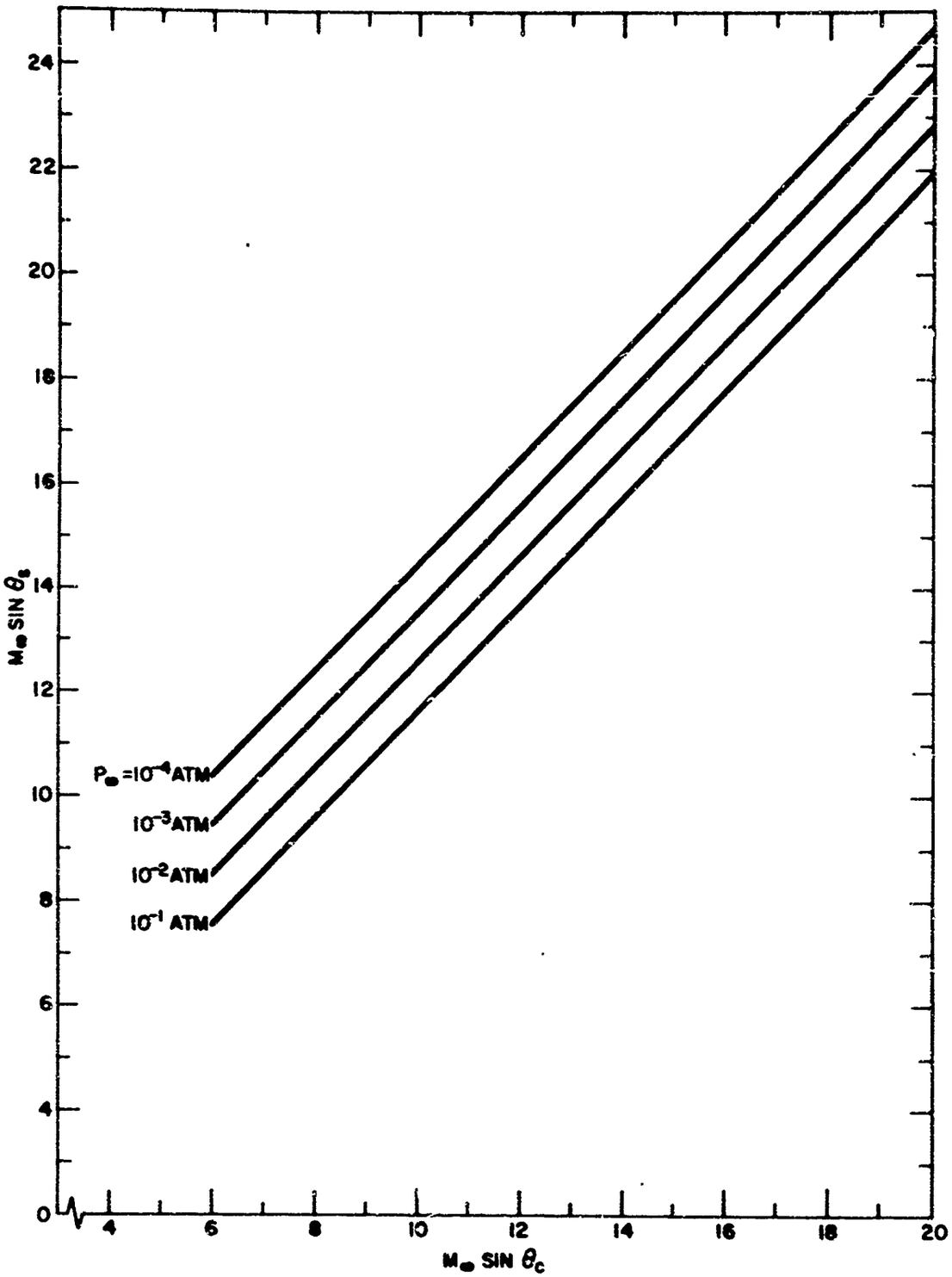

Figure 3.10. Cone shock wave angle versus hypersonic similarity parameter.

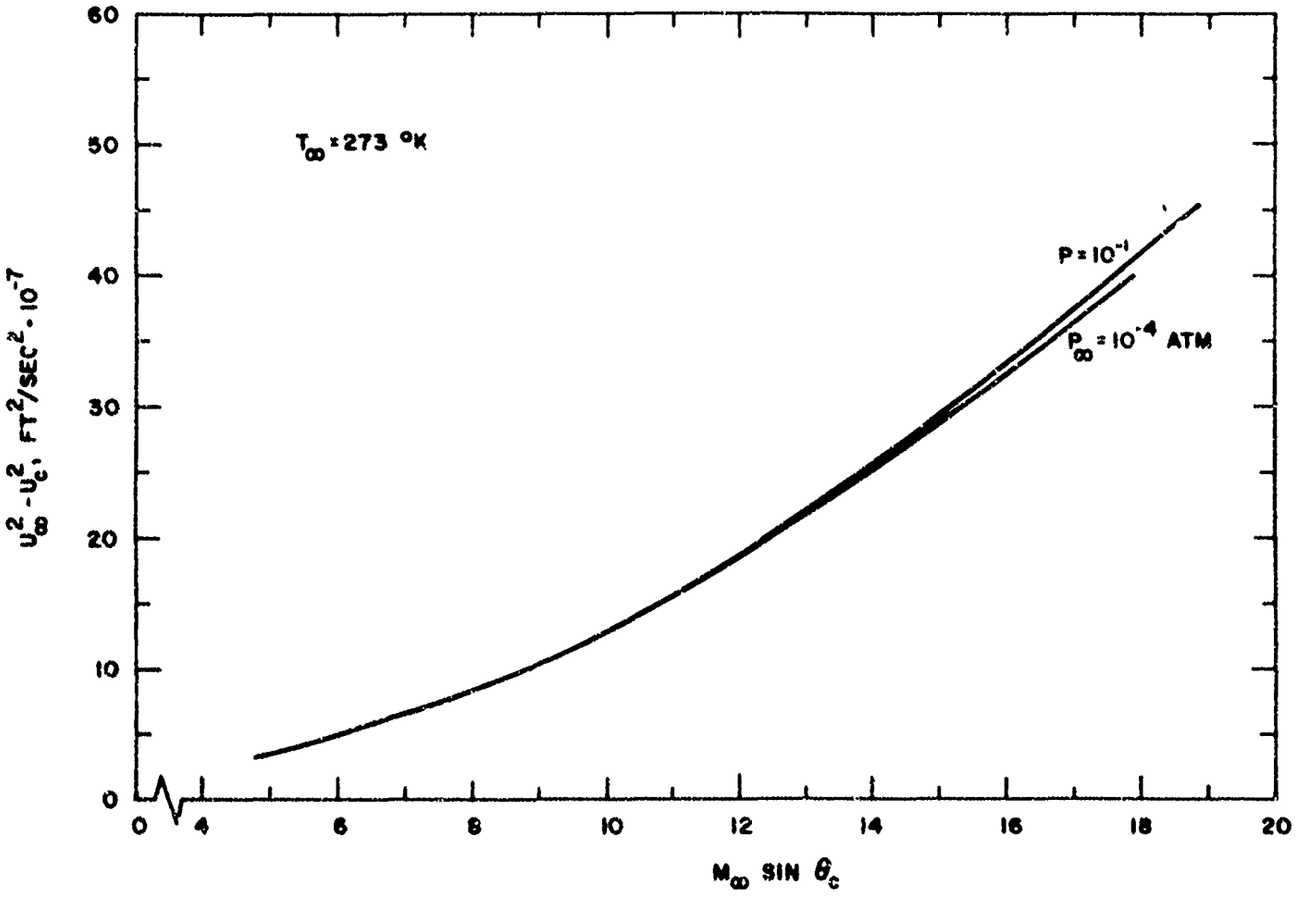

Figure 3.11. Cone surface velocity versus hypersonic similarity parameter.

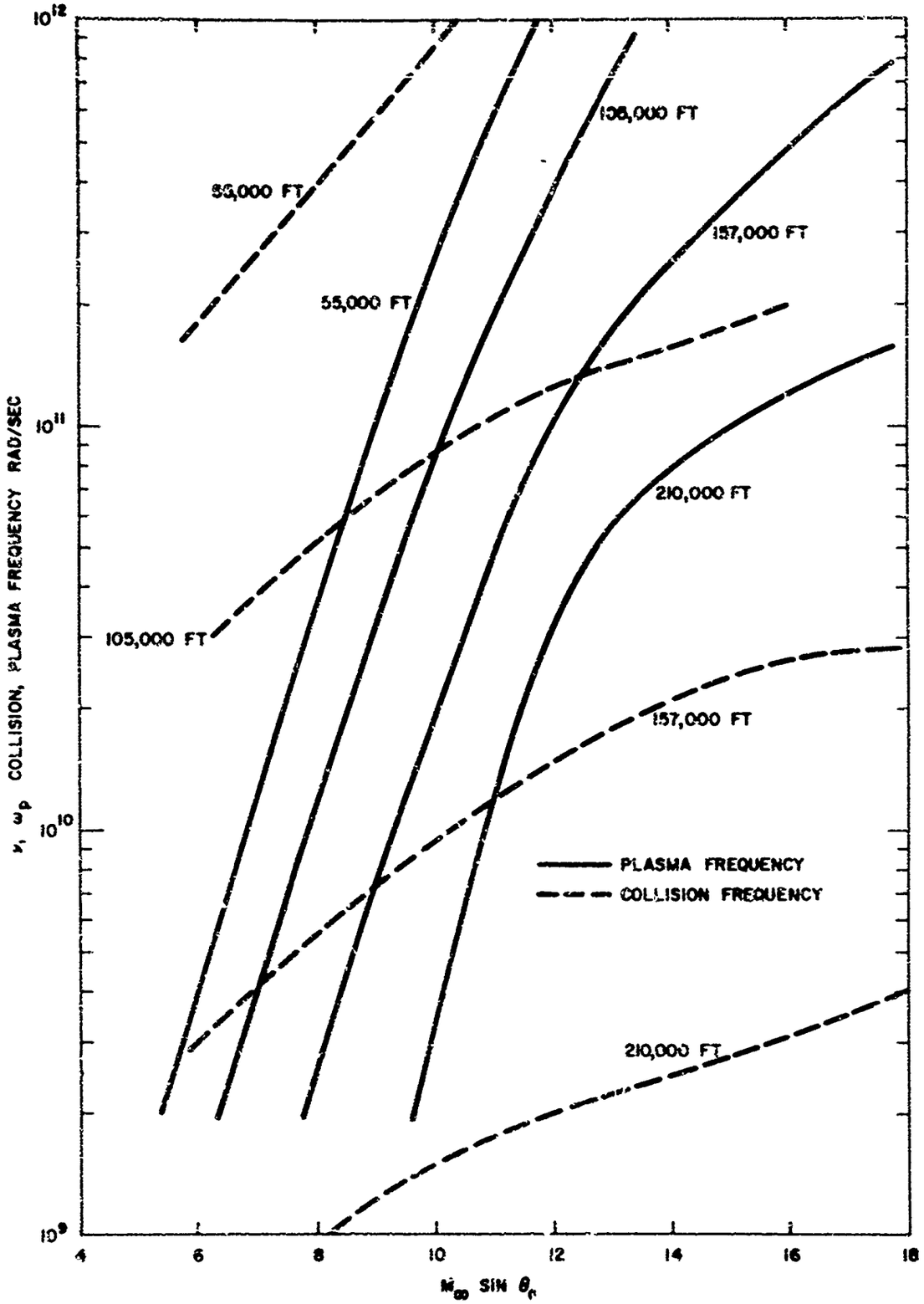

Figure 3.12. Plasma and collision frequencies as a function of the cone hypersonic similarity parameter.

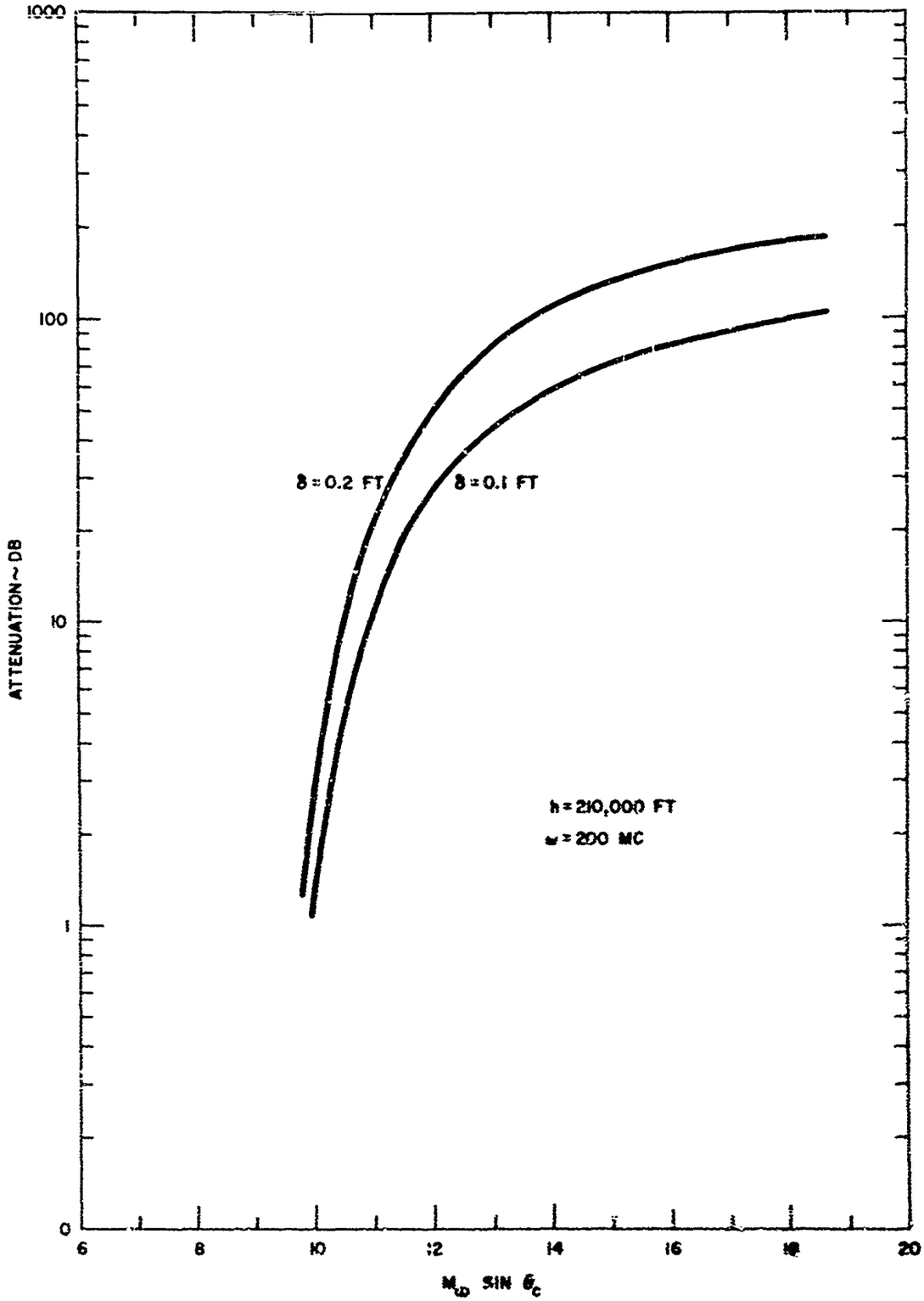

Figure 3.13. Attenuation as a function of the cone hypersonic similarity parameter for a plasma thickness of .1' and .2'.

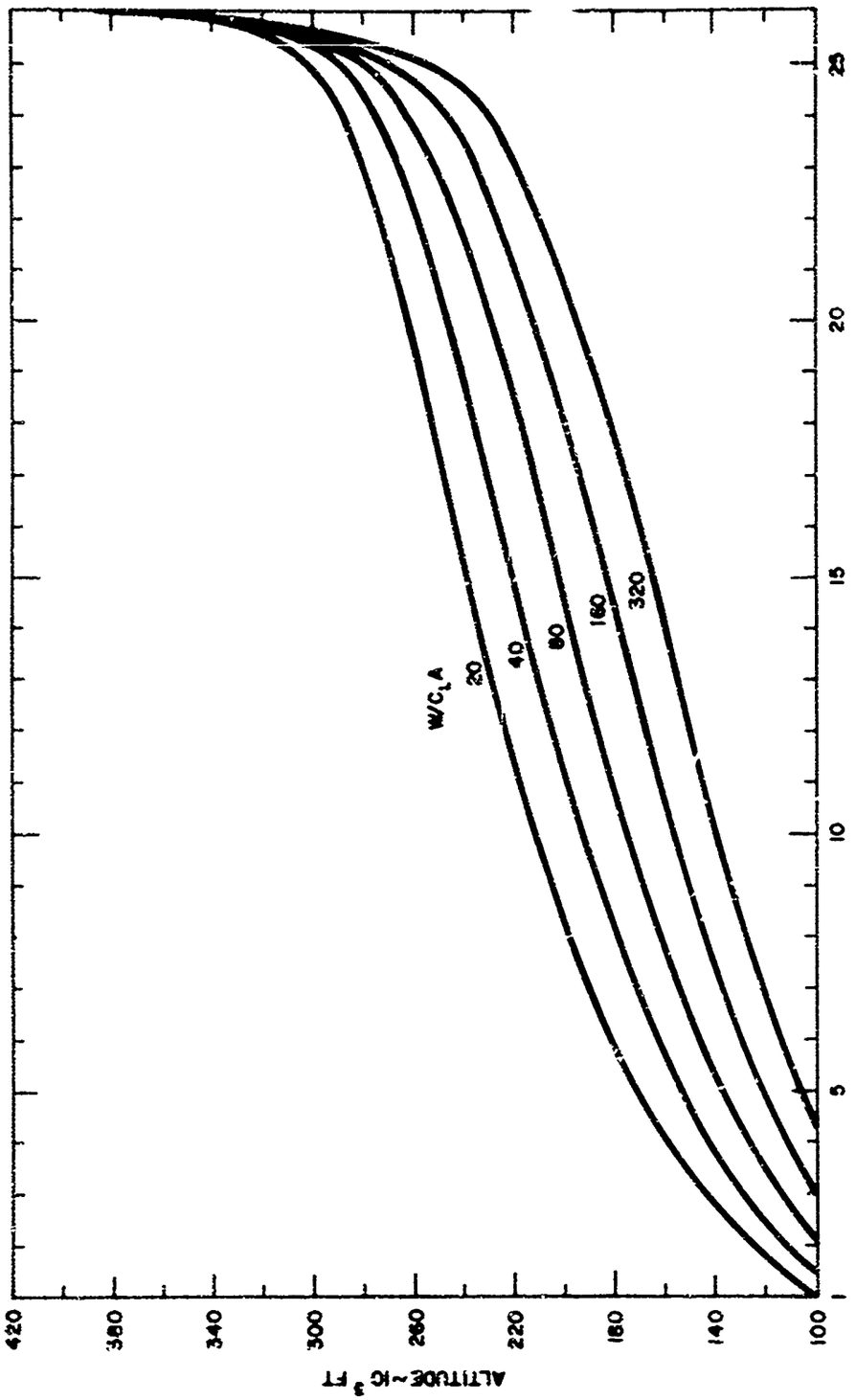

Figure 3.14. Equilibrium glide trajectories

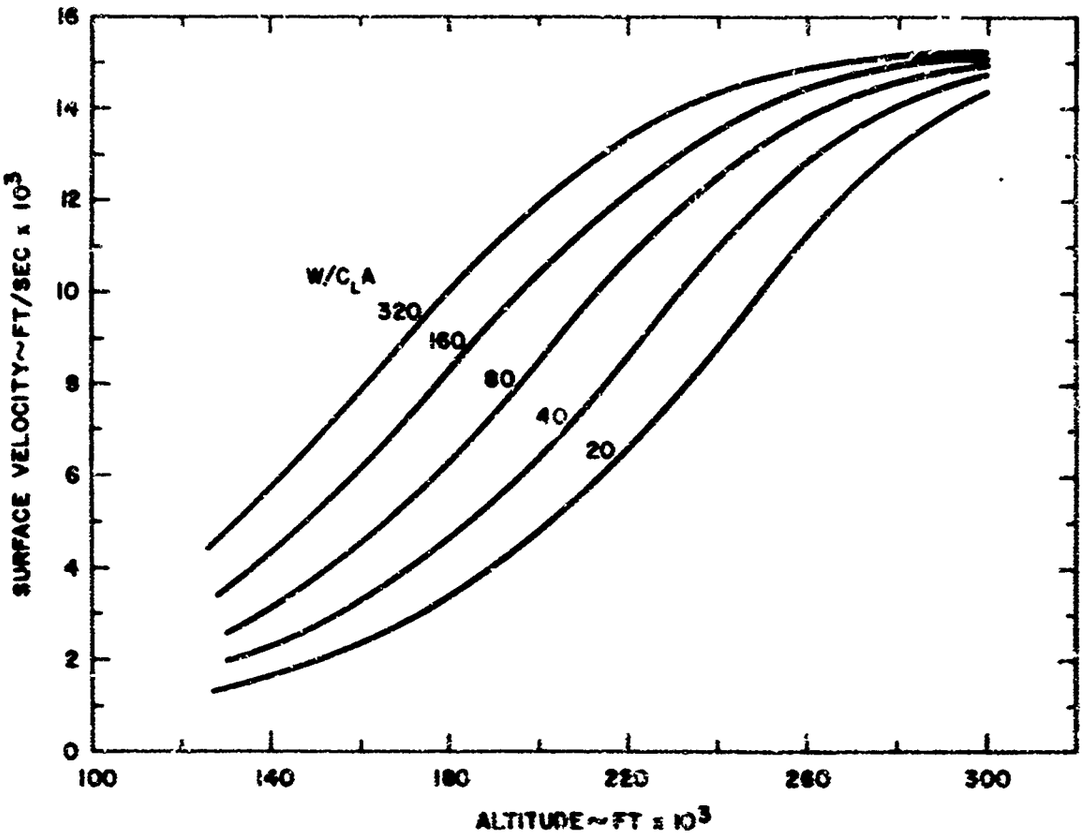

Figure 3.15. Surface velocities for equilibrium glide trajectories.

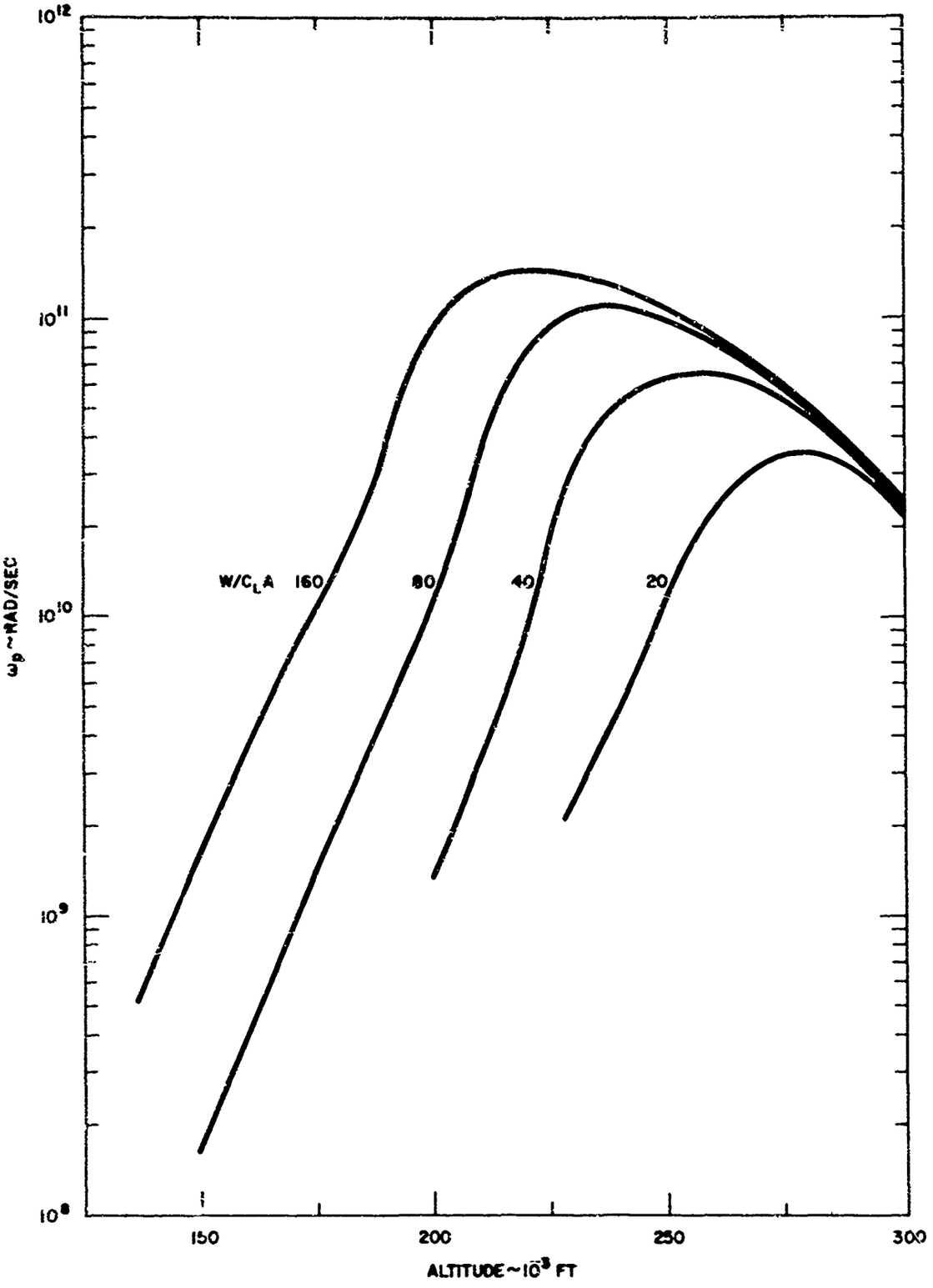

Figure 3.16. Equilibrium glide plasma frequency versus altitude.

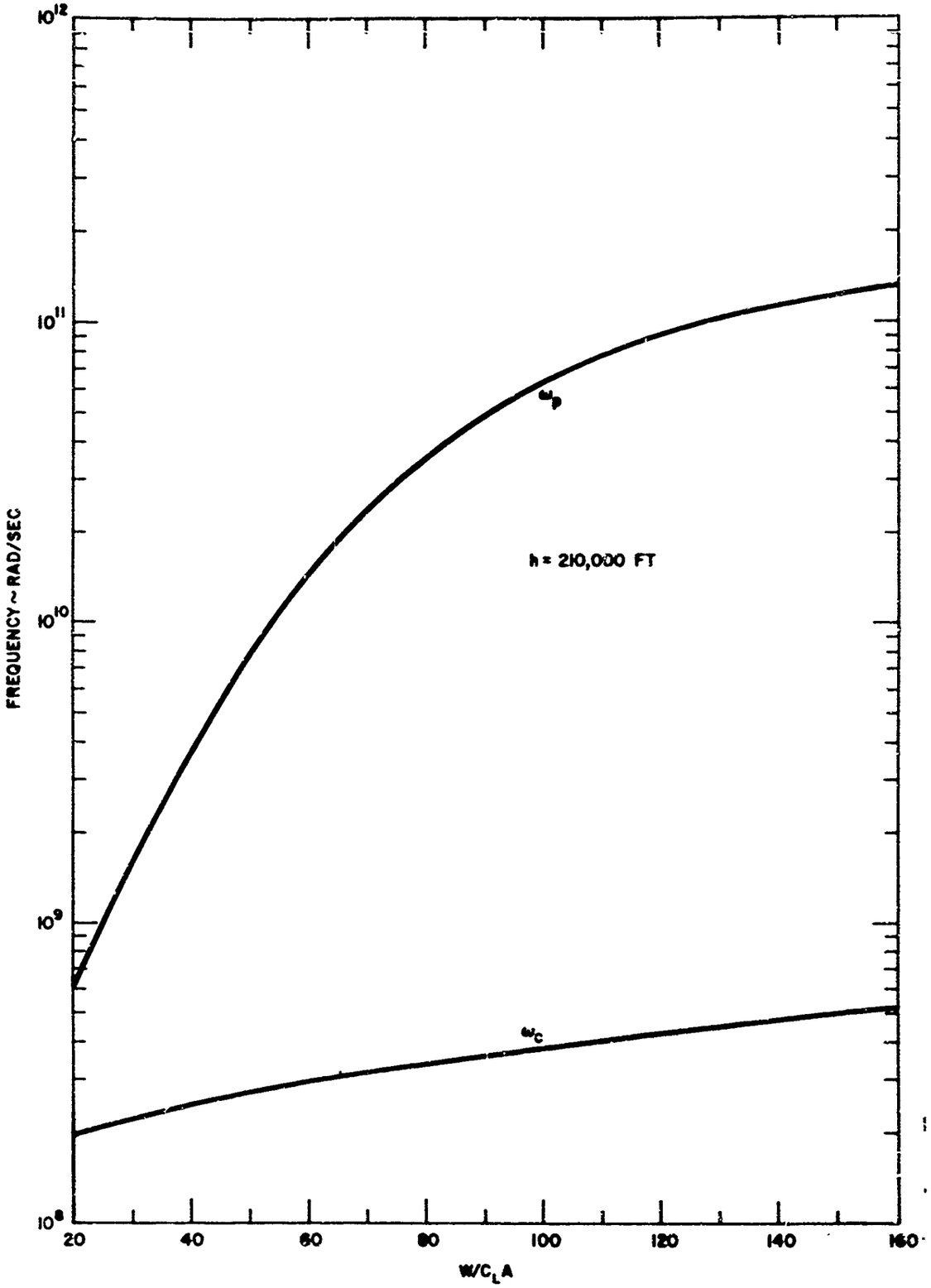

Figure 3.17. Plasma and collision frequencies versus the equilibrium glide parameter.

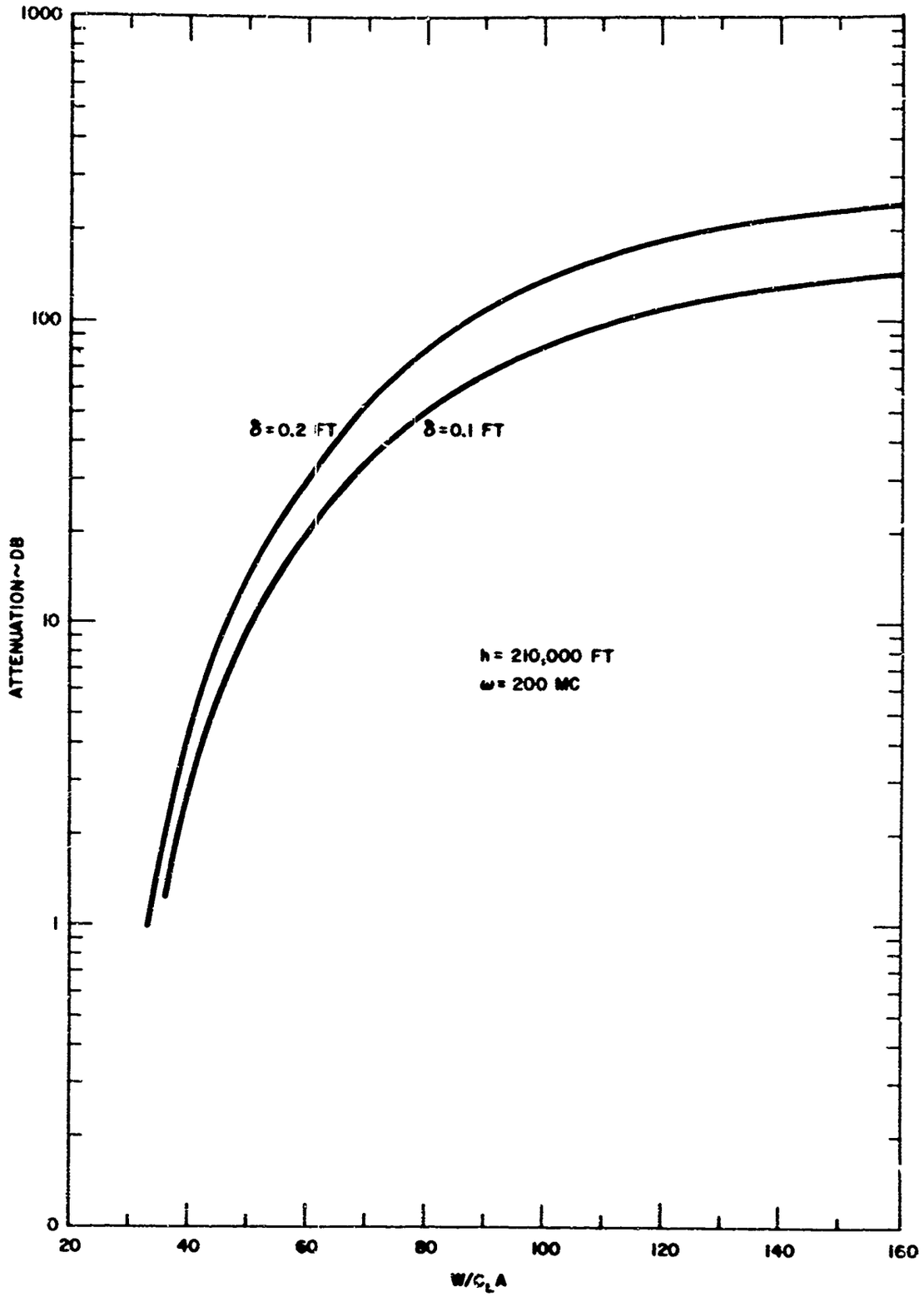

Figure 3.18. Attenuation versus the equilibrium glide parameter for a plasma thickness of .1' and .2'.

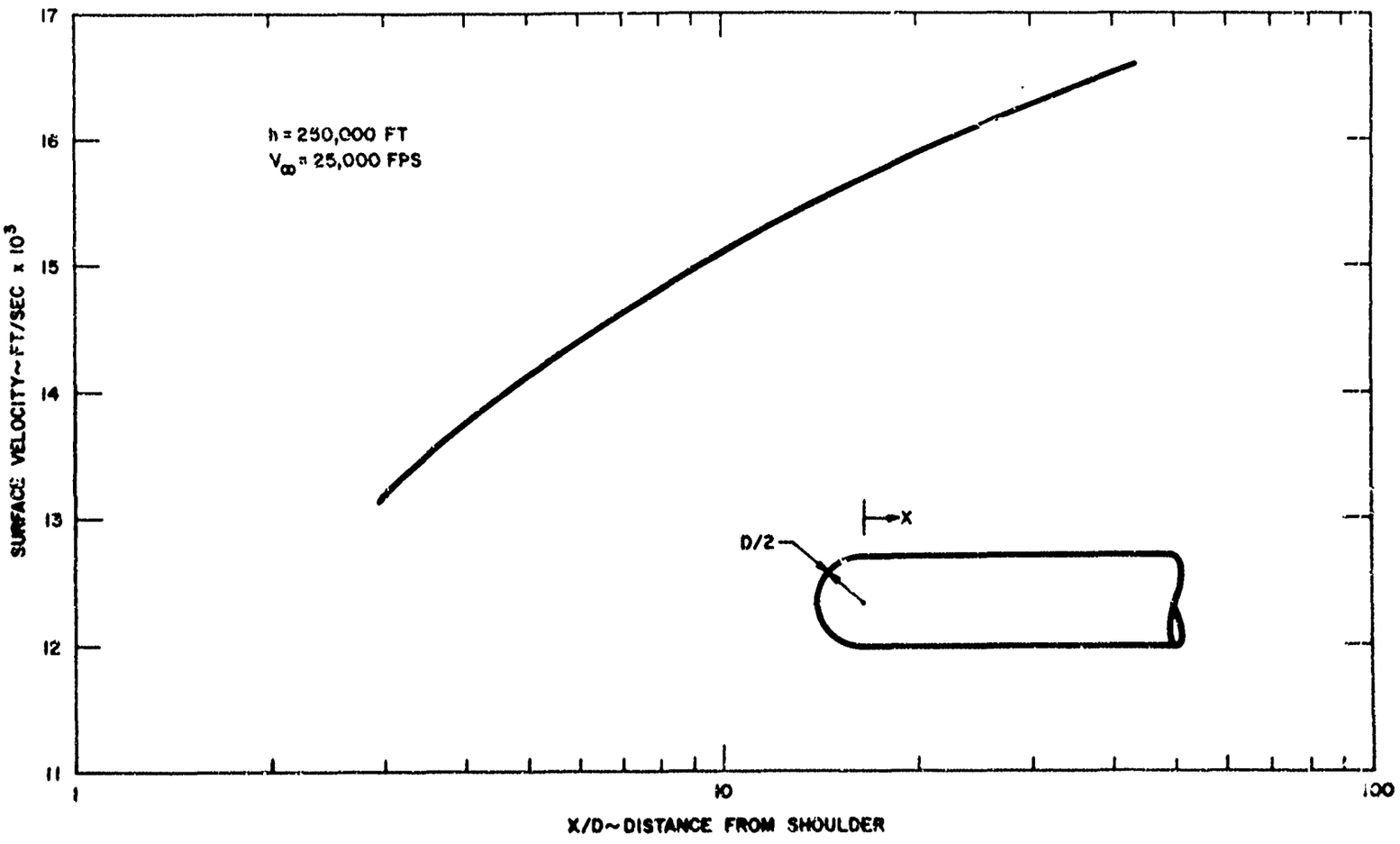

Figure 3.19. Blunt body surface velocity.

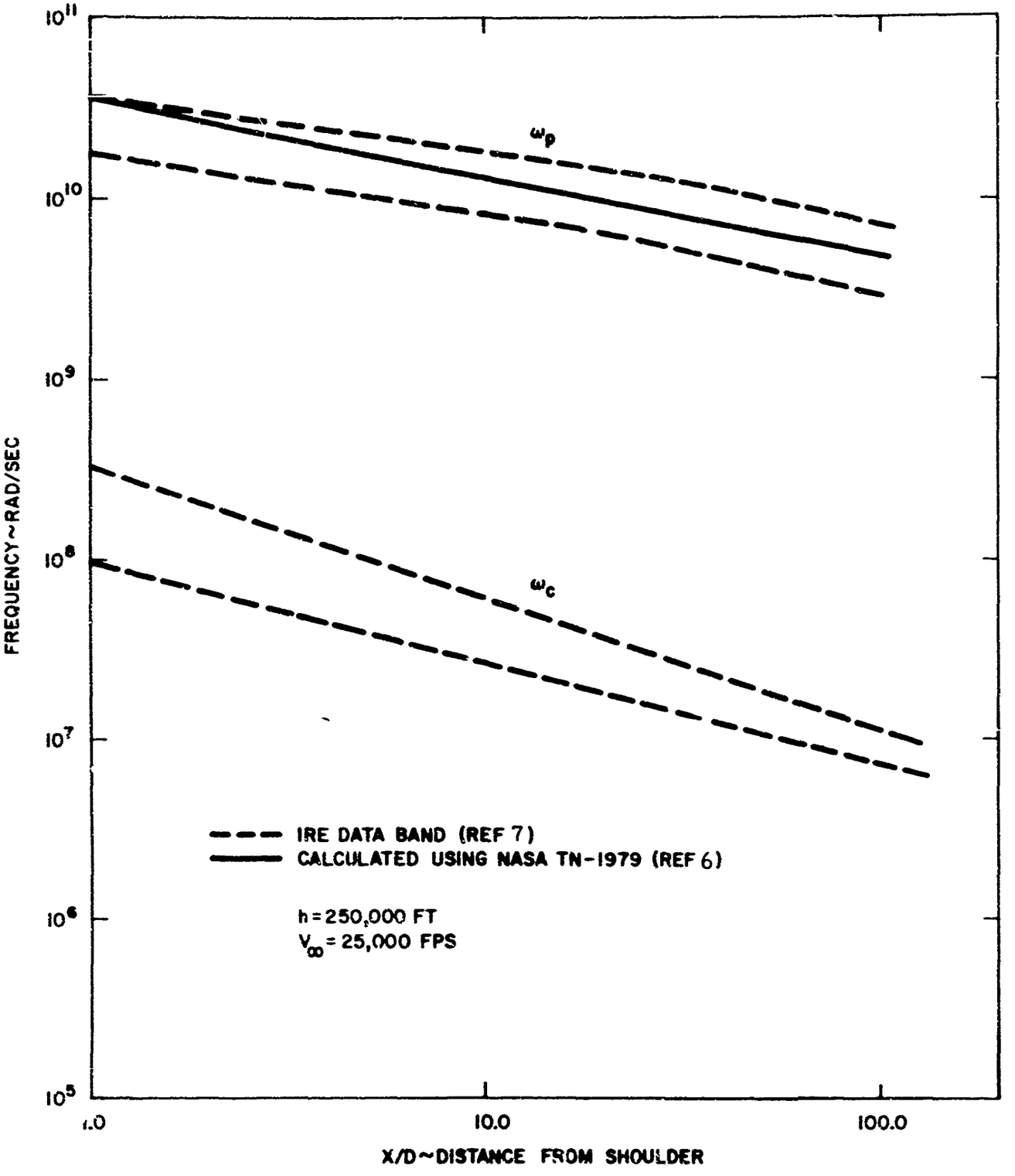

Figure 3.20. Plasma and collision frequencies versus distance.

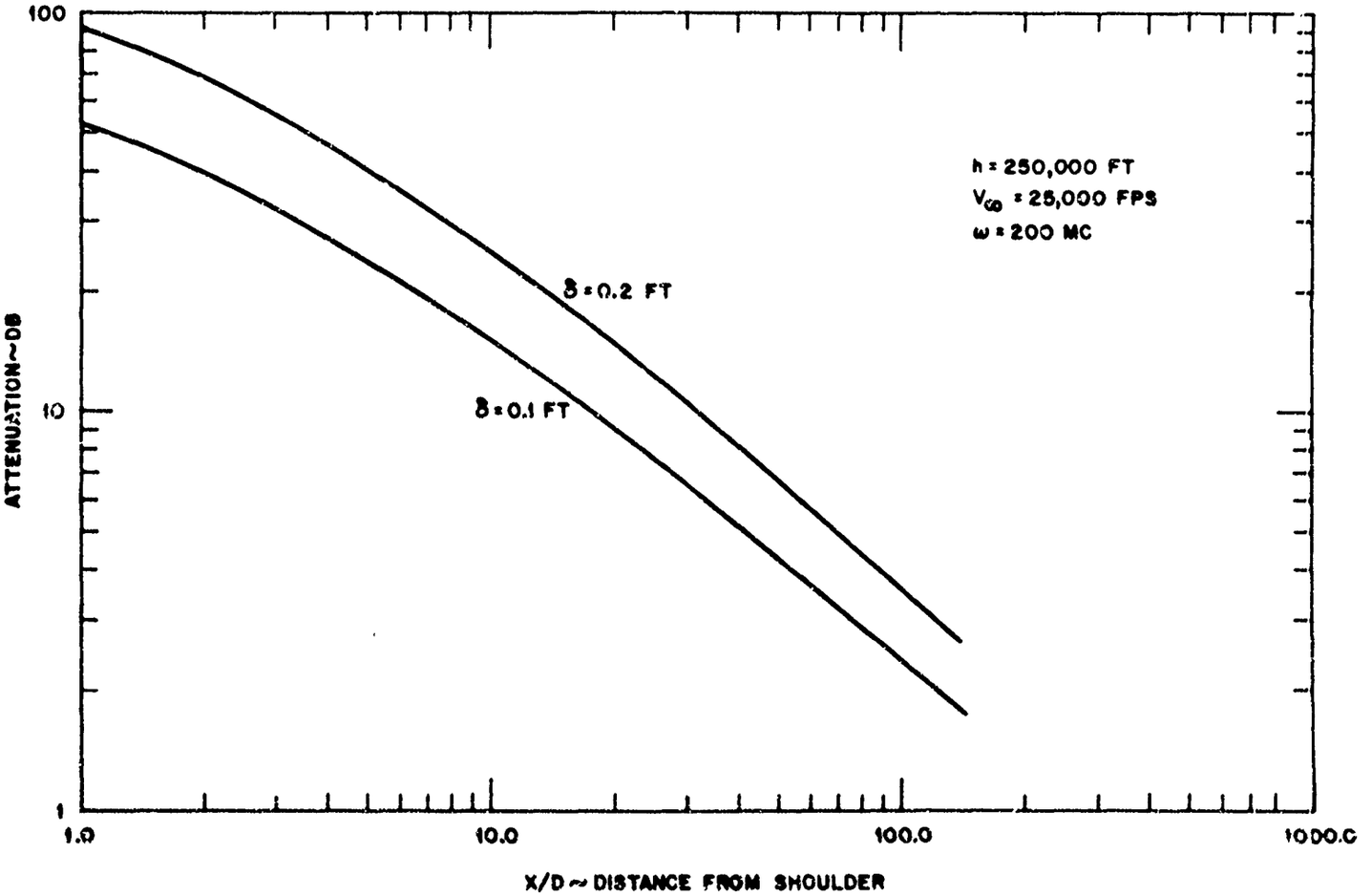

Figure 3.21. Blunt body attenuation as a function of distance for a plasma thickness of .1 and .2'.

4. USE OF JET PENETRATIONS AND MIXING TO CREATE A WINDOW

4.1 Basic Principle

One of the most attractive methods of creating a "window" in a plasma sheath is by cooling the plasma and reducing its electron concentration by injecting a jet of electrophilic gas into the plasma. The method considered herein is to use a jet from a flush mounted nozzle which penetrates into the flow before mixing in a streamtube carried downstream. The mixing within the streamtube serves to cool the plasma. Furthermore, reduction in the electron concentration by attachment to form negative ions may be obtained by using an electrophilic gas as the coolant.

4.2 Jet Penetration

In order to cool a supersonic flow by means of a jet the maximum lateral penetration must be achieved with as little disturbance of the main flow as possible. The specific method investigated here is to expand the injected fluid to a high Mach number, and to a pressure which balances the pressure of the free stream. This "correctly" expanded jet is directed across the main stream so that the momentum carries the jet fluid well out from the orifice before being swept downstream. The fluid spreads into the stream by turbulent mixing. The behavior of the flow, the mixing and the penetration distances will depend on injection Mach number, angle, fluid density, and free stream properties.

The situation is shown in Figure 4.1. A circular jet is represented by an expanding, curving tube in the free stream. The tube will have more and more free stream air in it as it moves outward; this air is entrained by turbulent mixing. Near the orifice, the upstream or "leading" edge will act like a bluff obstacle in the main flow. There will be a normal

shock in the flow before it spreads around the jet tube and closes behind it. In reality, part of the jet fluid will be torn away from the tube and carried downstream, thus distorting the circular form and reducing the total mass of the jet. The impact of the free stream on the jet tube will cause it to start curving downstream. As the jet progresses, it picks up mass by entraining free stream air, while maintaining a constant momentum. Since it will be curving there will be a centrifugal force which appears in the force equations. As the jet tube turns it presents a different angle to the free stream, thus changing the impact which the free stream exerts on it.

Two force equations, one along the stream tube and one normal to it are defined.

$$\text{a)} \quad \Delta F_s = (\Delta m)\, \mathring{V}_j$$

$$\text{b)} \quad \Delta F_n = (\Delta m)\, V_j\, \mathring{\sigma} \qquad (4.1)$$

$$= \mathring{m}\, \mathring{\sigma}\, \Delta S$$

Δm = mass of jet fluid in disc of diameter W and thickness S along the jet.

$\mathring{m}$ = mass flow of jet.

V_j = average velocity of jet along its center line at station S.

S = approximate path length from orifice along centerline of jet.

σ = arc tan (y/x).

ΔF_s = axial force acting on Δm.

ΔF_n = normal force on Δm (+ outward).

Equations (4.1) are decoupled by the following assumptions. First of all, the jet will be assumed to remain intact near the orifice (i.e. the

jet fluid torn away will be neglected). Second, after the jet has made a substantial turn, there will be a component of free stream velocity along the jet; in this event it is known that the law of entrainment must be modified[8] (see Pai, 1954 and Townsend, 1956). The form of modification is not known in the present example, and will be neglected. Third, the impact of the free stream takes place through a normal shock, so that the pressure surrounding the jet near the orifice will have a value well above free stream static. As the jet turns, the shock becomes oblique and the pressure rise becomes less. This decrement will be ignored in the first rough force balance. The effect of these assumptions is to fix the growth of mass flow in the jet at the same values as would occur in still air. Essentially the axial force balance is thus satisfied by hypothesis. For the situation where the stream and jet are different fluids, the growth rate is given by Ricou and Spalding (1961)[9]. Their formula is:

$$\frac{\dot{m}}{(\dot{m}_j)_o} = 0.32 \left(\frac{S}{d}\right) \left(\frac{\rho_{RA}}{\rho_{jo}}\right)^{1/2} \qquad (4.2)$$

$\dot{m}_j$ = mass flow in jet at station S.

$(\dot{m}_j)_o$ = mass flow of jet at orifice = $(\pi/4)\, d^2\, \rho_{jo} V_{jo}$

ρ_{RA} = density of air stream in contact with jet, here taken equal to ram density behind a normal shock. It is assumed that ram pressure P_{RA} of the air equals the jet exit pressure $(P_j)_o$.

d = diameter of the jet orifice.

Taking the momentum in the axial direction as constant, thus neglecting the contributions which variations in pressure might introduce, and

neglecting the effects ruled out by the second a ıumption above, the average velocity of the jet is found to be.

$$V_j = 3.1\,(V_j)_o \left(\frac{d}{S}\right) \left(\frac{\rho_{jo}}{\rho_{RA}}\right)^{1/2} \tag{4.3}$$

The width of the circular jet W_j is found by using equations (4.2) and (4.3) to substitute into the following equation:

$$\dot{m}_j = \pi/4\, W_j^2\, \rho_j\, V_j \tag{4.4}$$

Witn ρ_j taken to be equal to ρ_{RA} since the density of the jet is composed largely of ram air.
Solution for W_j gives;

$$W_j = .32\, S \tag{4.5}$$

The next step is to set up the force term for the left side of (4.1b); the right side is simply the centrifugal force of acceleration. The force term will have two parts: (1) the force owing to the accretion of free stream air to the jet; and (2) the force owing to the equivalent aerodynamic drag of the jet. (Both forces cause σ to decrease and therefore are negative). The first of these dpends on the increase in mass flow per unit distance along the jet $d\dot{m}/dS$. This mass before uniting with the jet had a velocity normal to the jet of $U^\circ \operatorname{Sin} \sigma$ which gives rise to a change in momentum normal to the jet or a normal force per unit length of jet of:

$$\left(\frac{\Delta F_n}{\Delta S}\right)_1 = - U^\circ \operatorname{Sin} \sigma \frac{d\dot{m}}{dS} \tag{4.6}$$

The normal force due to aerodynamic drag is given by;

$$\left(\Delta F_n\right)_2 = - \frac{1}{2} \rho^\circ U^{\circ 2}\, dA\, C_D \operatorname{Sin}^2 \sigma \tag{4.7}$$

According to Penland[10], the drag coefficient C_D is constant for supersonic Mach numbers and is independent of σ. With $dA = W\,dS$ and W given by equation 4.5 and $d\mathring{m}/dS$ obtained from the Ricou, Spalding relation equation 4.2, the force equation 4.1 can be written as:

$$\left(\frac{\Delta F_n}{\Delta S}\right)_1 + \left(\frac{\Delta F_n}{\Delta S}\right)_2 = -\mathring{m}\,\mathring{\sigma} \tag{4.8}$$

Now with substitution of equations 4.6, 4.7, and 4.2, and use of the relation

$$\mathring{\sigma} = \frac{dS}{dt} \cdot \frac{d\sigma}{dS} = V_j \frac{d\sigma}{dS}$$

with V_j given by equation 4.3, equation 4.8 above becomes:

$$\sin\sigma + \left\{\frac{2}{\pi}\left(\frac{\rho^\circ}{\rho_{jo}}\right)\left(\frac{U^\circ}{V_{jo}}\right)\left(\frac{\rho_{jo}}{\rho_{RA}}\right)^{1/2}\frac{C_D}{d}\right\} S \cdot \sin^2\sigma$$

$$= -\left\{3.1\left(\frac{V_{jo}}{U^\circ}\right)\left(\frac{\rho_{jo}}{\rho_{RA}}\right)^{1/2}\right\}\frac{d\sigma}{dS} \cdot d \tag{4.9}$$

The constant in the second bracket of equation 4.9 will be treated as a scaling parameter in the following way:

$$\alpha = 3.1\left(\frac{1/2\ \rho_{jo} V_{jo}^2}{1/2\ \rho^\circ U^{\circ 2}}\right)^{1/2}\left(\frac{\rho^\circ}{\rho_{RA}}\right)^{1/2}$$

$$= 3.1\left(\frac{q_{jo}}{q^\circ}\right)^{1/2}\left(\frac{\rho^\circ}{\rho_{RA}}\right)^{1/2}$$

where the dynamic press· at the jet exit is given by the modified Newtonian formula:

$$P_{jo} = P_{RA} = (.9)(2.)\, q^{\circ} \sin^2 \sigma_o$$

By defining,

$$\bar{S} = (S/d)\left(\frac{1}{\bar{\alpha}}\right)$$

$$\bar{\alpha} = 2.94 \sqrt{\gamma_j} \frac{M_{jo} \sin \sigma_o}{\left(\rho_{RA}/\rho^{\circ}\right)^{1/2}}$$

$$k = \frac{6}{\pi}\frac{2}{} C_D \left(\frac{\rho^{\circ}}{\rho_{RA}}\right)$$

equation 4.8 takes the form

$$\frac{d\sigma}{d\bar{S}} = -\sin\sigma - k\bar{S} \cdot \sin^2 \sigma \qquad (4.10)$$

The equation has one shape parameter k, which determines the precise form of the function $\sigma(\bar{S})$; k depends only on free stream Mach number. The parameter $\bar{\alpha}$ contains the effect of jet exit Mach number and angle of injection. Equation 4.10 cannot be solved analytically but can be easily programmed on a Recomp III computer as described by Bartlett[11]. The data required for this are initial conditions and values of k and $\bar{\alpha}$. Once σ is obtained as a function of $\bar{S}$, simple quadrature will yield the coordinates of the jet centerline

$$y/d = \int \sin\sigma\,(\bar{S}, k)\, d\,(S/d) = \bar{\alpha}\int \sin\sigma\,(\bar{S}, k)\, d\bar{S} \qquad (4.11a)$$

$$x/d = \bar{\alpha}\int \cos\sigma\,(\bar{S}, k)\, d\bar{S} \qquad (4.11b)$$

For the computation of k and $\bar{\alpha}$, the following conditions were chosen.

$$\gamma^{o} = 1.4$$

$$U^{o} = 14000 \text{ ft/sec}$$

$$T^{o} = 4100°K$$

$$M^{o} = 3.3$$

$$\rho_{RA}/\rho^{o} = 4.11$$

The injected fluid has a $\gamma_j = 1.67$ as would be the case for monatomic gas in the jet;

$$\bar{\alpha} = 1.8 M_{jo} \sin \sigma_o$$

$$k = .60$$

The solution to the above sets of conditions are shown plotted in Figures 4.2, 4.3, 4 4.

4.3 One-dimensional Flow with Coolant Injection

4.3.1 Basic Equations for Perfect Gases

In order to determine properties in a flow field after uniform mixing has occured, a one-dimensional stream tube analysis was performed. Schematically the problem is defined in the sketch on the following page:

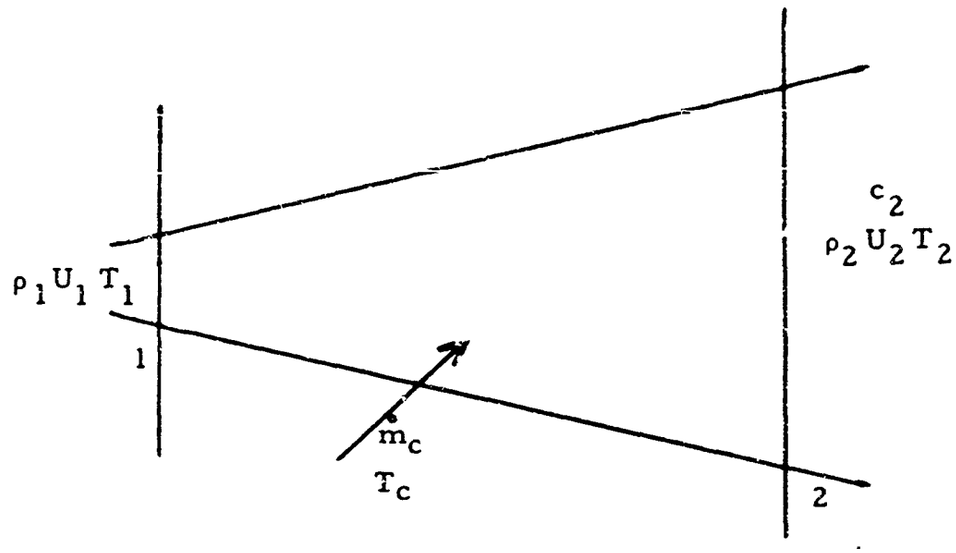

Flow at (1) is known; flow properties at (2) are to be determined. A coolant or electrophilic gas is injected into the stream tube between locations (1) and (2) with known properties. Complete mixing takes place in the region between (1) and (2), and the mixing of the initial flow and the coolant is assumed to take place at constant pressure.

Application of the conservation equations for mass, partial mass, momentum, energy and a state equation along this stream tube will determine properties of the mixed flow at (2).

The following conservation laws result.

$$\rho_1 U_1 A_1 + \dot{m}_c = \rho_2 U_2 A_2$$

$$\dot{m}_c / \rho_1 U_1 A_1 = c_2 / 1 - c_2$$

$$\rho_1 U_1 A_1 + \dot{m}_c U_c = \rho_2 U_2^2 A_2 \qquad (4.12)$$

$$\rho_1 U_1 A_1 H_1 + \dot{m}_c H_c = \rho_2 U_2 A_2 H_2$$

$$\rho_1 R_1 T_1 = \rho_2 T_2 R_2 = \bar{P}_{1,2}$$

c_2 is defined as the percent by weight of coolant present in the mixed flow;

$$\rho_2 \left(1-c_2\right) = \rho_{2\,air}$$
$$\rho_2 \left(c_2\right) = \rho_{2\,coolant} \qquad (4.13)$$

With this definition, weighted values for c_{p_2} and R_2, the partial enthalpy of air h_{2_a} and of the coolant h_{2_c} can be defined as follows.

$$h_2 = h_{2_a}\left(1 - c_2\right) + h_{2_c}\left(c_2\right)$$
$$c_{p_2} = c_{p\,air}\left(1 - c_2\right) + c_{p_c}\left(c_2\right) \qquad (4.14)$$
$$R_2 = R_{air}\left(1-c_2\right) + R_c\left(c_2\right)$$

With assumption that the momentum of the injected coolant or electrophilic gas $\left(\mathring{m}_c U_c\right)$ is much less than the momentum of the incoming free stream $\rho_1 U_1^2 A_1$, there results after defining $\mathring{m}/\rho_1 U_1 A_1 = C_{Q_1}$, the following values for the conditions at (2).

$$U_2/U_1 = 1/1+C_{Q_1}$$
$$A_2/A_1 = \left(1 + C_{Q_1}\right)^2 \cdot \rho_1/\rho_2 \qquad (4.15)$$
$$c_2 = C_{Q_1}/1 + C_{Q_1}$$

If the initial conditions, U_1, T_1, $P_{1,2}$ etc. are specified then for various values of the parameter C_{Q_1} one can solve for the downstream conditions using the relations above. The downstream temperature is found from the energy equation to be;

$$\frac{T_2}{T_1} = \frac{c_{p_1}}{c_{p_2}} \left[\frac{1}{1 + C_{Q_1}} \left\{ \frac{H_1}{h_1} + C_{Q_1} \frac{H_c}{h_1} \right\} - \frac{U_2^2}{2h_1} \right] \qquad (4.16)$$

H_1 remains constant and equal to its free stream value of

$$H_1 = H_\infty = h_\infty + \frac{U_\infty^2}{2} \qquad (4.17)$$

An alternate approach to the solution of this problem can be outlined if one wishes to determine what value of C_{Q_1}, and U_1, resulted in a specified downstream temperature T_2 for a certain flight velocity. This is done in the following way.

Substitution of U_2, c_2 h_2 from relations 4.15, and 4.14 into the energy equation results in an equation for U_1.

$$\frac{U_1^2}{2} = \left(1 + C_{Q_1}\right)\left[H_1 + C_{Q_1}\left(H_c - h_{2_c}\right) - h_{2_a}\right] \qquad (4.18)$$

Defining the stream tube mixing problem in this way allows us to select the final temperature of the mixture T_2, then with H_c a known coolant storage condition and $h_{2_c} = c_{p_c} T_2$, $h_{2_a} = c_{p_{air}}$. T_2, U_1 will be solely a function of C_{Q_1} or the ratio of coolant to initial mass flow necessary to achieve the desired final temperature.

What the initial temperature must have been in order to reach the final temperature T_2, with the proper ratio of coolant injected into the flow can be found from equation (4.17) to be:

$$T_1 = \left(H_1 - \frac{U_1^2}{2}\right) \frac{1}{C_{p_{air}}}$$

4.3.2 Special Method for Real Air in Thermodynamic Equilibrium

When the perfect gas assumption is discarded and the thermodynamic properties of air are obtained from a Mollier chart (assuming thermodynamic equilibrium) it is most convenient to use the method in which the downstream temperature is specified. It is also necessary in this case to specify the local pressure, $P_{1,2}$ of the flow.

The first step in the calculation is to choose a value of the partial pressure of air at station 2, P_{2a}. The partial pressure of the coolant is then

$$P_{2c} = P_{1,2} - P_{2a}$$

The partial densities at station 2 are

$$\rho_{2a} = \frac{P_{2a}}{R_A Z T_2}$$

$$\rho_{2c} = \frac{P_{2c}}{R_c T_2}$$

assuming Z = 1 for the coolant. The mixing ratio is

$$c_2 = \frac{\rho_{2c}}{\rho_{2c} + \rho_{2a}}$$

from which the injection coefficient C_{Q_1} can be computed as

$$C_{Q_1} = c_2 / 1 - c_2$$

Since the partial pressure and temperature of the air at station 2 have been specified, its enthalpy is also determined. Equation 4.18

can then be used to calculate the corresponding value of U_1, the local velocity before injection.

This straight forward method yields results of the type described in the next section, i.e. we obtain directly curves of C_{Q_1} versus U_1, with T_2 fixed.

4.3.3 Selection of a Coolant

Since data is yet unavailable to compare the electrophilic effectiveness of various gases the cooling effectiveness only will be considered herein. It should be kept in mind however that electrophilic additives could enhance the plasma suppression by the jet.

The effectiveness of a coolant may be judged by evaluating the heat it can absorb as it is raised from its storage temperature to the desired temperature of the coolant-air stream mixture which is on the order of 3000°K (5400°R). As may be recalled from Figures 3.4 through 3.7, 3000°K would lower the attenuation of a 200 Mc signal through a 0.2 ft plasma slab to about 3 db.

Figure 4.5 taken from Reference 12 shows the heat capacity per pound of hydrogen, helium, water and propane. Hydrogen,the most effective coolant could only be used where it could be shown that combustion would not occur, or if it does, would not be harmful. Water was included for comparison as NASA has been engaged in an intensive effort in plasma suppression by water injection. However, the prime interest in the studies at hand is in a light gas system. Helium and propane are quite comparable in the 5000°R range of interest.

Specific studies in section 4.3.4 will be based upon helium as the coolant.

4.3.4 Results of Coolant Injection

The equations developed in section 4.3.2 allow us to calculate an injection coefficient:

$$C_{Q_1} = \dot{m} / \rho_1 U_1 A_1$$

to obtain any desired temperature at station 2 by injecting a coolant into a given stream at station 1. Since the desired temperatures cover a wide range and the stream at station 1 can correspond to many different antenna locations on vehicles travelling at many speeds, a concise presentation of the results of our calculations requires some unifying scheme.

We have chosen to consider the problem in the following terms;

a) the basic independent parameter is the vehicle flight speed; together with nominal atmospheric temperature of 419°R, this defines a stagnation enthalpy H_1.

b) antenna location on the vehicle is defined in terms of the local velocity U_1 of the stream external to it. For antennas located on slender vehicles or on the shoulder of blunt-nosed vehicle $U_1 \geq 0.6\, U_\infty$ well beyond the sonic point.

c) the coolant temperature is fixed at 540°R.

d) the coolant is assumed to be helium, chosen as a typical example of a coolant with a large capacity to absorb heat.

The energy equations 4.16 and 4.18 show that it is possible with this scheme to either

1) choose U_1 and obtain a relation between C_{Q_1} and T_2.

2) choose a desired T_2 and obtain a relation between C_{Q_1} and U_1.

Both methods of presentation are used for the results shown in Figures 4.6, 4.7, 4.8, 4.9. Rather than use C_{Q_1}, however, which is normalized with respect to a streamtube area at the injection station we have used

$$C_{Q_2} = \frac{\dot{m}_c}{P_1 U_1 A_2}$$

which is based on the streamtube properties before injection and the area actually cooled at the antenna station. This parameter can be related more directly to the antenna requirements.

Most of the calculations so far have been performed for the sake of simplicity with the assumption that air behaves as a perfect gas. One set has been performed using equilibrium air properties to illustrate the differences to be expected in general. The coolant in all cases has been helium.

Figures 4.6, 4.7, 4.8 illustrate how the injection requirement varies, with the desired end temperature. Three flight speeds are represented and curves are drawn for constant values of the local velocity U_1. Note that each curve exhibits a peak at a value of T_2, which lies in the range of interest for plasma suppression. Thus for a given flight speed and local velocity the injection requirement is not very sensitive to the specification of T_2.

Figure 4.9 is a cross plot of these data for $T_2 = 2400°K = 4325°R$. It illustrates how the coolant requirement falls off as the antenna station is moved downstream to higher values of U_1. The curve for a flight speed of 18,000 ft/sec is reproduced in figure 4.10 where it is compared with equilibrium-air results for three values of the local pressure. The injection requirement predictions are considerably lower for equilibrium air than for air behaving as a perfect gas.

The shaded zones in the lower right-hand corners of some of the figures correspond to heating of the stream rather than cooling. The explanation for this unexpected behavior lies in the fact that coolant injection

decreases the velocity of the airstream as well as reducing the total enthalpy of the mixture. The decrease in velocity raises the ratio of static temperature to total temperature and under some conditions this process outweighs the total-temperature decrease. The practical consequence is that injection rates must exceed a certain critical value before any cooling is accomplished.

4.4 Effect on Vehicle Aerodynamics

The use of a side jet to create a "window" will create a moment, upsetting the vehicle trim. In order to get an order of magnitude estimate for trim angle with the side jet, a Trailblazer-type vehicle with the characteristics shown in Figure 4.11 will be considered. The flight conditions will be assumed constant as follows:

$$U_\infty = 18,000 \text{ ft/ sec}$$

$$T_\infty = 233°K$$

$$U_1/U_\infty = 0.67$$

$$\rho_1/\rho_\infty = 0.52$$

The coolant will be taken as helium and has a $\dot{m}/\rho_1 U_1 A_2 (C_{Q_2})$ of 0.13 as shown in Figure 4.10 for an equilibrium gas.

For a jet penetration into the shock layer, the axial force normal to the surface of the missile, N_j, has been assumed to be twice the exit jet momentum or,

$$N_j = 2 \dot{m} U_j \tag{4.19}$$

but

$$\dot{m} = C_{Q_2} \rho_1 U_1 A_2$$

so

$$N_j = 0.26\,\rho_1 U_1 A_2 M_j a_j \tag{4.20}$$

The area A_2 is the area that the jet cools and will be taken as $\frac{\pi\delta^2}{4}$ where δ is the plasma thickness. From Figure 4.11 we find that $A_2 = 0.00196\ell^2$. Also from Figure 4.11 note that the trim angle of attack is given by:

$$\alpha_{Trim} = \frac{127.6\,N_j}{C_{N_\alpha} q_\infty \ell^2} \tag{4.21}$$

Substituting equation (4.20) and the above value of A_2 into (4.21) we find

$$\alpha_{Trim} = \frac{0.13\,\rho_1/\rho_\infty\; U_1/U_\infty\; \dot{m}_j a_j}{C_{N_\alpha}\; U_\infty} \tag{4.22}$$

It now remains to find the jet Mach number, M_j. In order to cool the plasma layer of thickness, δ, it will be necessary that the jet penetrate a distance of $\delta/2$. For a typical jet the maximum jet penetration was given in Reference 13 as

$$y_\infty/d_j = 2.2\,M_J \tag{4.23}$$

We have said that we want $y_\infty = \delta/2$. The jet exit diameter d_j may be found from the mass flow of coolant required.

$$\dot{m} = \rho_J M_J a_j A_J = P_J M_J A_J \sqrt{\frac{\gamma_j}{R_J T_J}}$$

But from section 4.2,

$$P_J = 1.8q = 0.9\,\rho_1 U_1^2$$

therefore

$$\dot{m}_j = 0.9\,\rho_1 U_1^2 M_j A_j \sqrt{\frac{\gamma_j}{R_j T_j}}$$

As stated before $\mathring{m} = C_{Q_2} \rho_1 U_1 A_2$

so

$$C_{Q_2} \rho_1 U_1 A_2 = 0.9 \rho_1 U_1^2 M_J A_J \sqrt{\gamma_j / R_J T_J}$$

and

$$A_2 / A_J = \frac{0.9 U_1 M_J}{C_{Q_2}} \sqrt{\frac{\gamma_j}{R_J T_J}} \qquad (4.24)$$

where

$$A_2 = \pi \frac{\delta^2}{4.0}$$

and

$$A_j = \pi \frac{d_j^2}{4}$$

therefore

$$\frac{\delta^2}{d_j^2} = \frac{0.9 U_1 M_J}{C_{Q_2}} \sqrt{\frac{\gamma_J}{R_J T_J}}$$

From (4.23)

$$d_j^2 = \left(\frac{\delta/2}{2.2 M_J} \right)^2$$

and

$$M_J = \frac{U_1 \sqrt{\frac{\gamma_j}{R_J T_J}}}{21.5 C_{Q_2}} \qquad (4.25)$$

or for the values in the example

$$M_J = 2.16$$

The trim angle of attack may now be found by substituting in equation(4. 22)

$$\alpha_{Trim} = \frac{(0.13)\ (0.52)\ (0.67)\ (2.16)\ (3330)}{(.03)\ \ (18,000)}$$

$$\alpha_{Trim} = 0.6°$$

Such a value for the trim angle of attack is not considered a problem of much concern. In fact should a symmetrical installation be used the trim angle would be zero.

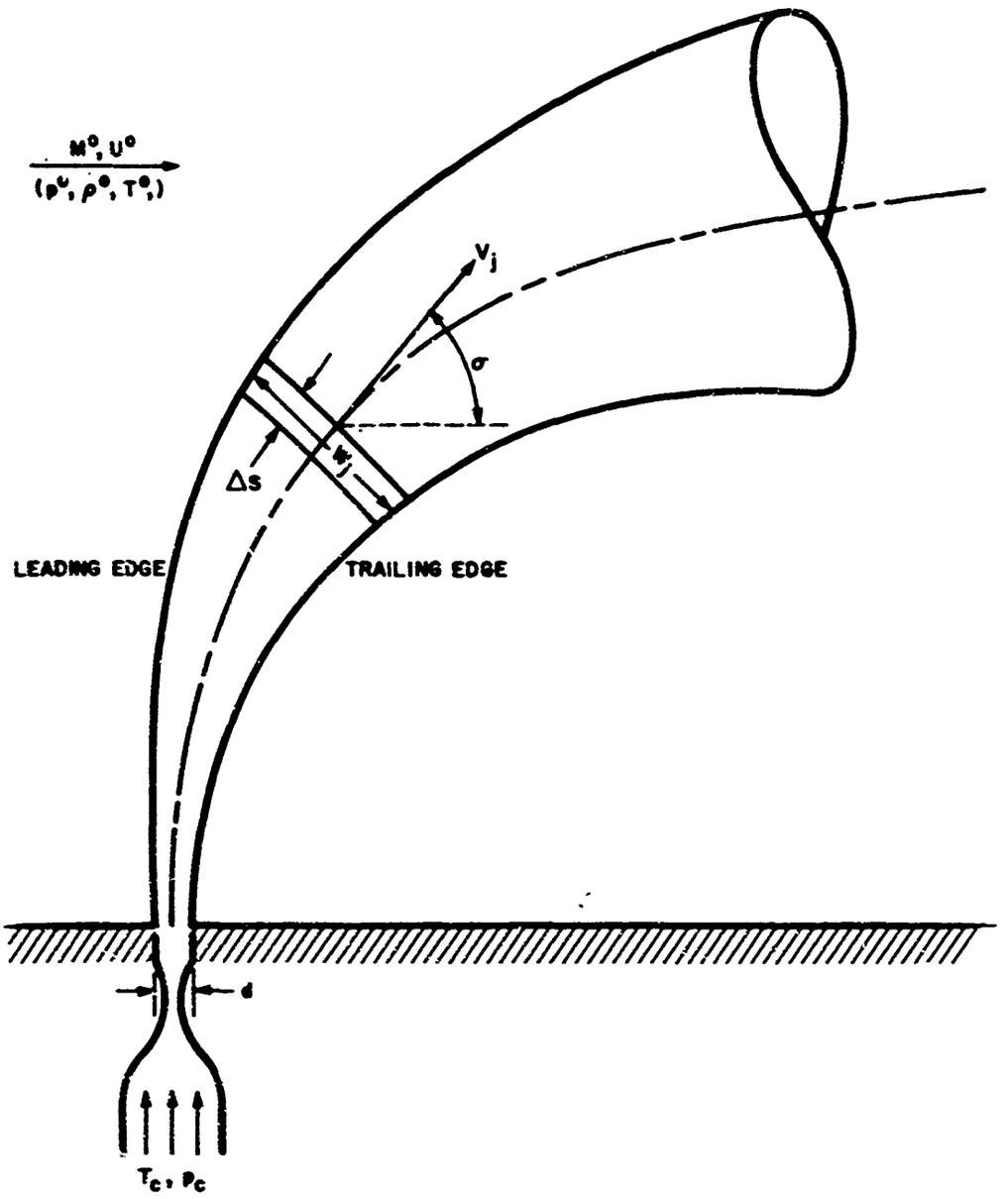

Figure 4.1. Circular cross jet in a supersonic free stream.

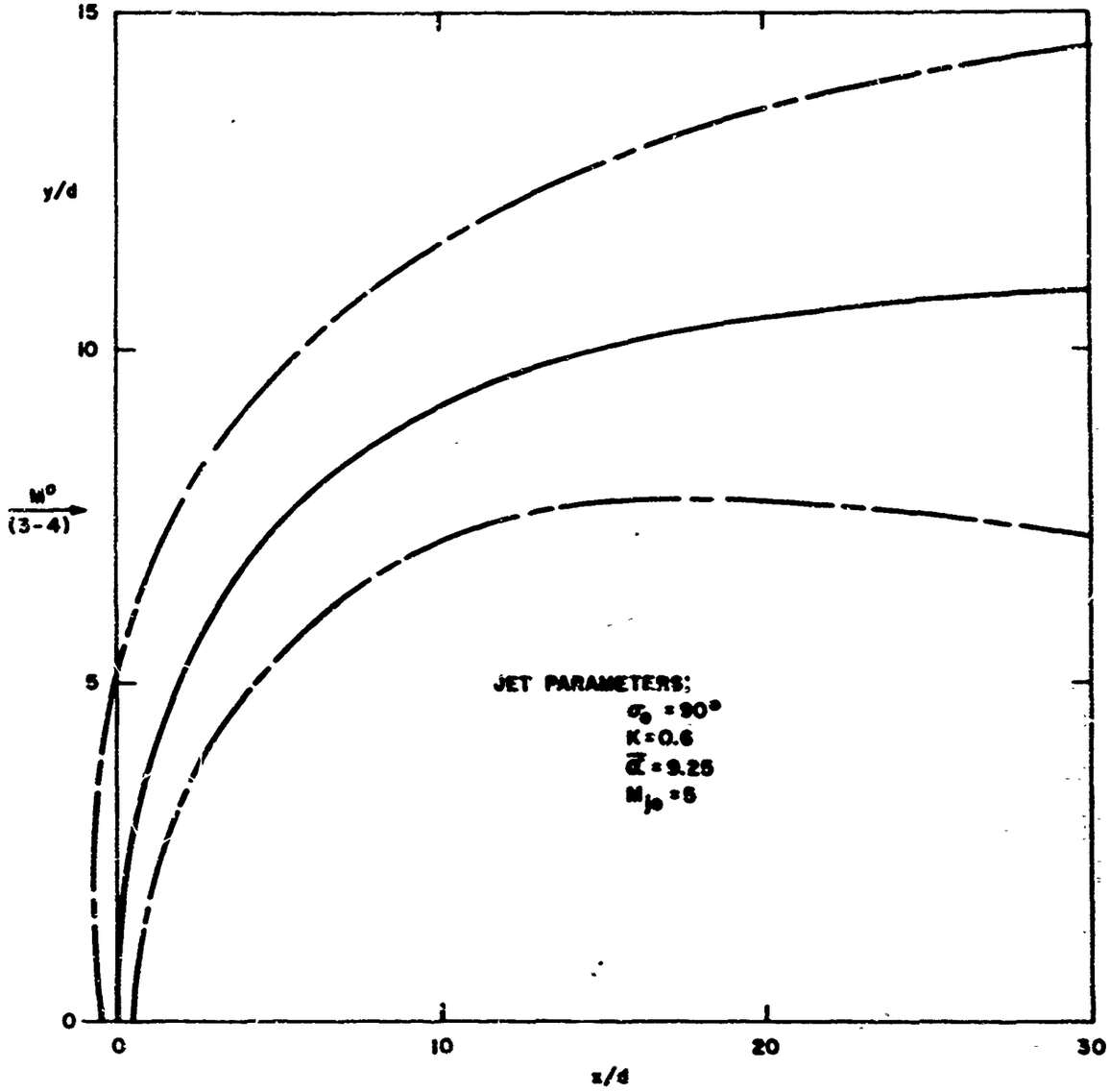

Figure 4.2. Jet centerline and boundaries.

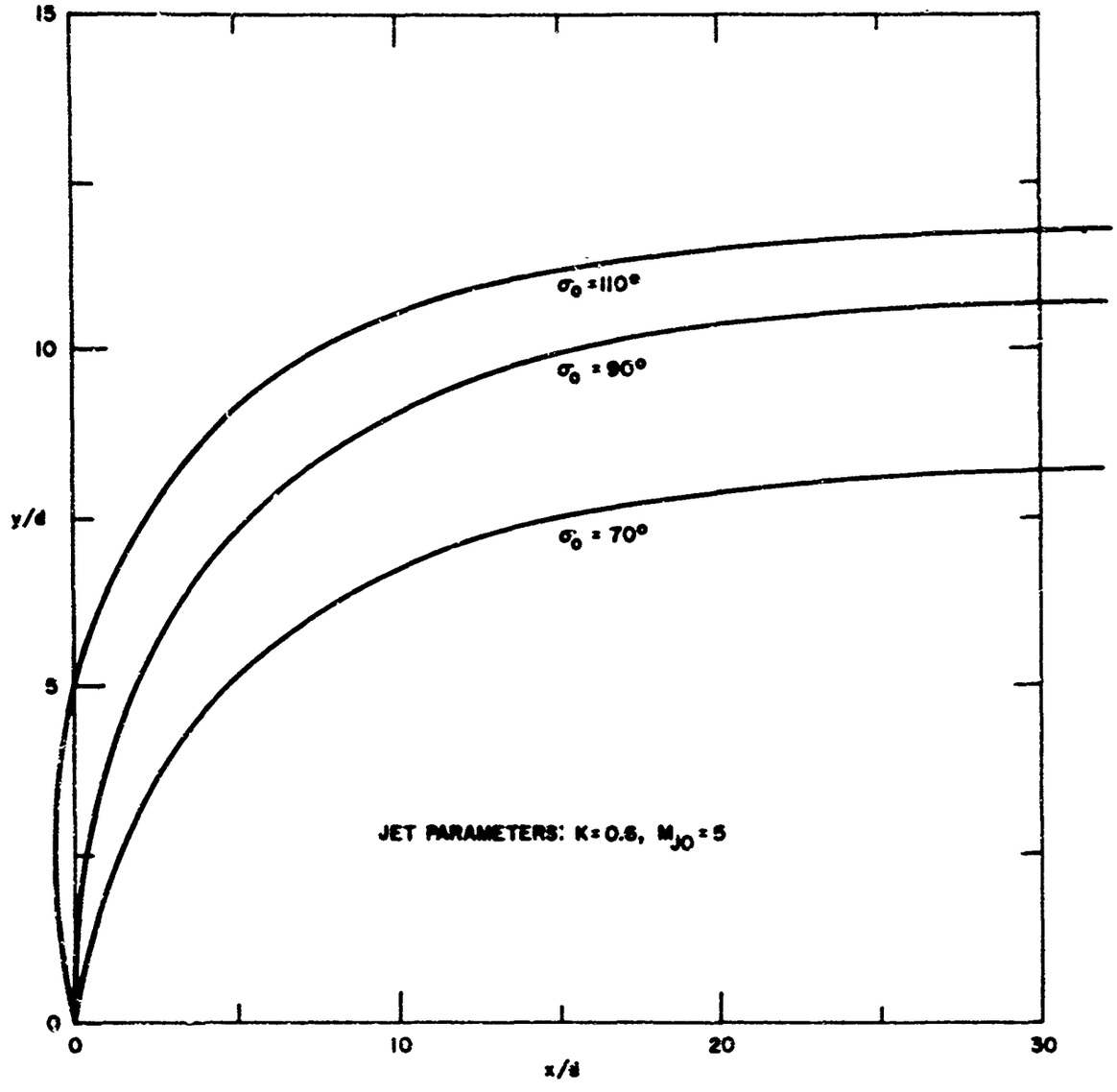

Figure 4.3. Jet centerline for M° = 3 — 4 and various angles of injection.

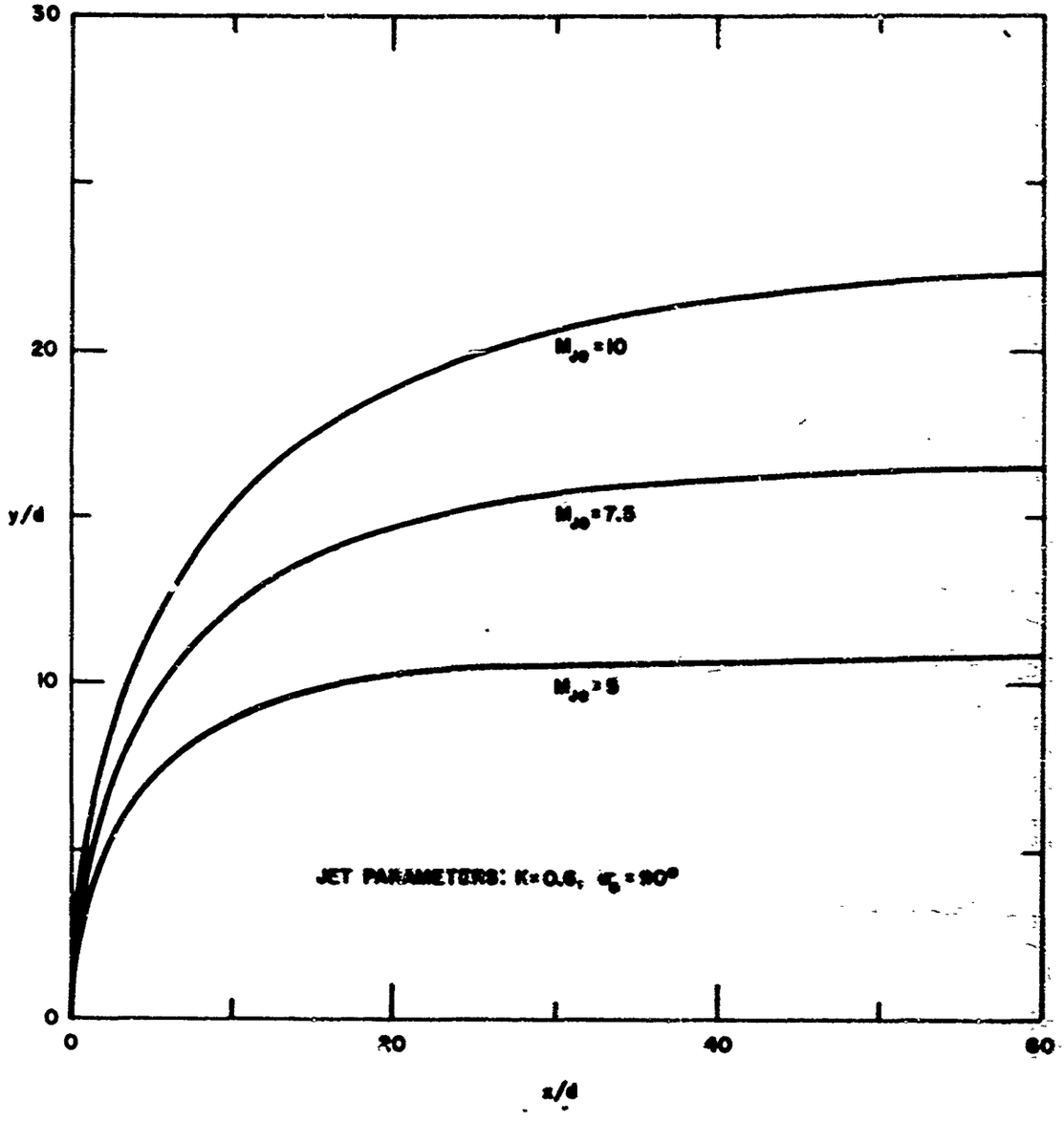

Figure 4.4. Jet centerline for M° = 3 — 4 and various jet mach numbers.

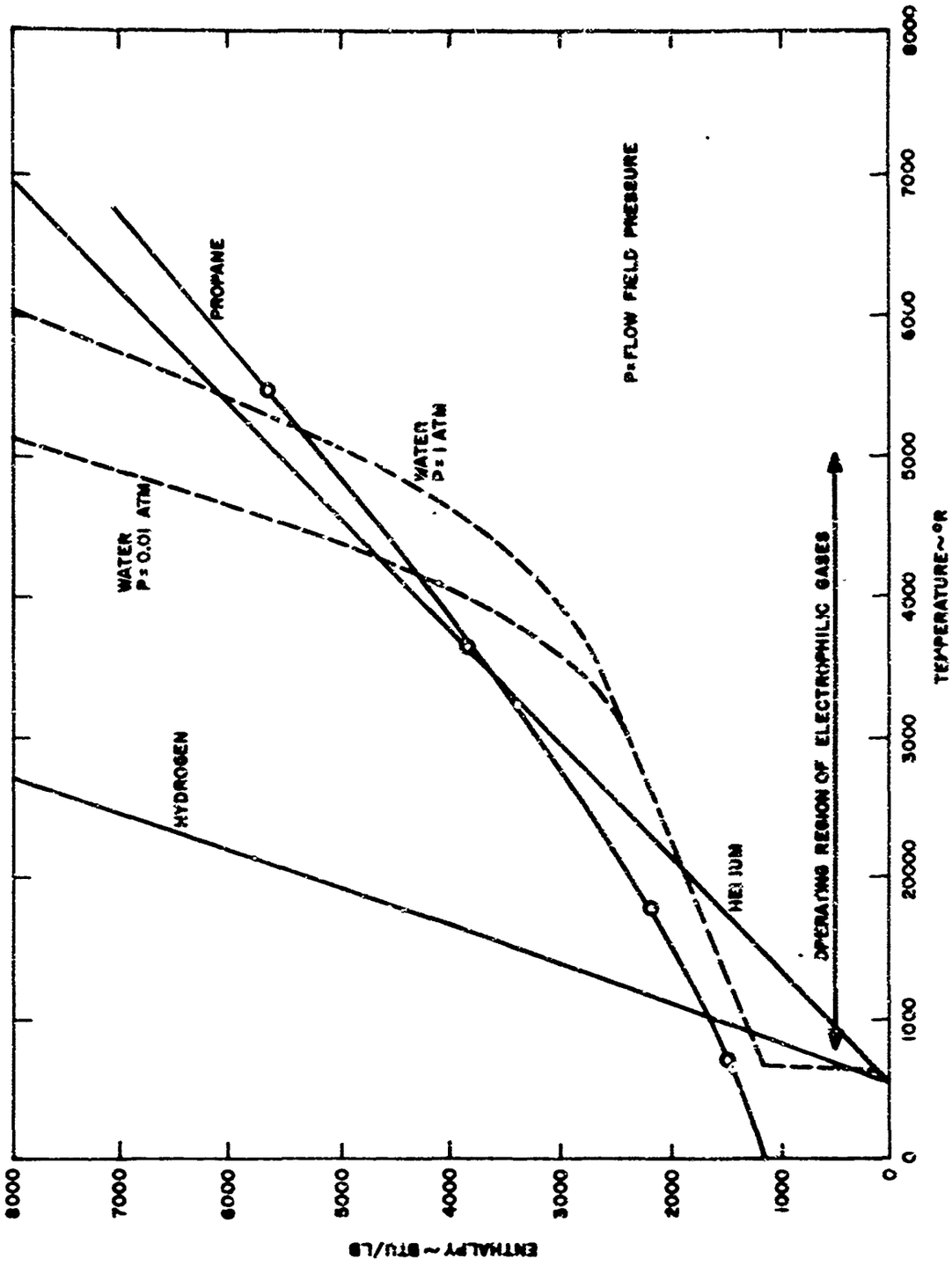

Figure 4.5 Cooling effectiveness as a function of temperature for various coolants.

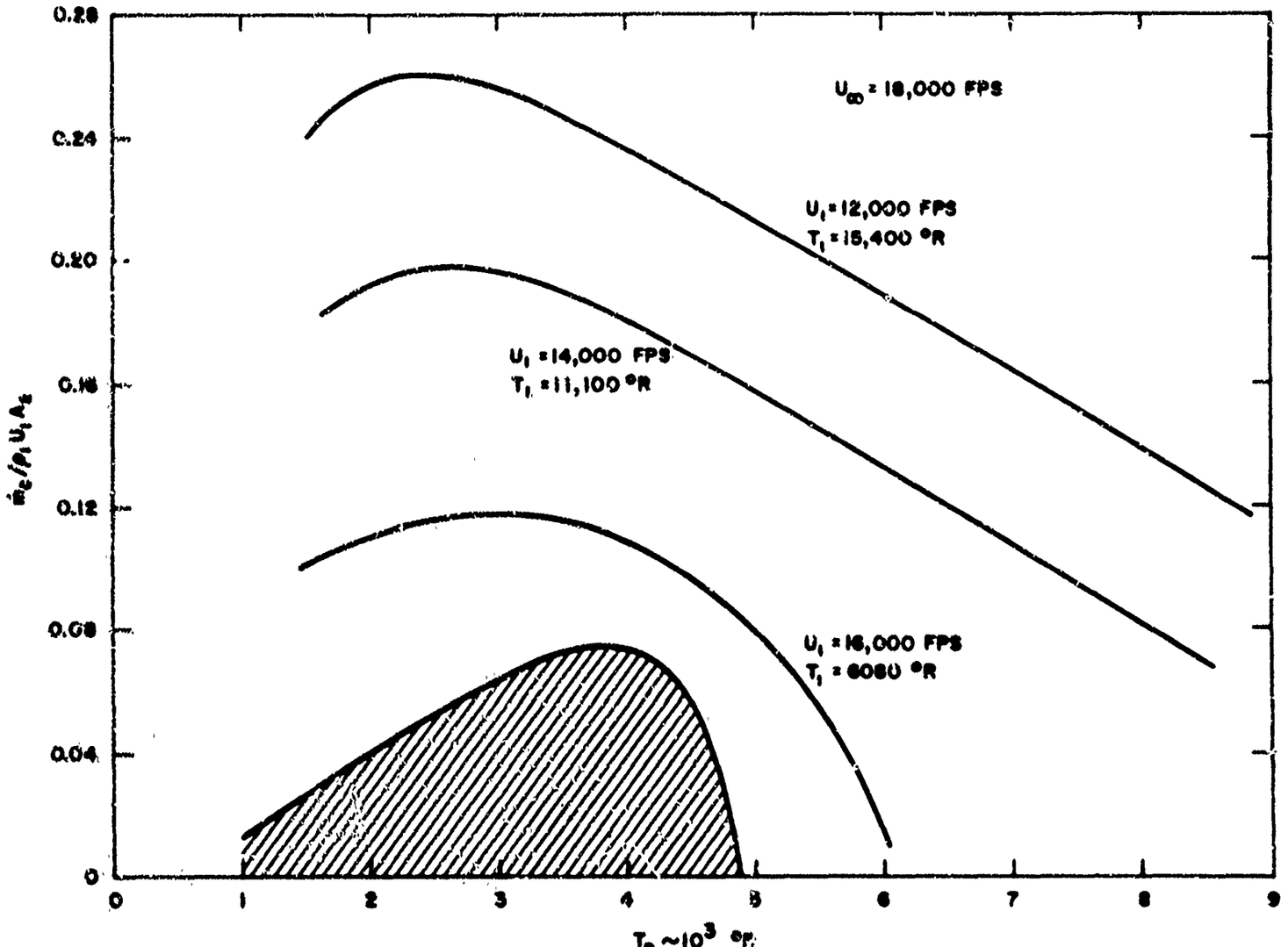

Figure 4.6. Coolant requirement as a function of temperature for a free stream velocity of 18,000 ft/sec.

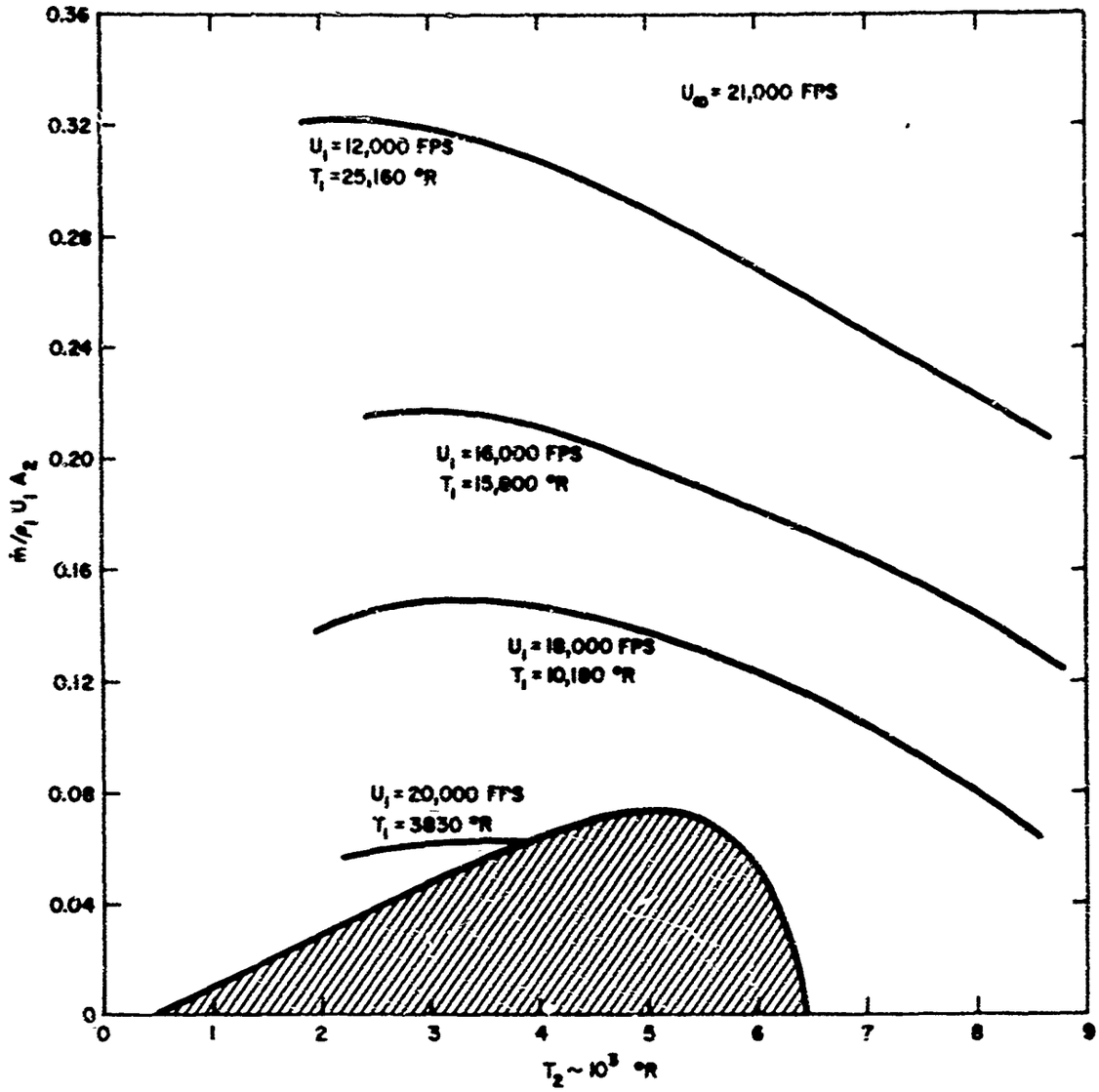

Figure 4.7. Coolant requirement as a function of temperature for a free stream velocity of 21,000 ft/sec.

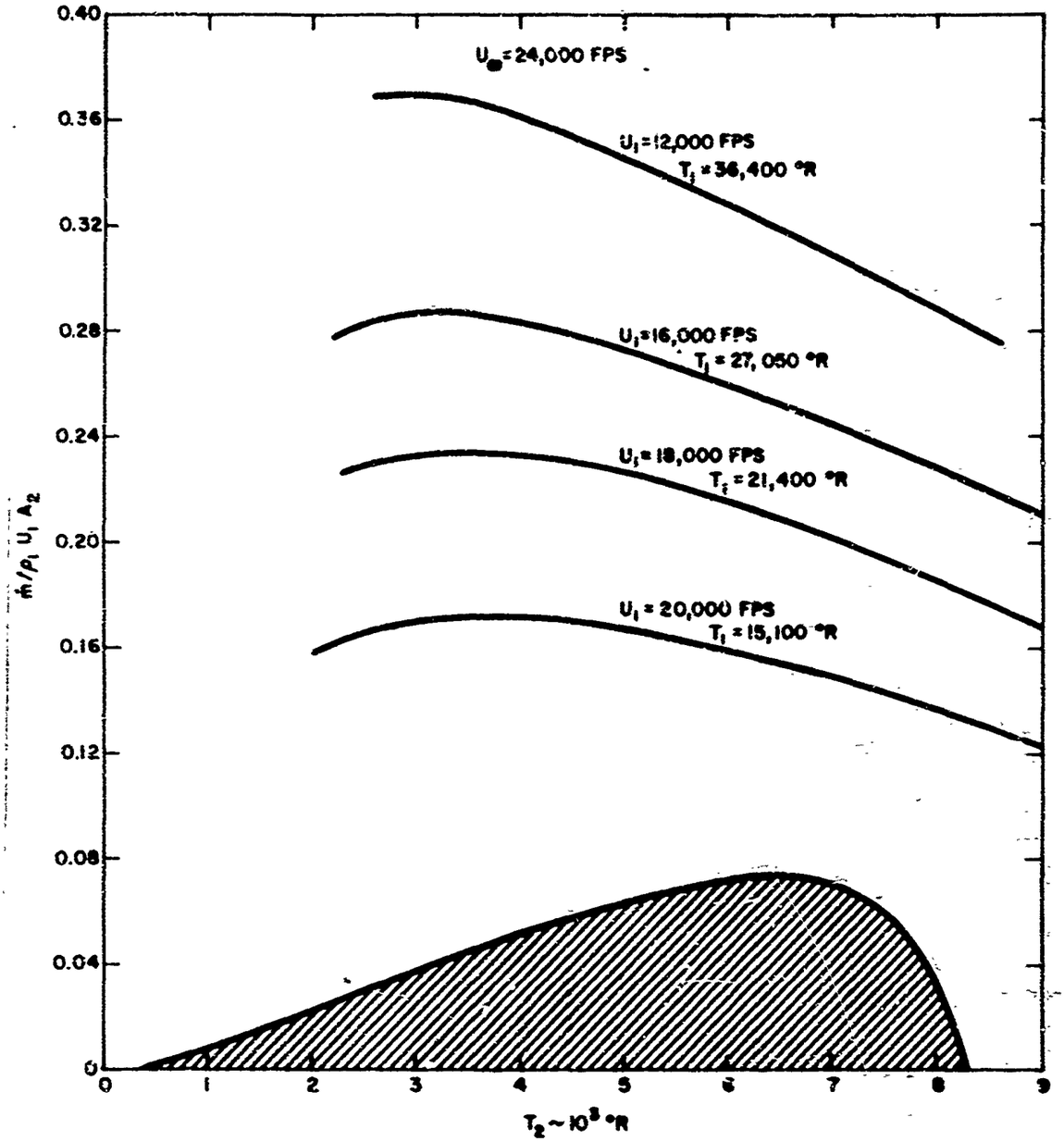

Figure 4.8. Coolant requirement as a function of temperature for a free stream velocity of 24,000 ft/sec.

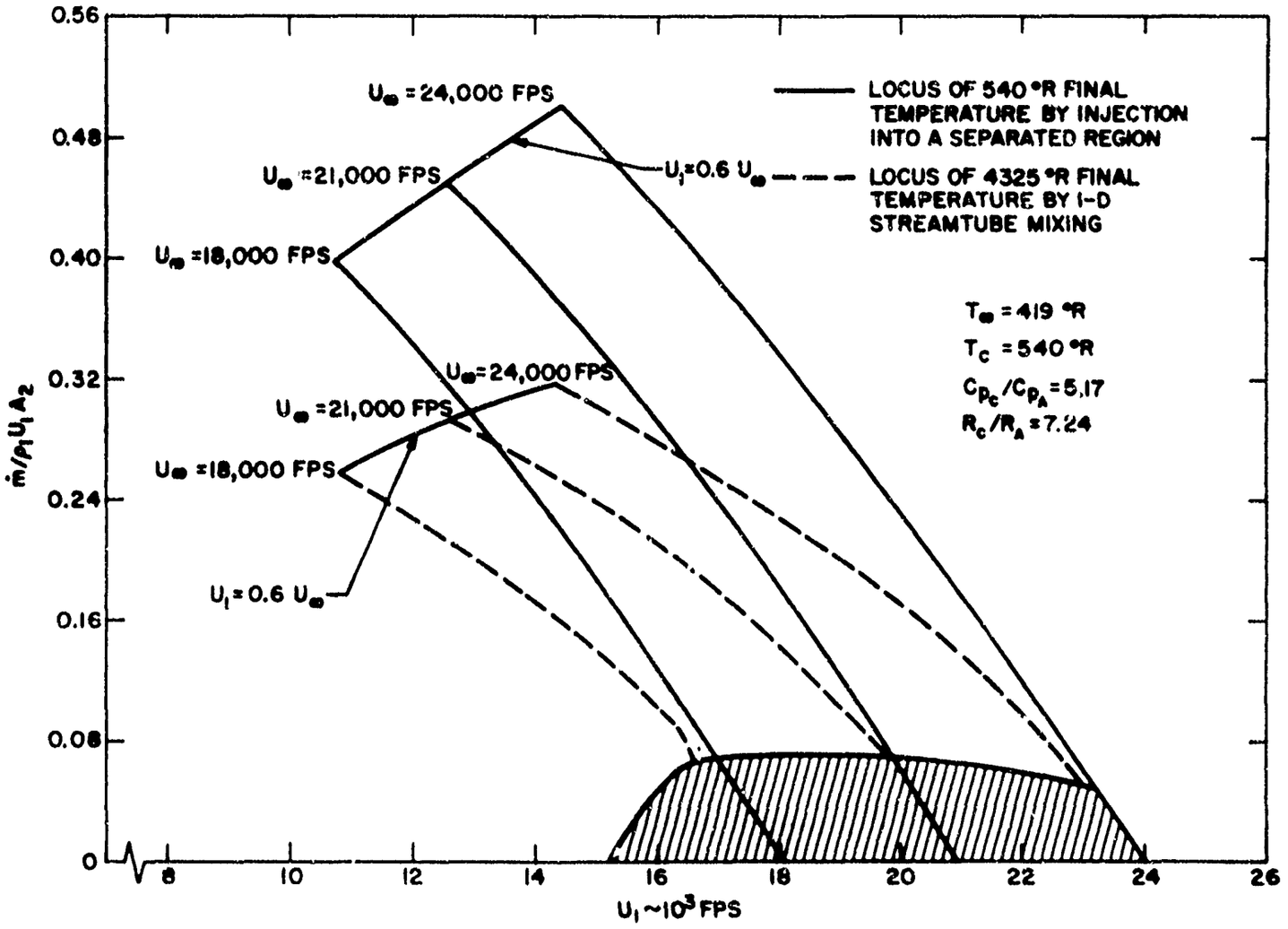

Figure 4.9. Comparison of separated flow cooling and cooling by 1-dimensional streamtube mixing.

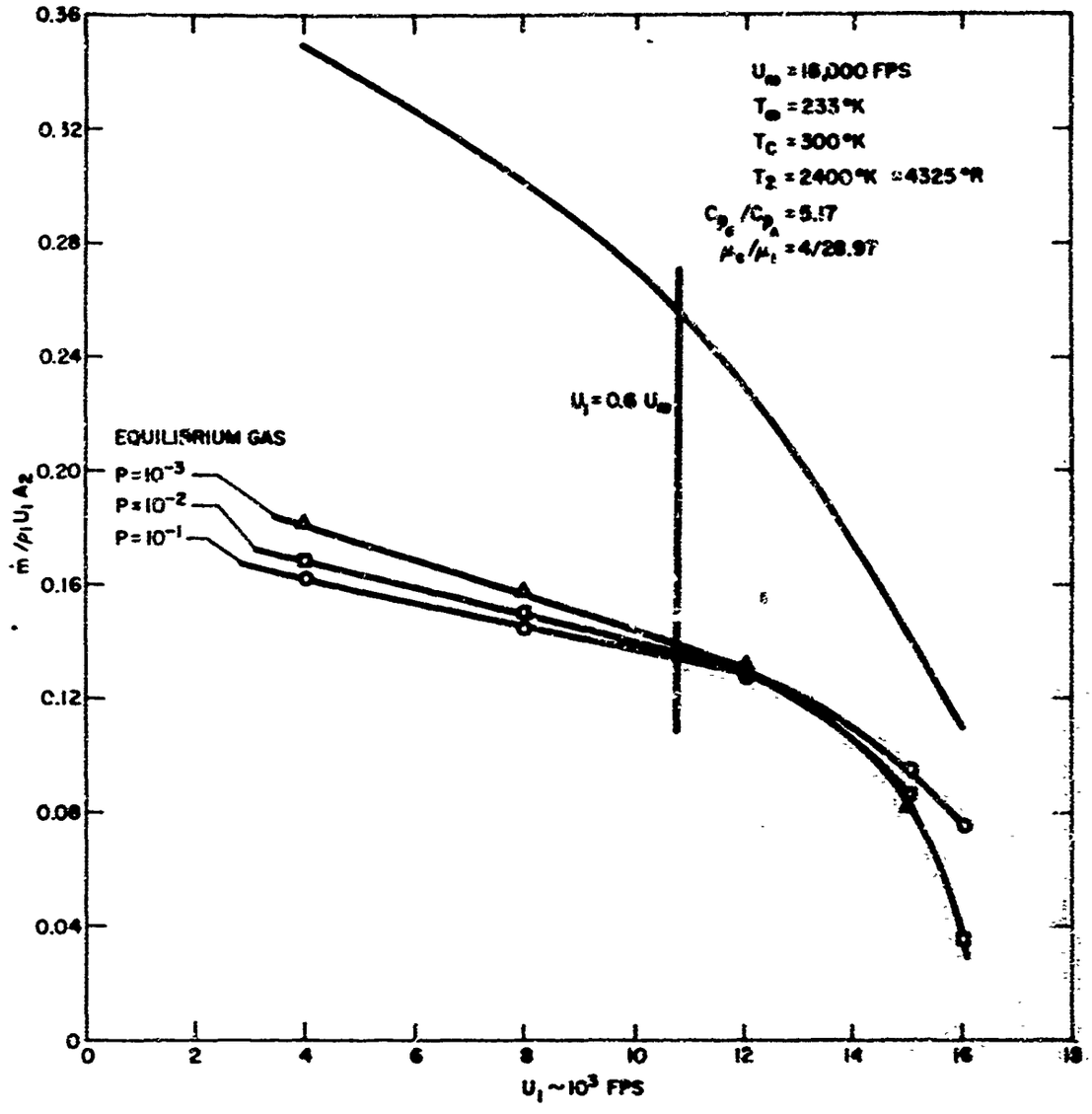

Figure 4.10. Comparison of coolant requirement for a perfect and an equilibrium gas model.

$$\alpha_{TRIM} = \frac{N_j \times 0.02\ell}{C_{N\alpha} \times q_\infty \times \pi (0.158\ell)^2 \times 0.02\ell}$$

$$= \frac{127.6\ N_j}{C_{N\alpha}\ q_\infty\ \ell^2}$$

WHERE $C_{N\alpha} \approx 0.03/\text{DEG.}$

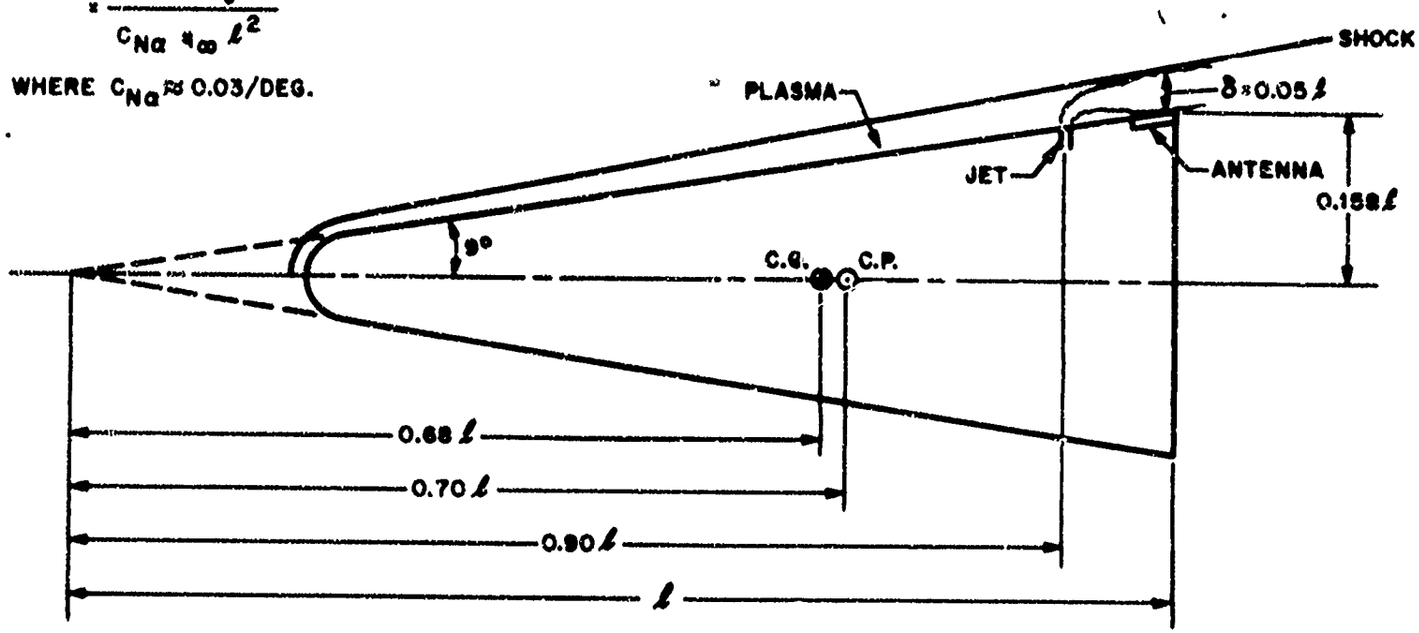

Figure 4.11. Trailblazer vehicle.

5. USE OF A FLOW DIVERTER AND BASE COOLING TO CREATE A WINDOW

5.1 Basic Principles

Re-entry vehicles are enveloped by a thin region of ionized gases which hinder communication from the vehicle to monitoring stations on the ground. A method of alleviating this communication problem would be to somehow eliminate this region of ionized flow locally over an antenna surface, thus creating a window through which transmission is possible. Locating a flow diverter just upstream of an antenna location is an attempt to create such a window by diverting the flow of ionized gases away from the antenna surface.

At the base of the flow diverter a "dead air" region will exist which will contain temperatures equivalent to those in a stagnation point. Therefore a coolant is injected into this region to keep temperatures here at a tolerable level for communication.

The simplest flow diverter to consider is one which extends out from the vehicle surface perpendicular to the stream. All the oncoming flow would be diverted laterally and a window would be created at its base (Figure 5.1A). Unfortunately, such a protruberance would be hard to protect against aerodynamic heating and would include significant aerodynamic forces on the vehicle. Generally, these considerations would eliminate the practical use of this type of two dimensional diverter with the exception of lifting re-entry vehicles with a "natural" flow diverter such as a dorsal fin.

A more versatile diverter must have a swept-back leading edge and be shaped more like a cone or pyramid (Figure 5.1B). Now, not all the flow is diverted around the side and some flows over the top for the antenna to look through. This kind of flow diverter will be useful only if the flow over the top is much more transparent than the original flow. Of course, the use of a diverter is only feasible in the first place if the region of high attenuation is more or less concentrated in a finite layer near the surface.

5.2 Diverter Effectiveness

For a communication gain to be realized with a flow diverter the plasma sheath must be either

a. completely diverted from flowing over the antenna at the base of the flow diverter.

b. geometrically thinned such that the plasma slab thickness at the antenna location is significantly less than the initial plasma thickness.

Since two dimensional flow diverters are only practical under special circumstances, due to drag and heating penalties, we will concentrate on the three dimensional flow diverter which thins the plasma sheath. Figure 5.2 shows the decrease in attenuation with decreasing plasma thickness for an antenna located on the aft portion of the conical surface of a Trailblazer II vehicle re-entering the atmosphere at 18,000 fps. A homogeneous finite thickness slab model of the plasma has been used for these calculations, and the local flow has been assumed to be in equilibrium.

As a means of geometrically thinning the plasma sheath, 2 types of flow diverters have been studied

a. conical flow diverters

b. conical flow diverters of elliptic cross-section

The elliptic cones were analyzed since it was felt that the cross-flow associated with this shape would contribute to the thinning of the plasma sheath by diverting part of the hot ionized air to the sides of an antenna. In the limit of very large elliptic ratios the flow over an elliptic cone flow diverter is seen to act like a two dimensional flow diverter.

5.2.1 Conical Flow Diverter

Figure 5.3 is a schematic illustration of the flow past a diverter which consists of half a circular cone. The flow approaching the diverter is first compressed in flowing over the conical surface and then re-expanded as it leaves the base. The flow over the antenna is thus

analogous to that in the near wake of a full cone. If we assume that the pressure at the antenna station is roughly equal to that in the undisturbed stream, we can calculate the thinning of the high-attenuation layer in the plane of symmetry as a purely geometrical effect. If

δ_1 is the original thickness the high attenuator layer

δ_2 is its thickness over the antenna

R is the radius of the base of the diverter

conservation of streamtube area requires that

$$\delta_2 = \sqrt{R^2 + \delta_1^2} - R$$

This relationship is illustrated in Figure 5.4 by a plot of δ_2/δ_1 versus R/δ_1.

The resulting gain in signal strength is illustrated in Figure 5.5 which combines the results in Figure 5.2 and 5.4 to show the decreased attenuation versus conical flow diverter radius.

Bearing in mind the 3 db criteria assumed for adequate transmission the reduction in attenuation is obviously inadequate. Figure 5.6 is merely an extension of Figure 5.5 to determine just what flow diverter heights are required to meet this criteria. Note that the flow diverter heights required are prohibitive.

5.2.2 Elliptic Cone Flow Diverter

An elliptic cone, as shown in Figure 5.7 experiences the same geometrical thinning of the plasma sheath as the circular cone. As before conservation of streamtube area requires that

$$\delta_2/\delta_1 = \sqrt{\left(\frac{a+b}{2\delta_1}\right)^2 + 1} - \left(\frac{a+b}{2\delta_1}\right)$$

b, a, major and minor axes of the ellipse.

This relationship is exactly the same as that shown plotted in Figure 5.4 if

$$R \equiv \left(\frac{a+b}{2}\right)$$

In order to make a comparison of the relative thinning effects of the elliptic and circular base cone, we define an equivalent circular cone as one whose base area is equal to that of the elliptic cone. This determines an equivalent radius for the circular cone to be the following

$$R_{equivalent} = \sqrt{a\,b}$$

To determine the relative merit of the circular and elliptic cone in thinning the high attenuation layer for the conditions shown below,

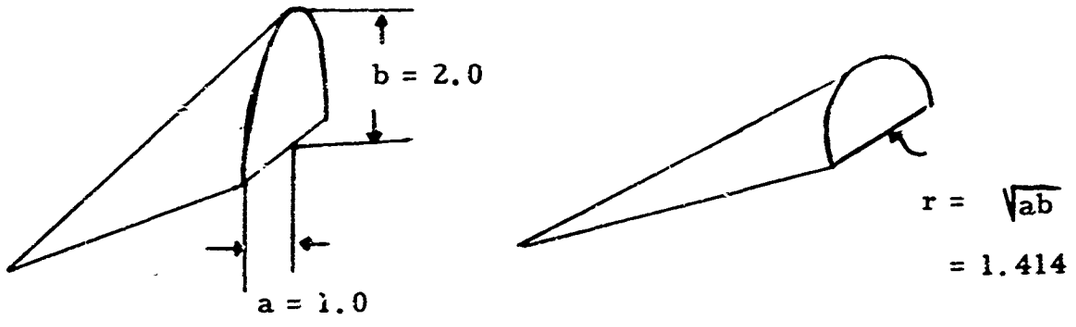

$$R \equiv \frac{a+b}{2}$$

$$= 1.5$$

$$\delta_1 = 2''$$

$$f = 200\ Mc$$

we have to refer to Figure 5.5 and note the attenuation for various altitudes for $R_{equivalent} = 1.414$ and $R = \frac{a+b}{2} = 1.5$.
The elliptic cone decreases the attenuation of a signal at all altitudes by approximately .5 db more than the circular cone. Hardly significant in comparison to the absolute value of the attenuated signal.

However by mounting an elliptic flow diverter with its major axis perpendicular to the flow we can take advantage of the cross-flow whose direction is from the major to the minor axis to divert part of the plasma layer to the sides and thereby further thin the plasma layer over an antenna.

Data taken from References 14, 15, 16 has been used to calculate the shock shape about two elliptic cones with axis ratios of 1.394 and 1.788. The Mach number of the flow over these cones was taken to be M = 3.088 and M = 5.9409 for each of the two elliptic cones.

Figure 5.8 shows the elliptic cones used in the analysis and their shock envelopes. The equivalent circular cone as defined previously above is that circular cone whose cross-sectional base area is equal to that of the elliptic cone. The antenna looks out through a window whose boundary is shown by the dotted lines.

As a means of comparing the effects of how thick the shock layers are for both the equivalent and elliptic cone flow diverters, the ratio

$$\Delta b_{ellipse} / \Delta R_{cone}$$

has been plotted in Figure 5.9 versus elliptic axis ratio b/a for constant Mach numbers. The mass flow contained in the shock layers for both the conical and elliptic flow diverters are approximately equal, so that the cross-flow effect in diverting the flow to the sides of an antenna can be determined from this figure. It is seen that for a Mach number 3.0 which corresponds to the local flow velocity at possible antenna locations on the Trailblazer II vehicle, the 2-dimensional effect of diverting flow to the sides with elliptic cone flow diverters is significant. For a cone of elliptic axis ratio of 1.5 the plasma thickness is 3/4 that of the flow over the equivalent circular cone. Referring to Figures 5.2 and 5.4 with "a" assumed equal to 1.0 and the initial plasma thickness = 2" the decrease in attenuation due to the cross-flow associated with the elliptic cone is approximately 3 db greater than that derived by use of the equivalent circular cone. This is again a relatively low gain in comparison to the

absolute magnitude of the signal loss. However it does point out the effect of cross-flow on thinning the plasma sheath in comparison to solely geometrical thinning.

5.3 Cooling the Near Wake

Even for the above gains to be realized it is of course necessary to maintain low electron concentrations in the separated flow behind the base of the diverter. This is accomplished by injecting a coolant, such as helium, into the base flow so as to avoid recirculation of the hot external flow.

The flow diverter scheme as a method of creating an antenna window is sketched in Figure 5.10. As Chapman[17] points out, if gas is injected at least as fast as the mixing layer scavenges it from the dead-air region, no flow is recirculated at the base, and the temperature in the dead-air region is equal to that of the injected gas. It does not matter whether the mixing layer is laminar, as considered in some detail by Chapman, or turbulent; however, the rate of gas injection required to avoid recirculation is much larger in the latter case. The theory presented here will concern itself with turbulent flows, which will occur in most cases of practical interest. In particular we consider rates of injection less than those required to avoid recirculation and calculate the variation with injection rate of the temperature in the dead-air region.

Since very little information is available about the structure of turbulent layers in high-speed flows, a simple analysis seems most appropriate. We shall assume that the profiles of total enthalpy and foreign gas concentration are linear functions of the velocity profile, corresponding to $P_r = L_e = 1.0$

$$H = H_s + (H_e - H_s)\, u^* \tag{5.1}$$

$$C = C_s\,(1 - u^*) \tag{5.2}$$

here

H	is the local stagnation enthalpy
H_s	is the enthalpy of the separated region
H_e	is the stagnation enthalpy of the free stream
C	is the local foreign gas concentration
C_s	is the foreign gas concentration in the separated region
u^*	is the local velocity divided by that of the free stream.

We shall also assume the form of the eddy viscosity law suggested by Ting and Libby[18], which relates the compressible profiles to the incompressible profile through the Howarth transformation:

$$Y = \int \rho^* \, dy \tag{5.3}$$

At reattachment the flow in the mixing layer splits as sketched in Figure 5.10. The dividing streamline ($y = 0$) splits the flow such that the mass flux flowing below it is equal to the total rate of mass entrainment from the dead-air region[17]. The reattachment streamline ($y = y_i$) splits the flow such that the mass flux flowing below it is recirculated.

If b is the width of the flow (or the perimeter in the axisymmetric case), the following relation holds:

The mass rate of injection: $m_j = b \int_{yi}^{c} \rho u \, dy$

the entrainment of foreign gas: $b C_s \int_{-\infty}^{0} \rho u \, dy$

the recirculation of foreign gas: $b \int_{-\infty}^{yi} \rho u C \, dy$

In terms of normalized variables, the balance of in-flow and out-flow of foreign gas may thus be written:

$$C_s \int_{-\infty}^{o} \rho^* u^* dy = \int_{yi}^{o} \rho^* u^* dy + C_s \int_{-\infty}^{yi} \rho^* u^* C^* dy \quad (5.4)$$

Using (5.2) and (5.3) this may be solved for

$$C_s = \frac{1}{1 + J} \quad (5.5)$$

where

$$J = \int_{-\infty}^{yi} u^{*2} dy \Big/ \int_{yi}^{o} u^* dy \quad (5.6)$$

For the case of zero heat transfer to the solid surface bounding the separated region (which will yield a "recovery factor" with injection), a similar balance may be written for the flux of total enthalpy:

$$H_s \int_{-\infty}^{o} \rho^* u^* dy = H_i \int_{yi}^{o} \rho^* u^* dy + \int_{-\infty}^{yi} \rho^* u^* H dy \quad (5.7)$$

Using (5.1), this reduces to:

$$\frac{H_s - H_i}{H_e - H_i} = \frac{J}{J + 1} \quad (5.8)$$

i - refers to injected coolant conditions.

For perfect gases with constant specific heats, this may be expressed in terms of temperature as:

$$\frac{T_s - T_i}{T_{t_e} - T_i} = \frac{J}{J + C_{p_i} / C_{p_e}} \quad (5.9)$$

Now J may be related to the location of the re-attachment streamline in the flow by (5.6), which is a transformed expression to be evaluated from the solution for incompressible flow. The same solution can be used to evaluate, ϕ, the ratio of the injection rate to the total entrainment rate of the mixing layer:

$$\phi = \int_{yi}^{o} u^* \, dy \Big/ \int_{-\infty}^{o} u^* \, dy \qquad (5.10)$$

The relation between ϕ and J is given in Figure 5.11 with the assumption made here that it is universal to all turbulent mixing layers.

Hill and Nicholson[19] have measured turbulent entrainment rates over a very wide range of conditions and have developed the following formula for the entrainment coefficient c_q:

$$c_q = \frac{\rho_s u_s}{\rho_e u_e} = 0.049 \left[\frac{R_e T_e}{R_s T_s}\right]^{0.4} \left[\frac{T_e}{T_{te}}\right]^{0.67} \qquad (5.11)$$

In this expression the gas constant ratio, R_s / R_e, in the separated region may be evaluated in terms of the molecular weight ratio, m_e / m_i, and the mixing ratio C_s:

$$R_s / R_e = 1. + C_s \left[\frac{m_e}{m_i} - 1.\right] \qquad (5.12)$$

This coefficient c_q has been normalized with respect to the base area of the flow diverter (Reference 20) such that proper comparison can be made with the coolant injection jet-penetration coefficient. It was found that;

$$C_{Q_2} = \frac{\dot{m}_i}{\rho_1 u_1 A_2} = 6\, c_q$$

To determine the coolant mass flux C_Q for varying temperatures in the mixing layer greater than the injected coolant temperature, equation 5.9 is solved for the parameter J which from figure 5.11 defines the ratio

of injection rate to the total entrainment rate of the mixing layer. Solution of equation 5.11 defines the total entrainment of the mixing layer. Thus curves showing the effect of mass injection as a function of separated region temperature can be drawn.

Figure 5.12 shows C_Q plotted versus local flow diverter velocity or body station for various separated region temperatures.

The temperature in the mixing layer in general varies monotonically from T_s, the temperature in the separated region, to T_e, the temperature in the free stream outside the region of influence of the flow diverter. However for some combinations of T_s and the local flow velocity U_e, at the flow diverter station, the mixing layer temperature varies nonmonotonically from its two boundary conditions, and in this case a peak temperature can exist which is higher than the free stream temperature T_e. When these conditions, shown circled in Figure 5.12, occur, there is obviously no gain in cooling the local flow by means of a flow diverter. This effectively sets a limit on flow diverter location.

2-DIMENSIONAL

5.1a

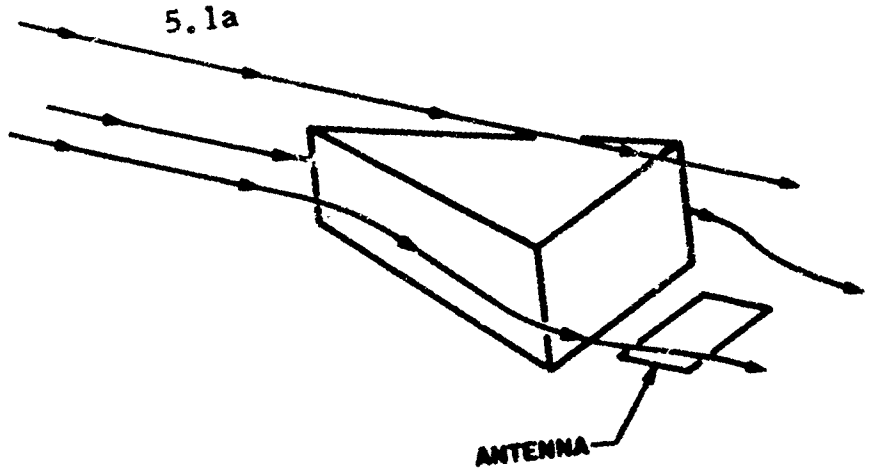

3-DIMENSIONAL

5.1b

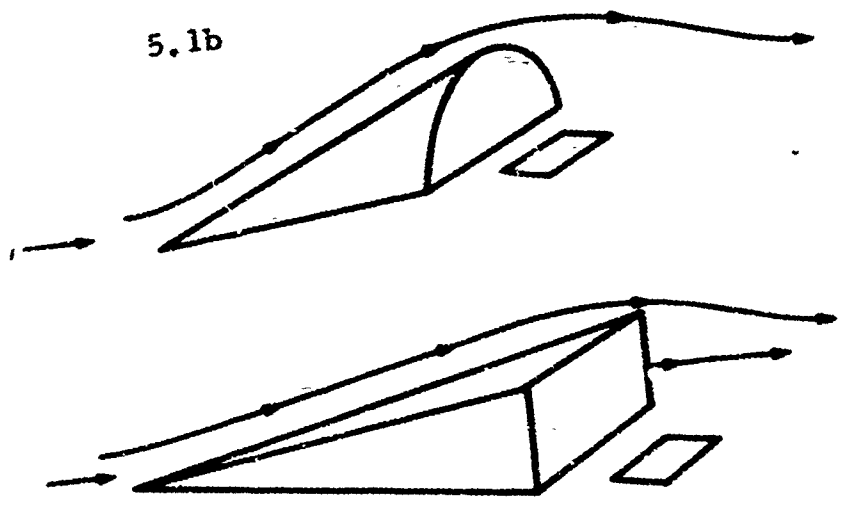

Figure 5.1. Flow diverter.

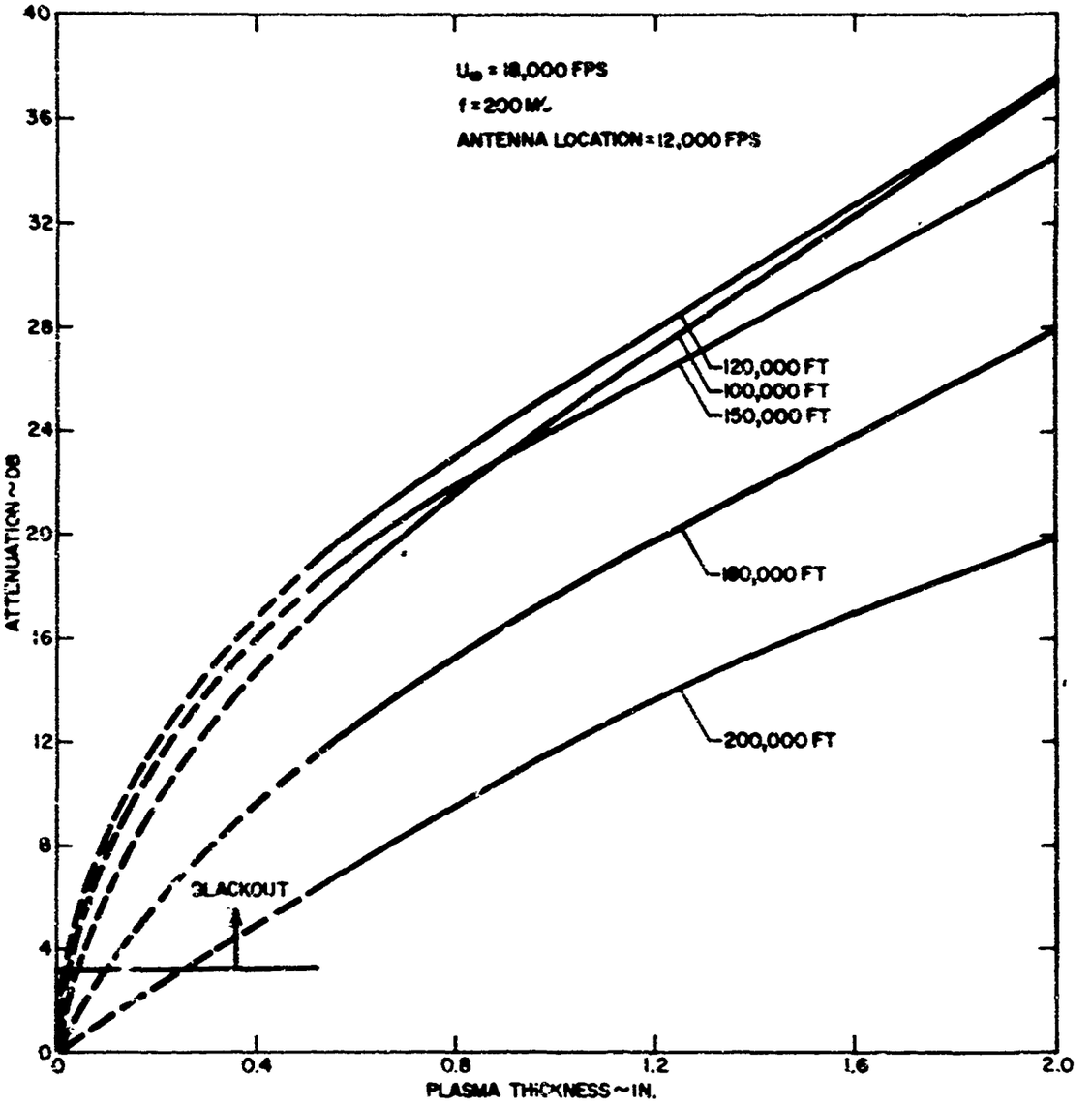

Figure 5.2. Attenuation as a function of plasma thickness.

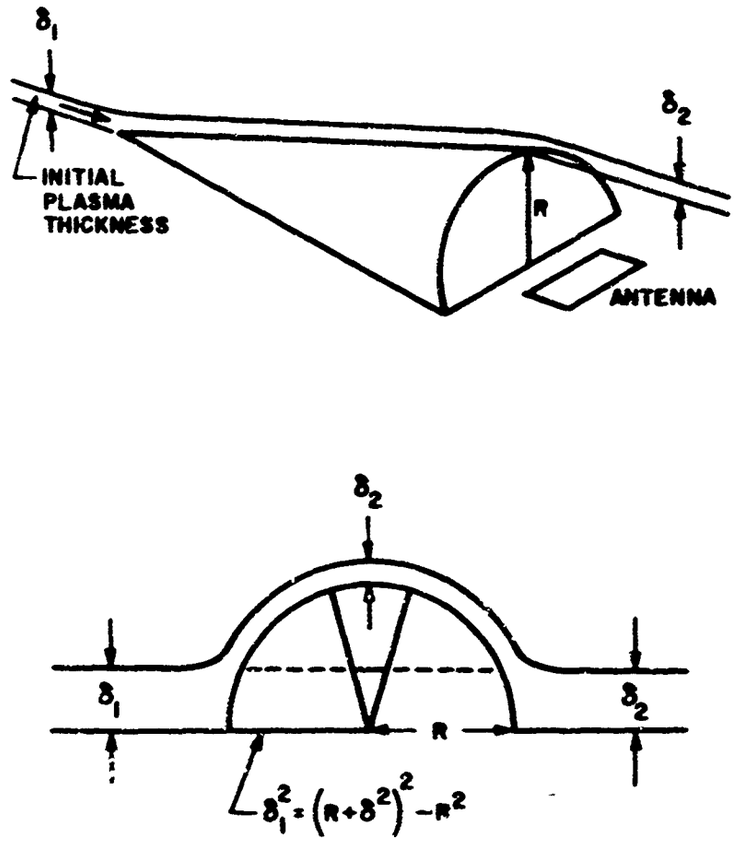

Figure 5.3. Schematic of flow diverter performance.

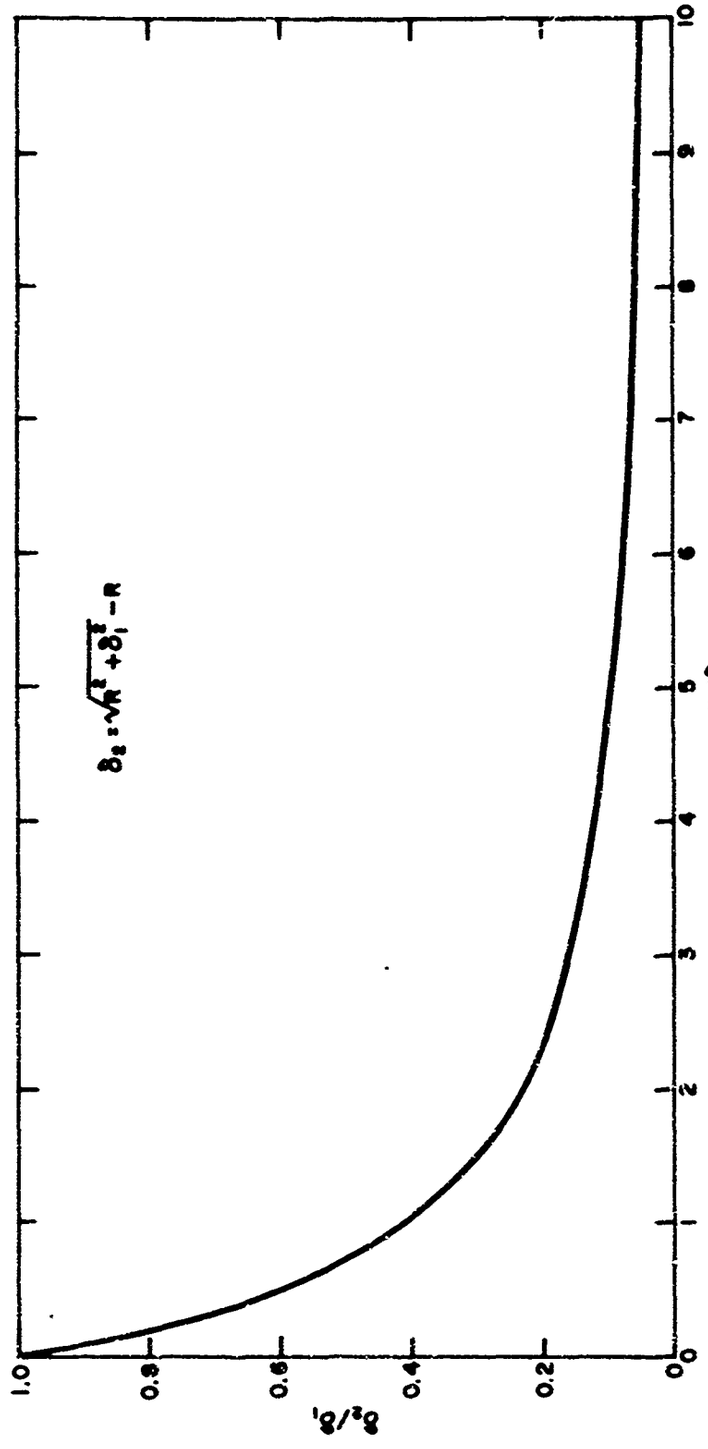

Figure 5.4. Decrease in plasma thickness as a function of flow diverter height.

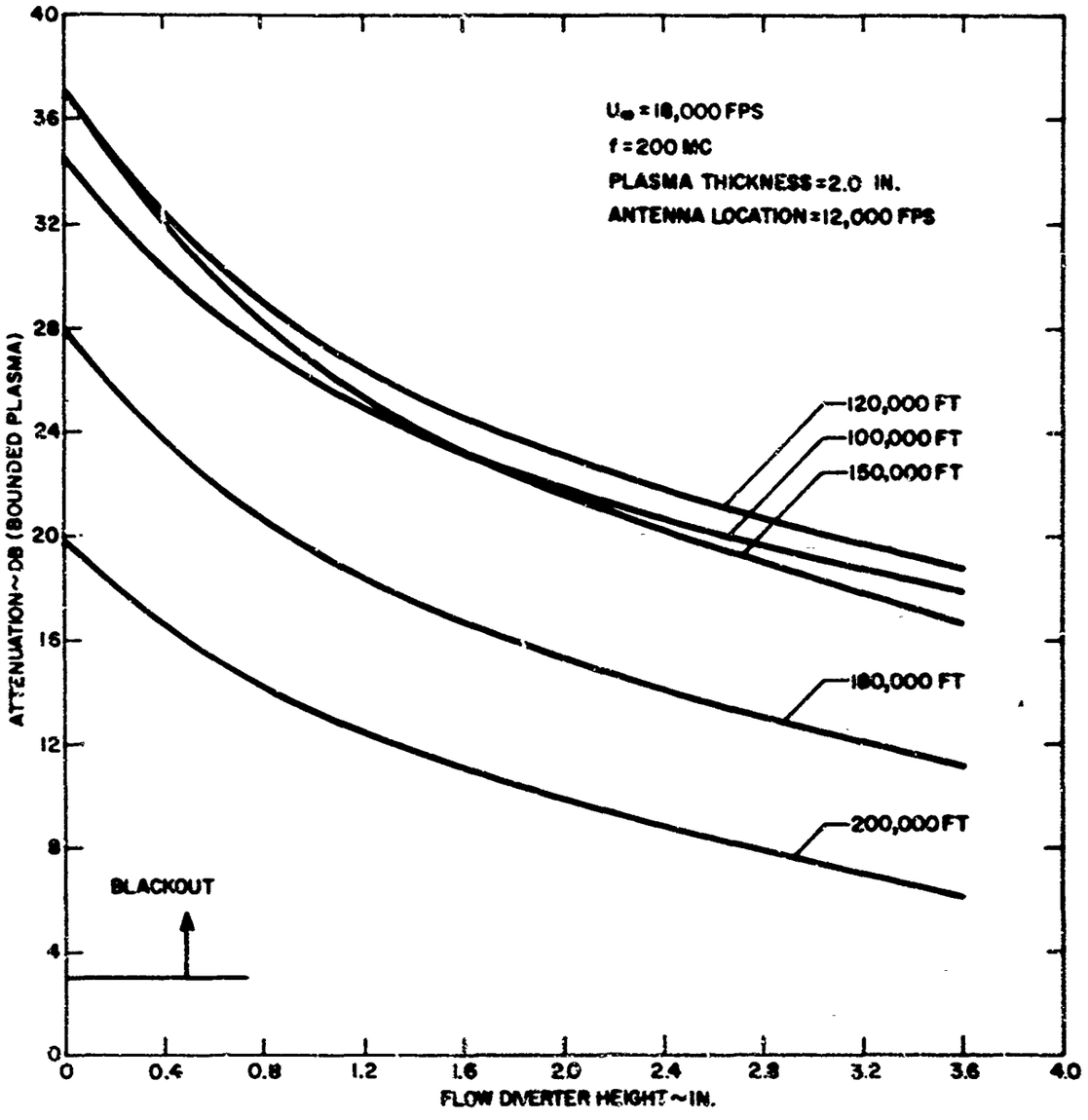

Figure 5.5. Attenuation versus flow diverter height as a function of altitude.

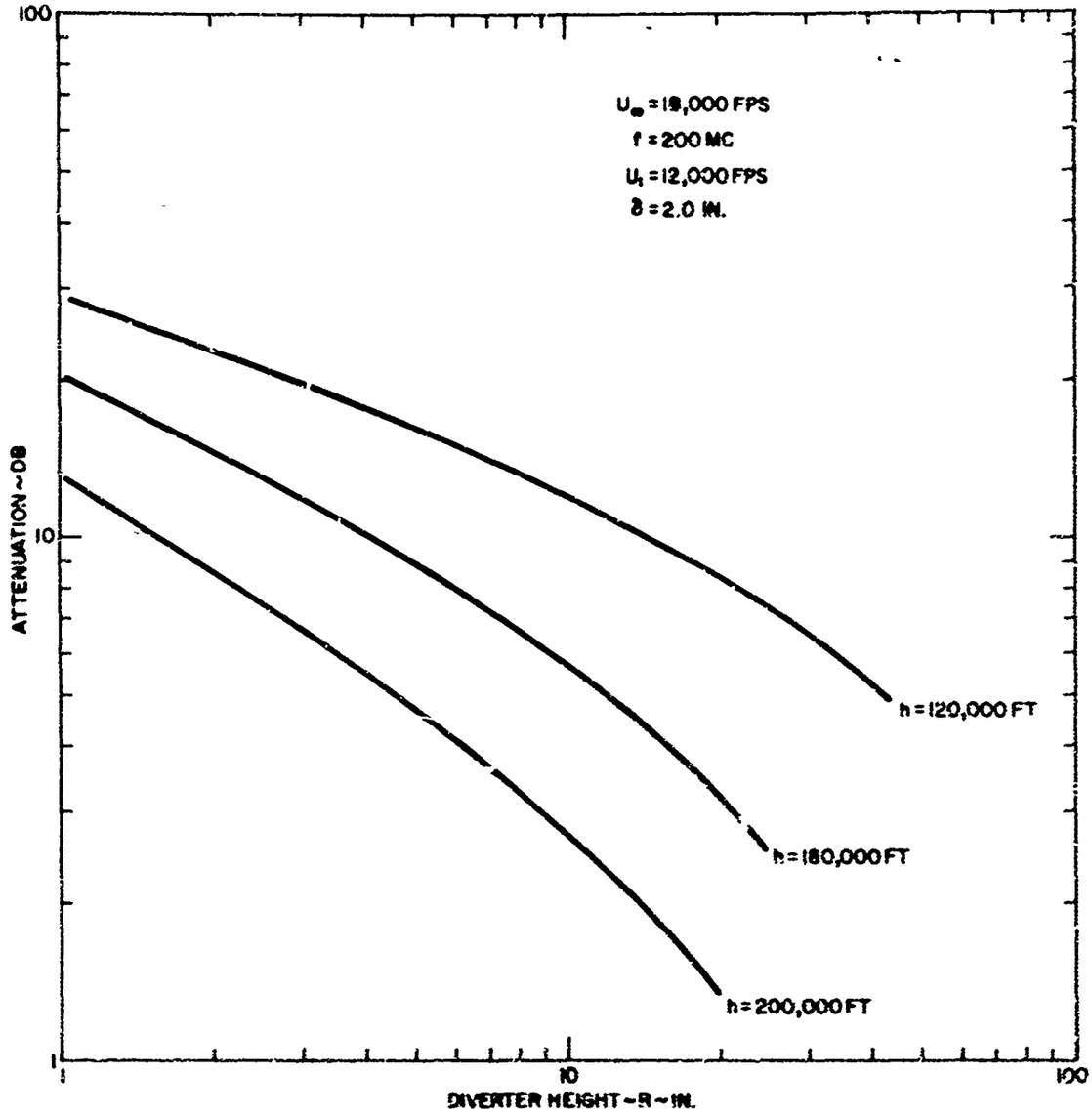

Figure 5.6. Attenuation versus flow diverter height as a function of altitude.

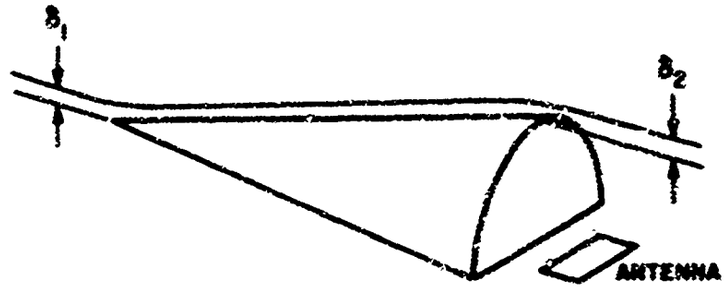

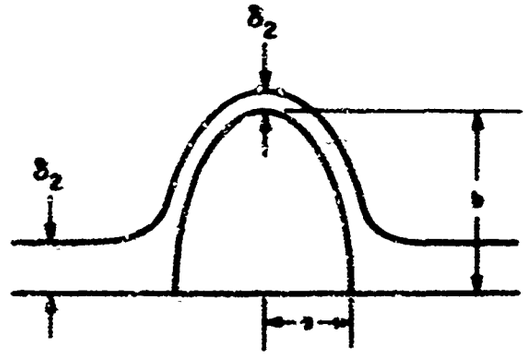

$$\delta_1^2 = (a+\delta_2)(b+\delta_2) - ab$$

Figure 5.7. Schematic of elliptic cone flow diverter performance.

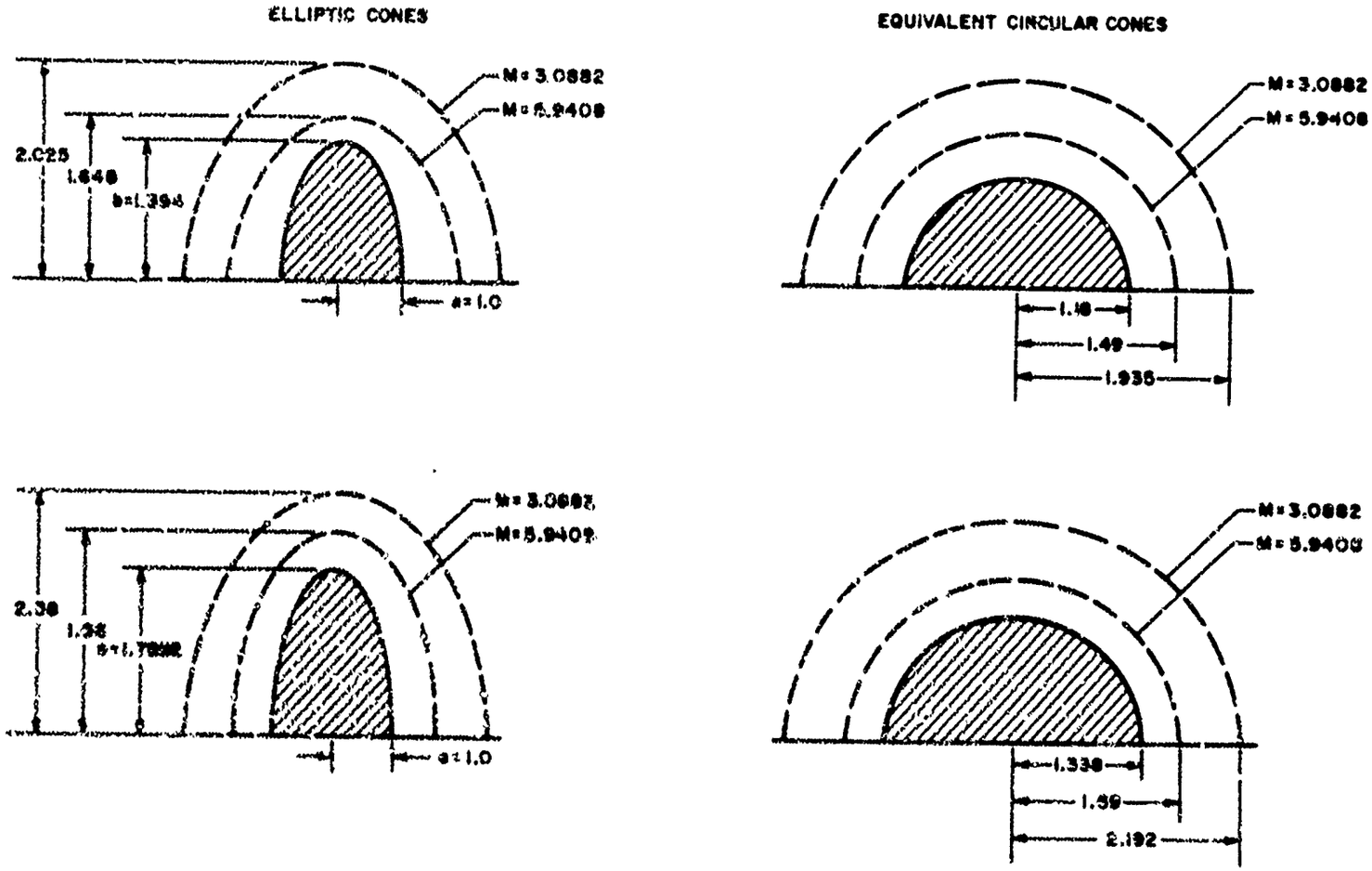

Figure 5.8. Shock envelopes of elliptic and equivalent circular cones.

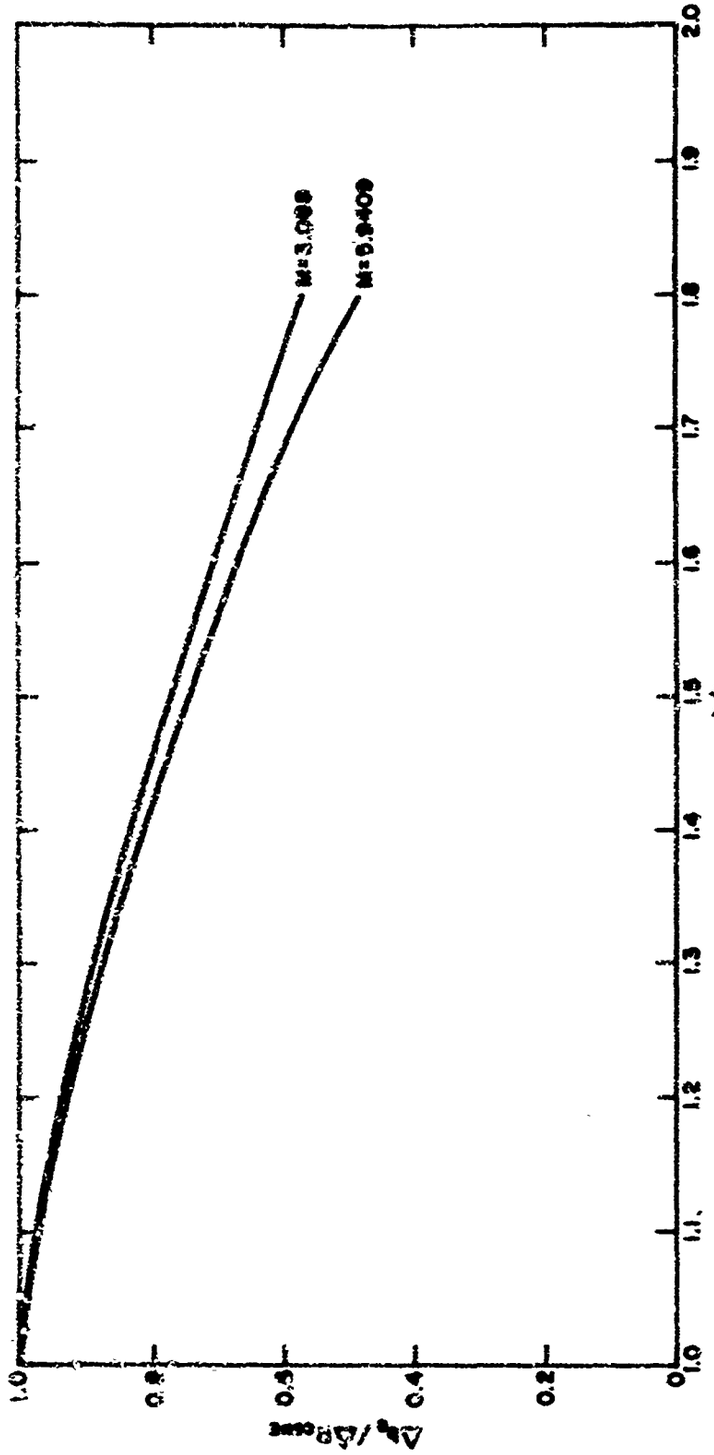

Figure 5.9 Elliptic cone cross flow effect on plasma thickness.

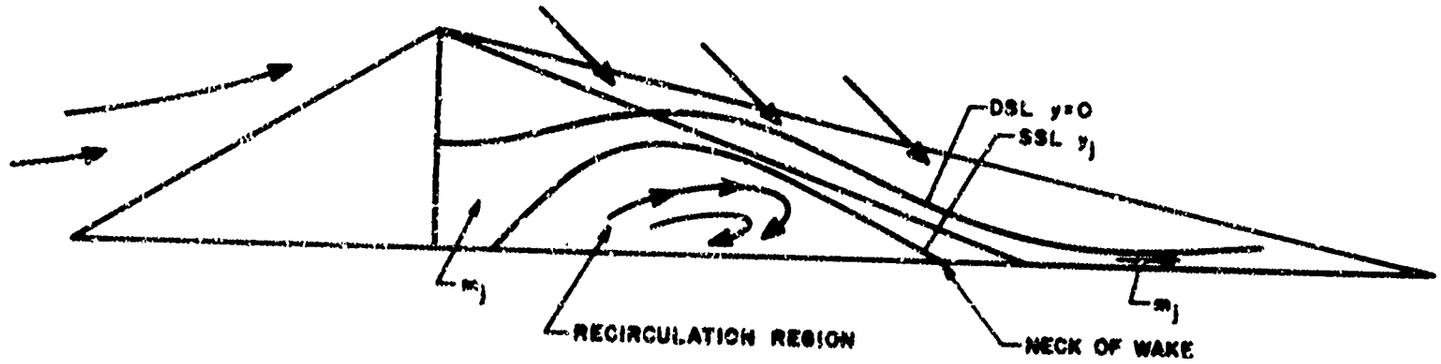

Figure 5.10. Schematic of flow separation at base of a flow diverter.

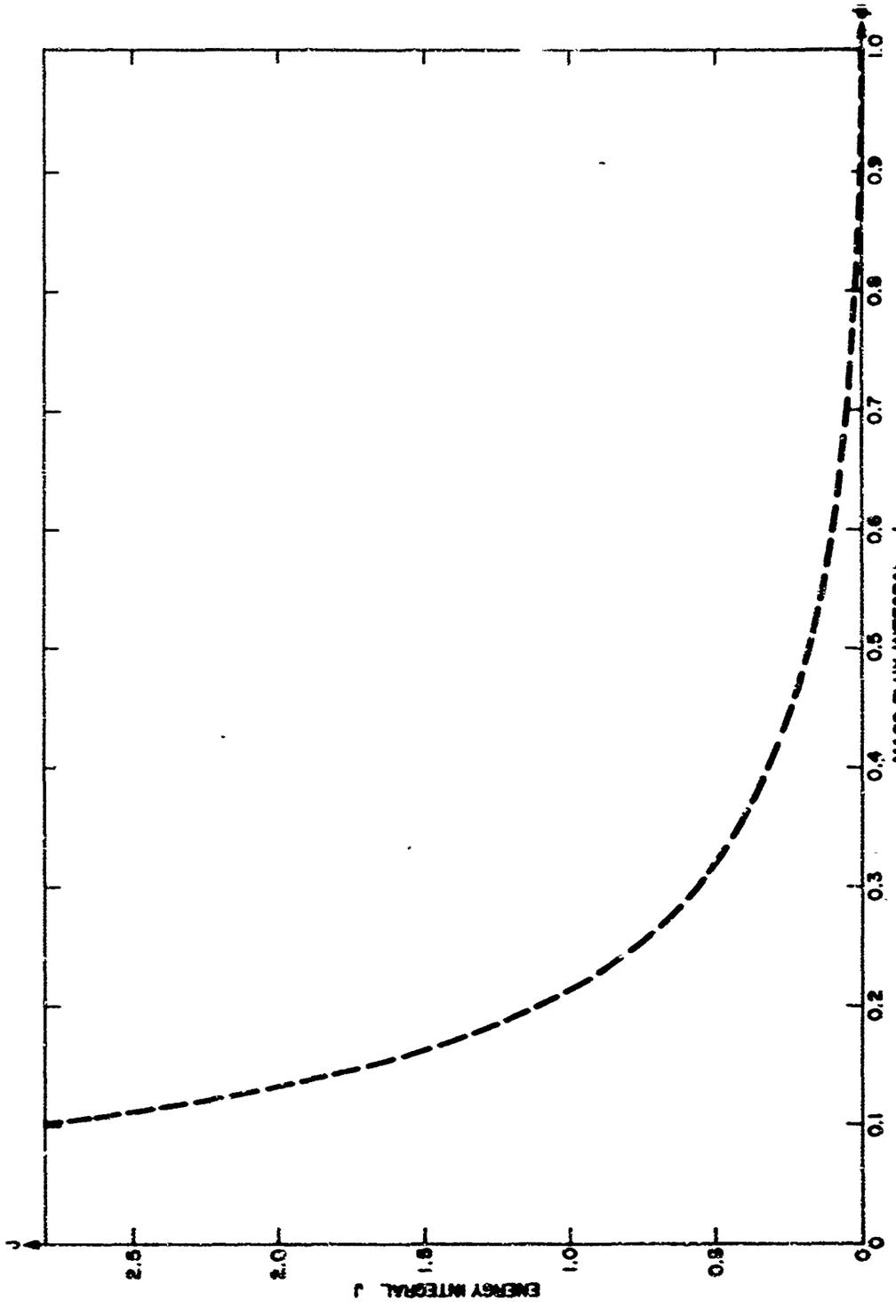

Figure 5.11. Energy integral versus mass flux integral for calculating separated region flow properties.

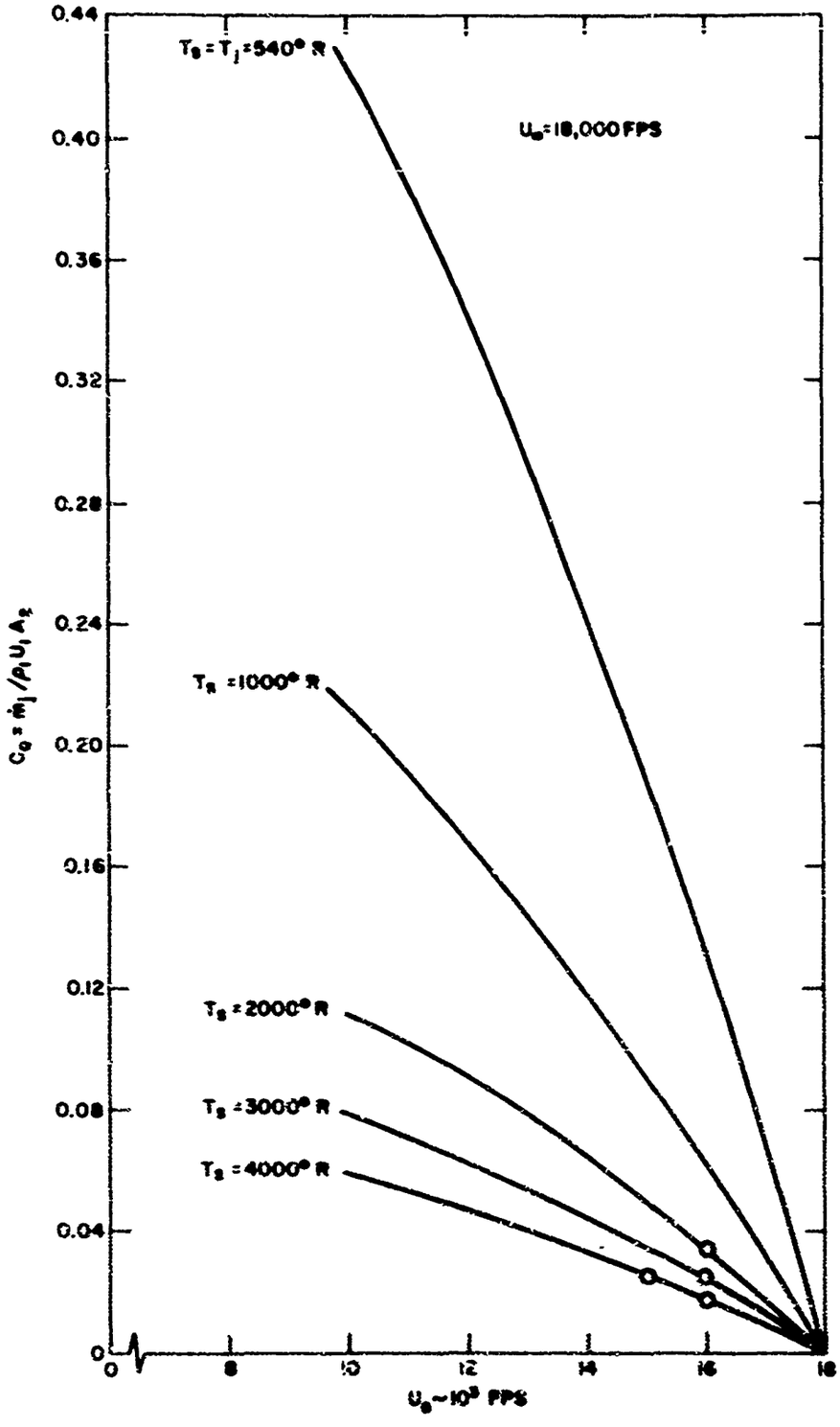

Figure 5.12. Coolant requirement for separated region cooling as a function of local velocity and temperature.

6. COMPARATIVE EVALUATION OF THE TWO WINDOWS

The work reported in the previous sections has been concerned with two methods of modifying and cooling the flow field in the vicinity of an antenna installation on a re-entry vehicle.

In one method nozzles flush with the vehicle surface are used to project jets of coolant into the flow. As it is carried downstream, the coolant cools the airstream by mixing with it. In the other method a physical flow diverter is used to displace the highly ionized flow laterally around the antenna aperture. A region of separated flow is formed over this aperture behind the base of the flow diverter. Coolant is injected to maintain low temperature both in this region and in the shear layer which bounds it.

The injection of a coolant with a flush mounted nozzle appears to be by far the most attractive and practical method for the following reasons:

1. The jet method can reduce the plasma temperature to levels at which transmission is possible (attenuation less than 3 db) with modest mass flows (see Figure 4.10).

The flow diverter method although reducing the attenuation will not reduce the attenuation to the 3 db level as was demonstrated in Figures 5.5 and 5.6.

2. The jet method allows the cooling of a plasma sheath located away from the body surface whereas the flow diverter is limited to relatively thin plasma sheath near the body surface.

3. The jet method allows all equipment to be located internally while the flow diverter is an external protuberance which must be protected against aerodynamic heating and loads.

REFERENCES

1. Bachynski M. P., Cloutier G. G., Graf K. A., Microwave Measurements on Finite Plasmas. RCA Victor Research Report 7-801-26 May 1963.

2. Evans John S. and Huber Paul W., Calculated Radio Attenuation Due to Plasma Sheath on Hypersonic Blunt-Nosed Cone. NASA-TN-D, 2043.

3. R. E. Good, Plasma and Collison Frequencies. MITHRAS Memo 63-01, March 1963.

4. Feldman, Saul, Trails of Axi-Symmetric Hypersonic Blunt Bodies Flying through the Atmosphere. AVCO R R-82 December 1959.

5. Romig, Mary F., Conical Flow Parameters for Air in Dissociation Equilibrium . Convair Scientific Research Laboratory, San Diego, California, Research Report No. 7, May 1960.

6. Kuehn, Donald M., Experimental and Theoretical Pressures on Blunt Cylinders for Equilibrium and Non-Equilibrium Air at Hypersonic Speeds. Ames Research Center, Moffett Field, California. NASA TN D-1979, November 1963.

7. McCabe, William M., and Stolwyk Carl F. Electromagnetic Propagation Through Shock Ionized Air Surrounding Glide Reentry Spacecraft IRE Transactions on Space Electronics and Telemetry, December 1962.

8. Pai, Shih-I, (1954) Fluid Dynamics of Jets. D Van Nostrand Company 1954, New York, New York.

   and

   Townsend, A. A., (1956). The Structure of Turbulent Shear Flow. The Cambridge University Press, Cambridge, England

9. Ricou, F. P., and Spalding, D. B. (1961) Measurement of Entrainment by Axisymmetrical Turbulent Jets. Journal of Fluid Mechanics, Vol. 11, Part I, August 1961, Unclassified.

10. Penland, Jim A., (1957), Aerodynamic Characteristics of a Circular Cylinder at Mach number 6.86 and Angles of Attack up to 90°. NACA TN 3861.

11. Bartlett, Stephen (1964) Relative Merit of Two Methods of Integrating the General Equation dy/dx = f(x, y). Memorandum 63-80

12. Hill, J. A. F., Comparison of Several Possible Materials for Plasma Suppression by Injection into the Flow Field, MITHRAS Internal Memo 432., January 10, 1964.

13. Hill, J. A. F., Alden, H. L., The Penetration of Supersonic Flows by Circular Cross Jets. MITHRAS Internal Memo 440 February 12, 1964.

14. Anthony Martellucci, An Extension of the Linearized Characteristic Method for Calculating the Supersonic Flow Around Elliptic Cones. Polytechnic Institute of Brooklyn Report No. 517.

15. Antonio Ferri, Nathan Ness, Thasseus T. Kaplita. Supersonic Flow over Conical Bodies without Axial Symmetry. J.A.S. August 1953.

16. Robert L. Chapkis, Hypersonic Flow Over an Elliptic Cone, Theory and Experiment. J.A.S. November 1961.

17. Chapman, D. R. A Theoretical Analysis of Heat Transfer in Regions of Separated Flows NACA Techn. Note 3792, 1956.

18. Ting, L. and Libby, P. A. Remarks on the Eddy Viscosity in Compressible Mixing Flows . Journal of the Aero/Space Sciences, October 1960.

19. Hill, J. A. F. and Nicholson, J. E. Compressibility Effects on Fluid Entrainment by Turbulent Mixing Layers, Final Report on NASA Contract NASw-601, MITHRAS, Inc., MC 62-39-R1, March, 1964 or NASA Contractor Report CR-131.

20. MITHRAS QPR No. 2, Contract AF 19(628)-3852, January 15, 1964-April 14, 1964, MC 63-78A.

UNCLASSIFIED
Security Classification

DOCUMENT CONTROL DATA - R&D

Security classification of title, body of abstract and indexing annotation must be entered when the overall report is classified.

1 ORIGINATING ACTIVITY (Corporate author) MITHRAS, INC. 701 Concord Avenue, Cambridge, Massachusetts 02138	2a. REPORT SECURITY CLASSIFICATION Unclassified 2b. GROUP

3. REPORT TITLE
Research of Aerodynamic Methods of Producing Antenna Windows in a Plasma Sheath

4. DESCRIPTIVE NOTES (Type of report and inclusive dates)
Scientific Report No. 1 Oct 14, 1963-October 19, 1964

5. AUTHOR(S) (Last name, first name, initial)
Adams, Richard H., and
Rossi, Joseph J.

6. REPORT DATE October 1964	7a. TOTAL NO. OF PAGES xii and 85	7b. NO. OF REFS 20
8a. CONTRACT OR GRANT NO. AF19(628)-3852 b. PROJECT NO. 4642 c. TASK 464202 d.	9a. ORIGINATOR'S REPORT NUMBER(S) MC 63-78-R1 9b. OTHER REPORT NO(S) (Any other numbers that may be assigned this report) AFCRL-65-65 AD	

10. AVAILABILITY/LIMITATION NOTICES
Qualified requesters may obtain copies of this report from DDC.
Other persons or organizations should apply to U. S. Department of Commerce, Office of Technical Services, Washington, D. C. 20230

11. SUPPLEMENTARY NOTES	12. SPONSORING MILITARY ACTIVITY AF Cambridge Research Laboratories Office of Aerospace Research (CRDM) United States Air Force Bedford, Massachusetts

13. ABSTRACT

Two aerodynamic methods of creating transmission "windows" in typical plasma sheaths surrounding re-entry vehicles have been investigated: (1) the use of jets of coolant from flush nozzles which penetrate across the plasma slab and then mix with the ionized gases as they are carried downstream, (2) the use of a physical flow diverter to bypass some of the ionized flow laterally around the antenna. Equations are developed for the lateral jet penetration in a supersonic stream and for one-dimensional mixing for both perfect gases and real gases in thermodynamic equilibrium. The assumption of real-air equilibrium thermodynamics yields coolant requirements considerably below the perfect gas values for the jet injection method. It is concluded that the jet injection method will reduce a 200 mc signal attenuation to 3 db with modest jet flow rates of helium on a typical re-entry trajectory. Conversely, the use of a physical flow diverter is not an effective method of creating a transmission window where the ionization layer is not adjacent to the vehicle surface or where the attenuation needs to be reduced more than 10 db. (Unclassified)

DD FORM 1 JAN 64 1473

UNCLASSIFIED
Security Classification

14. KEY WORDS	LINK A		LINK B		LINK C	
	ROLE	WT	ROLE	WT	ROLE	WT
Theory	8	2				
Transmission "Windows"	8, 7	1				
Jet Penetration Cooling	10	1				
Flow Diverter	10	1				
Separated Flow Cooling	10	1				
One-Dimensional Streamtube Mixing	10	1				
Plasma Sheath	6, 8	1				

INSTRUCTIONS

1. ORIGINATING ACTIVITY: Enter the name and address of the contractor, subcontractor, grantee, Department of Defense activity or other organization *(corporate author)* issuing the report.

2a. REPORT SECURITY CLASSIFICATION: Enter the overall security classification of the report. Indicate whether "Restricted Data" is included. Marking is to be in accordance with appropriate security regulations.

2b. GROUP: Automatic downgrading is specified in DoD Directive 5200.10 and Armed Forces Industrial Manual. Enter the group number. Also, when applicable, show that optional markings have been used for Group 3 and Group 4 as authorized.

3. REPORT TITLE. Enter the complete report title in all capital letters. Titles in all cases should be unclassified. If a meaningful title cannot be selected without classification, show title classification in all capitals in parenthesis immediately following the title.

4. DESCRIPTIVE NOTES: If appropriate, enter the type of report, e.g., interim, progress, summary, annual, or final. Give the inclusive dates when a specific reporting period is covered.

5. AUTHOR(S): Enter the name(s) of author(s) as shown on or in the report. Enter last name, first name, middle initial. If military, show rank and branch of service. The name of the principal author is an absolute minimum requirement.

6. REPORT DATE: Enter the date of the report as day, month, year, or month, year. If more than one date appears on the report, use date of publication.

7a. TOTAL NUMBER OF PAGES: The total page count should follow normal pagination procedures, i.e., enter the number of pages containing information.

7b. NUMBER OF REFERENCES: Enter the total number of references cited in the report.

8a. CONTRACT OR GRANT NUMBER: If appropriate, enter the applicable number of the contract or grant under which the report was written.

8b, 8c, & 8d. PROJECT NUMBER: Enter the appropriate military department identification, such as project number, subproject number, system numbers, task number, etc.

9a. ORIGINATOR'S REPORT NUMBER(S): Enter the official report number by which the document will be identified and controlled by the originating activity. This number must be unique to this report.

9b. OTHER REPORT NUMBER(S): If the report has been assigned any other report numbers *(either by the originator or by the sponsor)*, also enter this number(s).

10. AVAILABILITY LIMITATION NOTICES: Enter any limitations on further dissemination of the report, other than those imposed by security classification, using standard statements such as:

(1) "Qualified requesters may obtain copies of this report from DDC."

(2) "Foreign announcement and dissemination of this report by DDC is not authorized."

(3) "U. S. Government agencies may obtain copies of this report directly from DDC. Other qualified DDC users shall request through _____."

(4) "U. S. military agencies may obtain copies of this report directly from DDC. Other qualified users shall request through _____."

(5) "All distribution of this report is controlled. Qualified DDC users shall request through _____."

If the report has been furnished to the Office of Technical Services, Department of Commerce, for sale to the public, indicate this fact and enter the price, if known.

11. SUPPLEMENTARY NOTES: Use for additional explanatory notes.

12. SPONSORING MILITARY ACTIVITY: Enter the name of the departmental project office or laboratory sponsoring *(paying for)* the research and development. Include address.

13. ABSTRACT: Enter an abstract giving a brief and factual summary of the document indicative of the report, even though it may also appear elsewhere in the body of the technical report. If additional space is required, a continuation sheet shall be attached.

It is highly desirable that the abstract of classified reports be unclassified. Each paragraph of the abstract shall end with an indication of the military security classification of the information in the paragraph, represented as *(TS), (S), (C), or (U).*

There is no limitation on the length of the abstract. However, the suggested length is from 150 to 225 words.

14. KEY WORDS. Key words are technically meaningful terms or short phrases that characterize a report and may be used as index entries for cataloging the report. Key words must be selected so that no security classification is required. Identifiers, such as equipment model designation, trade name, military project code name, geographic location, may be used as key words but will be followed by an indication of technical context. The assignment of links, rules, and weights is optional.